Theses and Dissertations | 1. Thesis and Dissertation Collection, all items

2001

Evaluation and comparison of electric propulsion motors for submarines

Harbour, Joel P.

Monterey California. Naval Postgraduate School

https://hdl.handle.net/10945/10910

Evaluation and Comparison of Electric Propulsion Motors for Submarines

by

Joel P. Harbour

B.S., Electrical Engineering
University of Wyoming, 1991

Submitted to the Departments of Ocean Engineering and Electrical Engineering
in partial fulfillment of the requirements for the degrees of

NAVAL ENGINEER

and

MASTER of SCIENCE
in
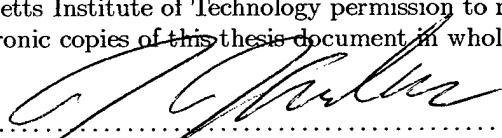ELECTRICAL ENGINEERING and COMPUTER SCIENCE

at the

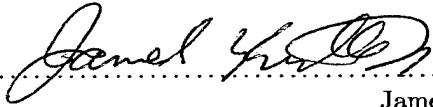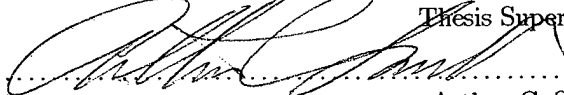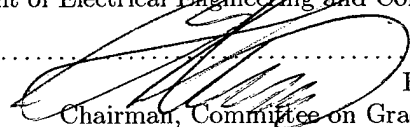MASSACHUSETTS INSTITUTE OF TECHNOLOGY

May 2001

The author hereby grants to Massachusetts Institute of Technology permission to reproduce and
to distribute publicly paper and electronic copies of this thesis document in whole or in part.

Signature of Author . . . .
Departments of Ocean Engineering and Electrical Engineering
11 May 2001

Certified by. . . . .
James L. Kirtley Jr.
Associate Professor of Electrical Engineering
Thesis Supervisor

Certified by. . . . .
Clifford A. Whitcomb
Associate Professor of Ocean Engineering
Thesis Supervisor

Accepted by. . . . .
Arthur C. Smith
Chairman, Committee on Graduate Students
Department of Electrical Engineering and Computer Science

Accepted by. . . . .
Henrik Schmidt
Chairman, Committee on Graduate Students
Department of Ocean Engineering

20010816 041

AQM01-10-2258

Evaluation and Comparison of Electric Propulsion Motors for Submarines

by

Joel P. Harbour

Abstract

The Navy has announced its conviction to make its warships run on electric power through the decision to make its newest line of destroyers propelled with an electric propulsion system [1]. Several ship construction firms and electric motor manufacturers are thus striving to develop enabling technology, including high power density motors [2]. The purpose of this thesis is to evaluate some of the proposed motor designs for use in a submarine.

Permanent magnet, superconducting synchronous and homopolar motors are modeled using computer programs. The application of these motors is optimized for submarine propulsion. The use of reduction gearing was not considered. Therefore, only low speed propulsion motors are evaluated. The permanent magnet motor utilized is the classic surface mounted magnet design scaled up to 21 MW with formed, rather than wound, coils. The superconducting synchronous motor utilized is loosely based on a design by American Superconductor [3] and uses equations developed from the doctoral research by James L. Kirtley [4]. The homopolar motor utilized is based on a novel design proposed by General Atomics [5].

For each motor concept, a repetitive optimization algorithm is used in which the design parameters of each motor are randomly generated and the motor attributes are evaluated. The attributes of the resulting motor, such as weight, volume and efficiency, are compared to a database of stored motor designs. If the new design's attributes dominate a previous design, it is included in the database and the dominated design is discarded. After several cycles the optimum motor designs are converged upon. The structure of this algorithm is based on the Novice Design Assistant developed at MIT by J.A. Moses et al. [6].

Thesis Supervisor: James L. Kirtley Jr.
Title: Associate Professor of Electrical Engineering

Thesis Supervisor: Clifford A. Whitcomb
Title: Associate Professor of Ocean Engineering

Biographical note

The author graduated from the University of Wyoming in December of 1991 with a Bachelor of Science in Electrical Engineering. In his junior year of college he was selected for the Nuclear Propulsion Officer Candidate (NUPOC) program and later received his commission at the navy's Officer Candidate School in Newport, RI. on 01 MAY 1992. He completed the navy's rigorous Nuclear Power School in Orlando, Florida and Prototype Training in Charleston, SC. Following Submarine Officer Basic School, he reported to his first sea command on a Nuclear Powered Ballistic Submarine out of Bangor, WA. He served as Sonar Officer, Reactor Controls Assistant, Main Propulsion Assistant, Strategic Missile Officer and Tactical Systems Officer on the USS Nevada (SSBN 733 (GOLD)) from OCT 1993 to DEC 1997. While serving on the Nevada he completed seven deterrent patrols, completed his Submarine Warfare qualifications, qualified Engineer for Naval Nuclear Propulsion plants and completed his Strategic Weapons Officer (SD2) qualifications. He was then selected for lateral transfer to the Engineering Duty Officer community and graduate studies at MIT. He reported to MIT in June of 1998 for a three year tour of full time graduate work in the Naval Architecture and Marine Engineering (13A) program of the Ocean Engineering Department and a second master's degree in the Electrical Engineering and Computer Science Department.

For my wife Tara

Who has always been there for support throughout my naval career

and my children

Megan

Cassandra

and

Ethan

Acknowledgments

Contents

List of Figures

List of Tables

Chapter 1

Introduction

Electric propulsion motors have been utilized in naval ships in the past, as early as the 1910's [2][7]. However, following WWII, reduction gear manufacturing techniques outpaced electric motor technologies and were able to make faster, lighter and more economical mechanical propulsion drive trains for ships. Electric drives were, and still are, being utilized in low power diesel electric submarines and as emergency propulsion drives in high power submarines. In the commercial and cruise ship industries, electric propulsion drives are becoming more prevalent. Recent technological advances in electric propulsion have brought about a renewed interest in electric propulsion for use in high power submarines.

1.1 Why Electric Propulsion?

Shown in Figures 1-1 and 1-2 are schematics of a traditional mechanical drive train with a separate electrical power plant and, conversely, a combined electrical propulsion drive train integrated into the electric distribution system. Several compelling arguments to move away from mechanical drive and to electric drive follow.

1.1.1 Reduction Gearing Approaching Limitations

Mechanical reduction gears, although historically smaller and more efficient than electric motors, have reached their limits, and electric propulsion motors have now started to become more appealing. This is especially true in high power submarine applications where the size of the reduction
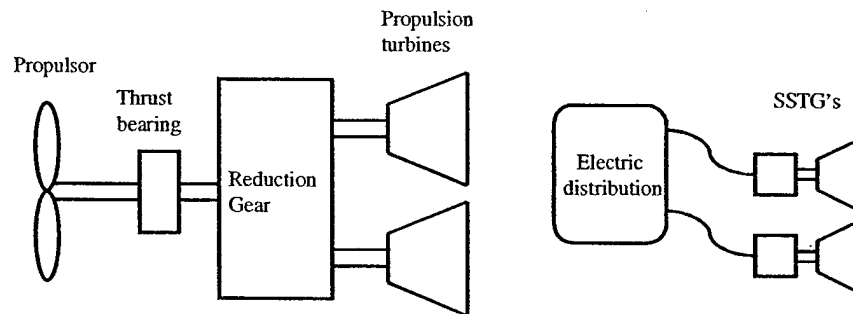
Figure 1-1: Mechanical drive schematic.
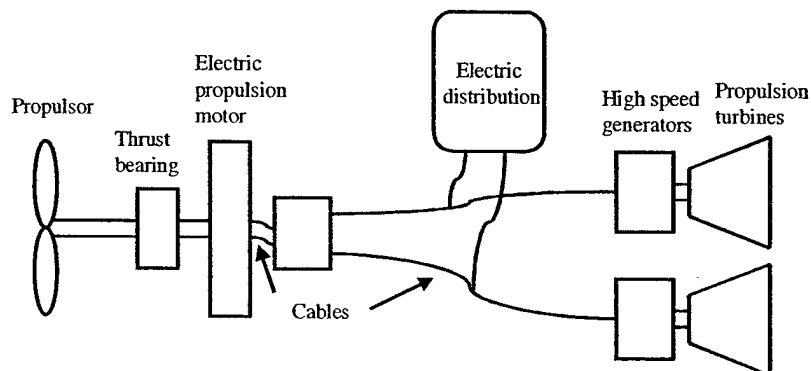
Figure 1-2: Electric drive schematic

gears is constrained by the diameter of the cylindrical hull form of a submarine. In addition, in order to make the propulsor as quiet as possible, rotational speeds have decreased to the point where the required reduction ratio from the high speed prime movers requires larger diameter gearing in the reduction gears themselves. Electric motor technology has the potential to enable a smaller and quieter propulsion transmission system than the historically mechanically driven submarine.

1.1.2 Installed Reactor Power Under Utilized

The installed reactor power on current mechanical drive submarines is predominantly used for propulsion. Roughly 80% of the total reactor power is available exclusively for propulsion[8]. Further, the operational speed profile of a submarine rarely uses the submarine's top speed. Most of the time, the submarine travels at a modest cruising speed. It would be beneficial to be able

16

to utilize the remaining installed power for other uses. With an electric drive submarine the installed reactor power of the submarine is first converted to electrical power and then delivered to an electric propulsion motor. The now available electrical potential not being used for propulsion could easily be tapped into for other uses[1]. In the large tanker ship industry, for example, this power distribution design is already being utilized. The same prime movers that power the electric propulsion motors for high speed transits are employed to power the large pumps that off-load and on-load cargo in port. There are numerous ongoing design projects to research and solve the design issues associated with integrating the propulsion plant and the electrical power generation and distribution systems [9]-[19].

1.1.3 Off Design Point Turbine Efficiency Low

The efficiency of the prime movers, the steam turbines, vary with load (see Appendix A)[20]. A steam turbine operating at 60% of its rated power has a 2% decrease in efficiency. Also, the propulsion power necessary to drive a submarine a certain velocity follows a cubic power law; to increase the speed of the submarine by a factor of 2, the shaft power must be increased by a factor of 8. Roughly 50% of the installed shaft power is used to drive a submarine up to 80% of its top speed. The remaining 50% is used to for the last 20% of speed[21]. By de-coupling the propeller speed from the turbine speed, a single turbine, operating at high efficiency, can be utilized at cruising speeds. If higher sprint speeds are necessary, the second turbine can be brought on-line. In a nuclear powered submarine, this translates to longer operational time between refueling with a corresponding savings in the overall operational cost of the platform.

1.1.4 Engine Room Arrangement

In mechanical drive propulsion systems, the components must be installed in the submarine sequentially and with their axes of rotation aligned. This involves extremely high manufacturing tolerances to ensure smooth operation of the installed components, which increases the manufacturing and assembly costs of the submarine. Further, the required stack length, or combined lengths of the different components connected in series, complicates the submarine design and limits the

---

[1]Notional submarine uses include: Electric launching of torpedoes and other unmanned vehicles, pulsed energy weapons such as lasers and electromagnetic energy and kinetic projectile launchers, to name a few.

available space and flexibility the naval engineer has in arranging the necessary (and desired) equipment within a submarine design. An electric drive propulsion system, however, can be arranged flexibly within a given compartment. The prime movers and the propulsion motor need not be aligned, and are connected to each other with high power cabling which will require lesser manufacturing and assembly tolerance. A point paper and submarine design by Dade[22] evaluated the possible design impacts and potential benefits of integrating the propulsion and electrical power generation systems.

1.2 Candidate Electric Propulsion Motors

A broad search of open source literature was conducted to determine the best suited propulsion motor options for submarines. There are five generally accepted electric propulsion motor options for ship application [2] [23]: synchronous motors, induction motors, permanent magnet motors, superconducting synchronous motors and superconducting homopolar motors, all of which generate sufficient shaft power for submarine use. The first two, the synchronous motor and induction motor, are prevalent in industry and the electrical designs are well known and understood. However, for the shaft power required in a high power submarine, these two machines are prohibitively large for installation within a submarine hull form. Further, they have considerably larger vibrational harmonics that cause them to run loudly, more so than the reduction gearing they would be replacing in a submarine. That leaves the permanent magnet, superconducting synchronous and superconducting homopolar motors, which are the motors evaluated in this thesis.

1.3 Future Benefits of Electric Propulsion

A long term benefit of utilizing electric propulsion motors in nuclear powered submarines is the possibility of removing the steam system and replacing it with direct conversion technologies. The steam system (see Figure 1-3) consists of feed water storage, feed piping and pumps, steam boilers, steam piping and valves, steam turbines and condensers, as well as a seawater cooling system to condense the steam back to feed water. The steam system is one of the larger maintenance burdens on the submarine's crew. Hundreds of steam valves are needed to properly direct the steam throughout the engine room, all of which need constant preventative and corrective maintenance.

18

Numerous spare valves, gaskets and tools must also be carried on board to maintain the steam valves.
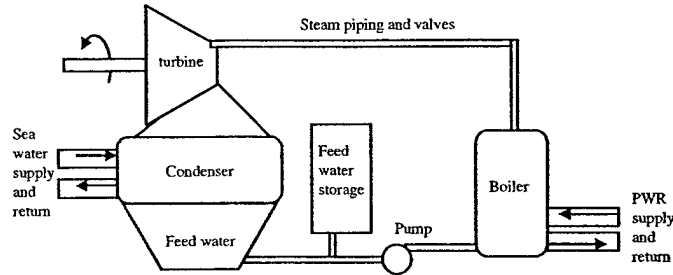
Figure 1-3: Rankine steam cycle.

Utilizing electric propulsion motors, direct conversion technologies can be used in place of a complex steam system. Thermoelectric and thermionic cells can produce electricity directly from a heat differential. By directly coupling the direct conversion electrical cells to the electric propulsion motor, the entire steam system can be eliminated. However, these technologies are just emerging and are beyond the scope of this thesis; therefore the removal of the steam system is not further developed.

Chapter 2

Baseline Submarine

In Chapter 1, the potential benefits of electric propulsion motors are discussed. In order to evaluate the actual benefits of electric propulsion motors, a benchmark or baseline design is needed for comparison. A baseline submarine design was developed in conjunction with a separate design project. The detailed design can be found in [21]. The summary of the baseline mechanical drive submarine developed is discussed below.

2.1 Submarine Design Summary

The main design objective of the baseline submarine, as defined in the mission need statement of the year long design project, was to enable a rapidly re-configurable submarine platform which could incorporate new technologies and developments as they evolved. To achieve these objectives, a module section consisting of three 20 ft×20 ft module bays was inserted in the center section of a modern submarine hull form (See Figures 2-1 to 2-2). The specifications of the resulting submarine are given in Table 2.1.

The propulsion power plant is a pressurized water reactor (PWR). The heat generated from the reactor core is used to create saturated steam. The steam is piped into the engine room where it drives the turbines for both the electrical power generation (7200 kW) and for the propulsion engines (28, 100 SHP, or roughly 21 MW).

A modern submarine propulsion propeller is most efficient at relatively slow revolutions per minute (rpm), while the efficiency of a steam turbine is best at much higher rpm. Thus, the
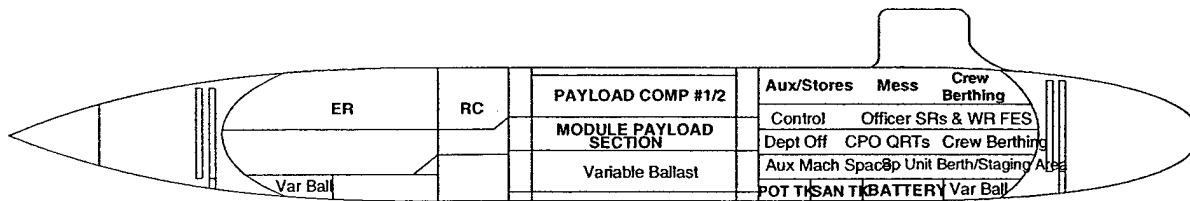
Figure 2-1: Baseline ships profile view.

Table 2.1: Baseline Design Summary.

Parameter	Baseline Design
Displacement (surfaced)	8499 ltons
Displacement (submerged)	9562 ltons
Length	372.4 ft
Diameter	40 ft
SSTG's (combined)	7200 kW
Payload Section Length	64 ft
Propulsion Motor Power (combined)	28,100 shp
Speed (submerged)	28.08 kts
Endurance Range	90 days
Complement	100

steam turbines are coupled to the propulsion shaft through a set of reduction gears. In the baseline submarine, the propeller rotates at 140 rpm and the steam turbines rotate at 3600 rpm. To achieve the desired reduction, a double reduction gear is used. The size and weight of the reduction gears, turbines and electrical generators is calculated in Appendix B[1] and summarized in Table 2.2.

Table 2.2: Summary of Baseline Mechanical Drive Train

	units	Reduction gear	Propulsion turbines (2)	Electrical turbines (2)	Electrical generators (2)
Weight	ltons/tonnes	89.3/90.7	41/41.7	33.3/33.8	26.8/27.2
Diameter	ft/m	12.3/3.8	5/1.5	4/1.2	4/1.2
Length	ft/m	8.5/2.6	12/3.7	8/2.4	6/1.8
Volume	ft^3/m^3	1017/28.8	471/13.3	201/5.7	192/5.4

Shown in Figure 2-3 is a notional engine room section for the baseline mechanical drive sub-

---

[1]Uses data and equations from [24] and [25]. The baseline electrical generators are each assumed to be 6ft×4ft×4ft cubes with an average density of 5000 kg/m^3
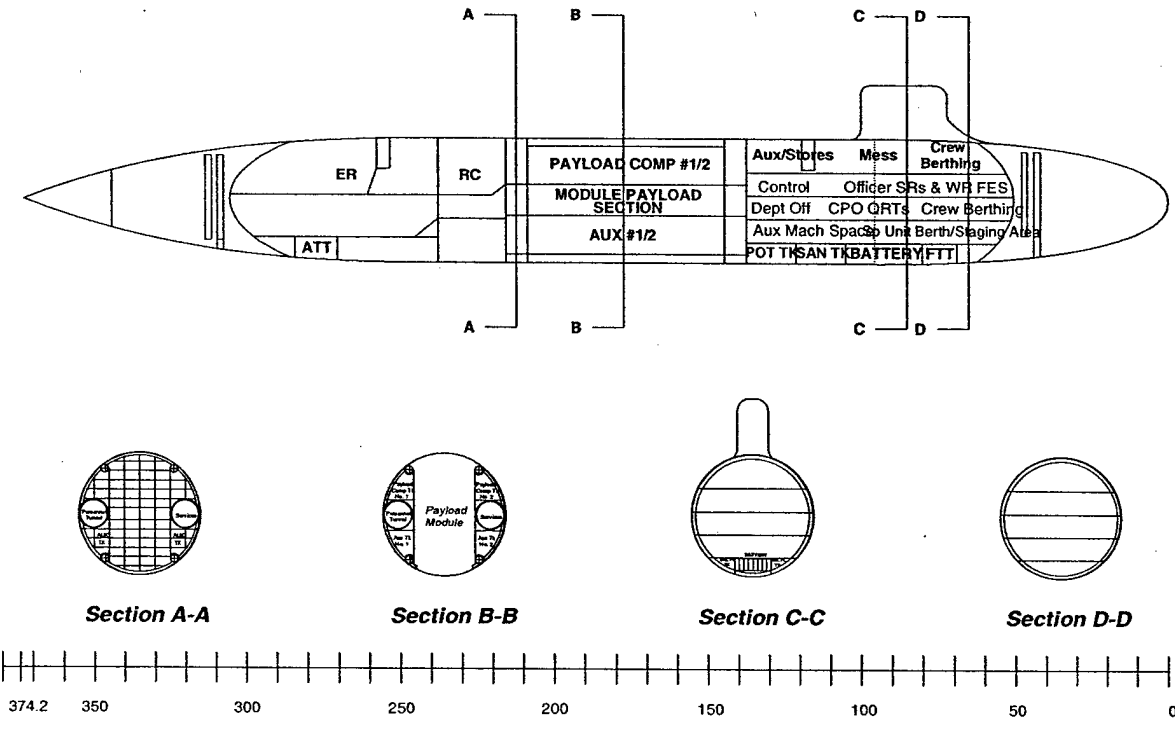
Figure 2-2: Baseline ship's arrangement drawings (profile view with selected sectional views).

marine. The propulsion turbines and reduction gearing are just above and aft of the cylindrical main condenser. The ship's service turbine generators (SSTG) are just above and forward of the main condenser. These are the items that will hopefully be made more functionally power dense through electric propulsion.

For the electric propulsion motor based system to be a worthwhile alternative it needs to have attributes that exceed the baseline mechanical drive train. At the very least, the electric motor, converter and controls and high speed turbine generators should deliver equal power, yet be smaller, lighter and quieter.

In subsequent chapters, several electric propulsion motor alternatives are evaluated in detail. In an effort to reduce the noise induced by the submarine propeller, the shaft rpm also needs to be reduced. Therefore a nominal 100 rpm will be the target speed for the electric motor propulsion

system. In order to evaluate them, each electric motor design, along with the necessary electric power generator, converter and motor controls, will be compared to the 140 rpm mechanical drive train data in Table 2.2.

Assuming that the electric propulsion based system's attributes, including weight, volume geometry and efficiency, are better than the baseline mechanical based system, a true potential will be realized.
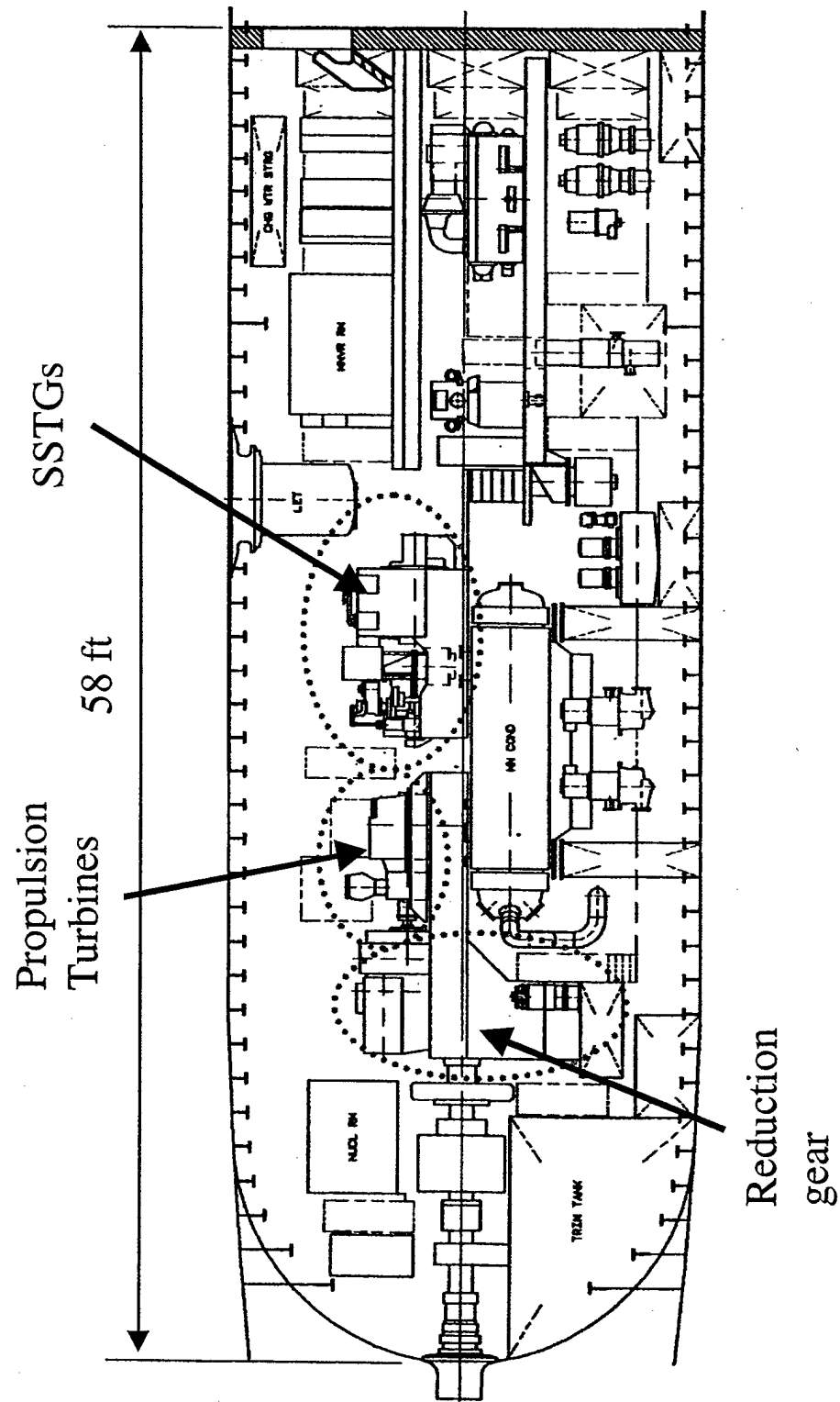
Figure 2-3: Engine room arrangement drawing for a PWR mechanical drive submarine (profile view), scanned image from [22].

Chapter 3

Relevant Electric Motor Attributes

In order to determine which design, within in a given range, is better than the others, the relevant attributes to be compared must first be determined. The relevant attributes are by nature strongly dependant upon the intended use of the design itself. In electric motor design, for example, an industrial manufacturing facility may not deem the motor's diameter to be of significance. There is abundant space inside a land based customer facility for a large, cumbersome electric motor that never moves. However, in a naval submarine, space and volume are at a premium. Ever increasing demand is placed on program managers to maximize the percentage of a submarines's war fighting capability. This translates to maximizing the payload that can be carried on board. Therefore, the smallest electrical motor, both in volume and footprint, is extremely important for the naval submarine designer.

3.1 Specific Navy Needs

As already discussed, size is important. Other desired attributes for a submarine, which may not be important for another customer, include weight, reliability, graceful degradation, noise level, efficiency and resistance to mechanical shock, as well as the ever important bottom line: cost. The cost here is not just the purchase price or acquisition cost, but is the life cycle cost (LCC). LCC is the overall cost of the system, from design to disposal. It involves the day to day operation of the motor, the fuel costs, maintenance and supply costs, as well as the disposal costs if necessary.

Of these, some are easily determined. The volume and weight of the motor will be determined

in the first order design process outlined in subsequent chapters. Others, such as cost, can be partly determined. The cost of the raw materials, for instance, can be determined. Finally, attributes such as noise and reliability are best evaluated later in development. A rough estimate can of course be drawn from reasonable engineering arguments. However, the design will need to be tested and will evolve in development.

3.2 Attribute Selection

The attributes to be considered and how they will be evaluated are discussed in this section.

3.2.1 Weight (Buoyancy and Balance)

In submarine design, a careful balance between the ships total envelope volume, or displacement, and the internal weight distribution of the ship is maintained.

First, the submarine must be made neutrally buoyant when submerged. Submarines are designed with reserve bouyancy for future modifications and for possible design errors. Permanetly mounted "margin" lead ballast is used to maintain the submarine's weight balance. In order to change systems on board the submarine, the weight change must be calculated and compensated by adding or removing "margin" lead.

The longitudinal center of gravity is carefully controlled in order to maintain the submarine at a level attitude while submerged. Unlike a surface ship, the submarine does not have a large waterplane area to counteract shifts or changes in weight distribution. Rather, the buoyancy of the hull and variable ballast seawater tanks are used to counteract the gravitational force of the weights within the hull. Complicating this is the fact that submarine hulls have evolved into a tear drop hull form in order to minimize the drag forces on the hull and maximize their speed at a given volume. The detrimental effect of this is that the displacement of the hull in the after section of the submarine is considerably less than in the forward sections. This is precisely where the bulky and heavy reduction gearing is located. To counteract the resulting large aft moment, large amounts of "stability" lead ballast are permanently added to the forward section of the ship.

For the above reasons, the addition of weight within a submarine is carefully controlled. Lighter electric propulsion motor systems, used in place of mechanical reduction gear systems, would greatly

ease the placement of lead ballasting on board.

3.2.2 Length and Diameter

Length, diameter and geometry define the volume and the space allocated to the propulsion motor. There is a finite amount of deck space available to mount equipment and house the crew within a cylindrical hull form. Also, certain pieces of equipment must be installed in the submarine in line. For example, the shaft, thrust bearing, reduction gearing and steam turbine all must be connected in series. For these reasons, the length and diameter will be evaluated as relevant attributes of the electric motors.

3.2.3 Efficiency

The efficiency of the propulsion drive train directly affects the naval ship designer's ability to size the propulsion plant. In order for the submarine to achieve a desired mission speed, a given amount of shaft torque must be supplied to the propeller. The electric propulsion motor must supply the shaft torque plus any losses in the shafting. Efficiency losses in the motors will directly affect the required size and weight of the prime movers, the turbines, as well as the total power which must be supplied by the pressurized water reactor (PWR). All of the combined losses directly contribute to the necessary size and weight of the PWR, as well as the useful lifetime of the reactor core itself, with a corresponding reduction in the amount of time the submarine will have between refueling of the reactor core. The size and weight of the PWR must also be factored into buoyancy and center of gravity issues described in 3.2.1 and 3.2.2. Therefore, the efficiency will be evaluated as a relevant attribute of the electric motors

3.2.4 Harmonics

The primary mission of the naval submarine is to remain undetected and covert. Any vibrational radiation emanating from the submarine has the potential to give the submarine's presence, or even location, away, rendering the primary mission capability impossible. As discussed in chapter 2, the current reduction gear technology has evolved as gears about as quiet as they can be. Thus, in order for an electric motor to be considered in place of the reduction gears, it must operate with a comparable or better level of vibration. However, this is one of the attributes of an electric motor

that is difficult to quantify during the early design phase since it is usually analyzed with small scale prototype motors and doesn't scale well to full size. An engineering qualitative analysis will be made to determine the expected harmonics created by the electric propulsion motors.

3.2.5 Converter

The power converter and motor controller are features that must be added to the submarine to facilitate electric drive propulsion. They are necessary in order to convert the supplied power from the ship's propulsion electric generators to the required power needed by the electric motor for a torque. For a synchronous motor, this will require a variable voltage and frequency motor. For a DC motor it will require a variable voltage or current source. In order for the propeller to be reversed for slowing, stopping and backing, the phase rotation, supplied to the AC synchronous motor, will need to be reversible as well. The enabling technology to allow this is power semi-conductor switches. However, in order to reduce the level of electrical harmonics they induce, large filtering reactive elements are required. Thus, for a high power power converter, the size and weight must be evaluated along with the electric motor.

3.2.6 Reliability

In any piece of equipment used in a military application, the reliability is a concern. In the propulsion motor of a PWR submarine this concern is even higher. The submarine must have propulsion power available at all times. The reliability of the electric motor, its power converter and its support systems must be at an optimum to enable it to safely and efficiently carry out its mission. Reliability issues need to be addressed and evaluated for each electric motor design.

3.2.7 Degradation

Degradation is the ability of the electric motor to continue operating, albeit at a lower power level, when there is a failure of one of its systems. If something does fail, for whatever reason, some minimal amount of propulsion power is desired in order for the submarine to continue its mission, at least in a degraded capacity. At the very least, the submarine must be able to transit out of harm's way and back to port for repairs. The ability of the electric propulsion motor to continue operating in a degraded condition will be evaluated.

3.2.8 Torque

The output torque is important for quick and responsive maneuvering of the submarine. The torque for each propulsion motor at rated speed will be calculated to ensure adequate power output. However, the propulsion motor must also have high torque at all speeds in order to deliver adequate acceleration for the submarine to perform its many missions successfully. A propulsion motor with poor torque characteristics will render the submarine sluggish and hard to maneuver. Therefore, the torque characteristics of the motors at all other speeds will be qualitatively evaluated.

3.2.9 Risk

Risk is the amount of uncertainty in the feasibility of a design. This includes the developing and foreseen technologies expected to enable the design to function as desired. It also involves the current state of technology for the design itself. An immature technology will need to be validated in small steps in order to convince program managers to incorporate it in a ship design. This validation process involves proof-of-concept testing. Normally, several sub-scale designs of increasing complexity are built and proof-of-concept testing is performed on each to validate the engineering calculations. The actual feasibility of the design will become more and more apparent as the proof-of-concept testing progresses. However, until the final testing is completed there will be some risk associated with the design. The risk involved with each motor candidate can be qualitatively evaluated by the state of the individual components as well as the current state of proof-of-concept testing for each concept.

Chapter 4

Optimization Routine

In chapters 5,6 and 7, the selected motor candidates for submarine application are described and the process in which a defining set of input motor parameters is transformed into the motor's qualitative attributes is outlined. In this chapter, the method used to determine the input parameters and to evaluate the relative "goodness" of the resulting attributes is described.

4.1   Multi-Attribute Dominance

To determine the best out of a set of designs, it is not enough to say that the lightest or the cheapest or the smallest is best, since single attributes rarely distinguish overall design goodness. All of the attributes of two motors must be compared to each other, and the design with the best *overall* combination of attributes will be determined to be the best, or dominant, motor design. The motor which is inferior, or dominated, should not be considered further. However, the dominant motor is not necessarily the *most* dominant design. Several other permutations of parameters should be evaluated to determine if a better motor design can be obtained. An engineer can of course accomplish this multi-attribute evaluation of motors, but it would necessitate constant input to vary the motor's design parameters and perform the pair-wise comparisons of the resulting attributes. Both would be tedious and laborious.

A computer algorithm is used to replace the engineer in the loop. The parameters that comprise a given motor design are determined by a computer program. A separate evaluation program is then used to determine if the given set of parameters describes a motor that has at least a minimum

set of performance characteristics. If so, the attributes of the resulting motor are determined and returned for comparison to a stored set of attributes in the design space.

4.2 Parameter Selection

Each motor design has a set of design parameters (rotor radius, rotor length etc.), which fully describes the construction of the motor. The design parameters are determined through a combination of random and deterministic search techniques. A parent design set of parameters is altered, within a given upper and lower bound, to create a new set of parameters. The amount of deviation away from the given parent parameter is determined by random selection within a normal distribution set with its mean value shifted to that of the parent parameter value and variance scaled up to the range of the upper and lower bound. The random number taken from this distribution set is completely random, a "roll of the dice."

The parameter generation process is deterministic in that the defining parameter space is ever decreasing. Each time a motor design is determined to dominate a previous design, the parameters of the dominant motor are saved as the new parent parameters, from which new motor parameters will be created. Also, the variance of the parameter distribution is reduced by a pre-determined amount. Thus, in time the entire parameter space will be searched. However, the parameter sub-space defining the most dominant motor designs will be searched the most heavily

The parameter selection and pair-wise comparison routines are integrated into an algorithm program called NDAxxx. The structure of this algorithm is based on the Novice Design Assistant (NDA) developed by Moses et al. [6] and [27]. A program call for attributexxx is imbedded into each to evaluate the motor's attributes. The specific programs used for each motor topology can be found in Appendices G, H and I.

4.3 Overall Measure of Effectiveness (OMOE)

Given a design space populated by the dominant motor designs, there are several decision making methods available to determine which design is best (See Whitcomb [26]). For the design attributes of the electric propulsion motors developed in this thesis, a scaled and weighted sum of the motor's attributes is used, similar to Whitcomb's Multiattribute Utility Analysis (MUA). The particular

31

formulation of the chosen design decision making method follows.

Each attribute (length, weight etc.) is given a goal and a threshold value. The actual range of attribute values is set as the attribute design space. The attribute with the lowest value is set as the threshold value and the largest value is set as the goal. For example, the lightest motor's weight is used as the goal weight and the heaviest motor's weight is used as the threshold weight. Each motor is given an OMOE score. The OMOE is calculated by comparing the individual motor's attributes to the goal and threshold values. An individual $OMOE_i$ score of between 0.0 and 1.0 is assigned to each attribute, based on the objective function of the attribute (4.1). The scores from each attribute are multiplied by a weighting factor.

The individual weighting factors are developed by ranking the individual attribute's importance against one another and then normalizing their sum. For the purposes of this thesis, the attributes were all given a relative importance of one. However, the relative importance of the attributes can be easily adjusted, within the OMOExxx computer code, given a particular customer's desires.

The motor OMOE is then the sum of the individual $OMOE_i$ attribute scores. Because the weighting factors sum to 1.0, the maximum possible score for the OMOE is 1.0. This process is shown in Equation 4.2.

$$OMOE_i = \frac{X - X_T}{X_G - X_T} \qquad (4.1)$$

$$OMOE = \sum \frac{X - X_T}{X_G - X_T} * w_X \qquad (4.2)$$

where

T = threshold

G = goal

w = weight fraction

X = attribute (weight, length, diameter volume and efficiency)

The individual motor OMOE's are then plotted against their respective costs. The result is a Pareto chart, a visual indication of which motor has the best attributes for the least cost. A trade-

off between how much OMOE is desired against how much it costs can now be made. Unfortunately, since the motor cost is purely a material weight based model and the OMOE's objective function is weighted towards the smallest and lightest motors, the motors with the highest OMOE, by definition, have the lowest cost (see appendix C, D and E). However, if an additional cost analysis tool was developed and included, such as the labor cost to manufacture superconducting field coils and large copper drums, than the OMOE analysis may show something else entirely.

In addition to the quantitative OMOE results above, a qualitative analysis is made with regard to the other motor attributes discussed in chapter 3. The "best motor" should have the best overall combination of weighted size, weight and efficiency. However, it should also have better qualitative attributes. These include the motor's vibrational harmonic signatures that need to be isolated from the submarine's surrounding environment, electrical harmonics that can be reflected onto the distribution bus and interfere with electronic equipment operation and the torque output, which needs to be high at all propeller speeds for maneuverability.

Chapter 5

Surface Mount Permanent Magnet Motor (SMPM)

5.1 Design Overview

The surface mounted permanent magnet motor (SMPM) is a synchronous type motor. The magnetic flux of the permanent magnets B_r interact with the sinusoidal current through the Lorentz force $\vec{F} = \vec{J} \times \vec{B}$, imparting a torque on the rotor. Shown in Figure 5-1 is a crude illustration of a four pole rotor, $p = 2$, within a twelve slot stator.
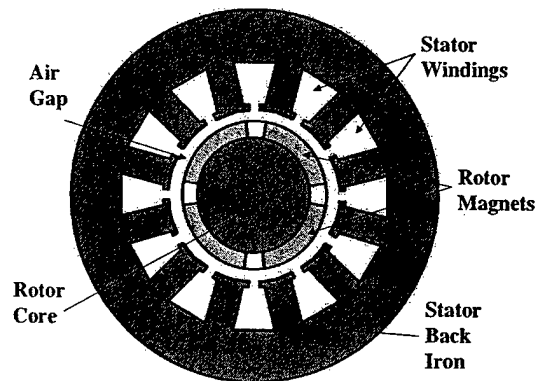
Figure 5-1: SMPM motor axial view showing twelve stator slots and two pole pairs.

The motor characteristics are solved for using a lumped element method where the structure

and mechanical composition of the motor is used to define equivalent electrical circuit lumped elements. The lumped elements are then used to evaluate the characteristics of the motor.

To solve for the lumped elements, *Maxwell's* equations in their magneto-quasi-static form are employed[1].

The governing equation is the magnetomotive force (mmf) (5.1)

$$mmf = \mathrm{Ni} = \oint H \cdot dl \tag{5.1}$$

However, in the presence of discrete coils, the mmf, as well as the majority of the characteristics of the motor are described by a square wave with Fourier series components of the form (5.2):

$$\sum_{n=1,3,5,7,...}^{\infty} \frac{4}{n\pi} \sin(n\omega t) \tag{5.2}$$

From mmf, the other characteristic properties of the lumped elements can be found through their constituent relationships (5.3).

$$\text{magnetic flux} \quad = \quad \phi = \frac{mmf}{\text{Reluctance}} \tag{5.3}$$

$$\text{flux linkage} \quad = \quad \lambda = N\phi \tag{5.4}$$

$$\text{induced voltage} \quad = \quad Eaf = \frac{d\lambda}{dt} \tag{5.5}$$

$$\text{Inductance} \quad = \quad L = \frac{\lambda}{i} \tag{5.6}$$

5.2 Design Parameters

The variable design parameters used to generate an SMPM motor are given in Tables 5.1 and 5.2. Table 5.1 gives the continuously varying inputs and Table 5.2 gives the variables that vary by integer steps. For the continuous variables, an upper and lower bound is defined. The deviation value is that amount which is multiplied by a random number generated from a normal distribution[2],

---

[1]magneto-quasi-static means that the displacement-current terms in *Maxwell's* equations will be neglected.

[2]Normal distribution is the set of real numbers with mean zero and variance one.

scaled and shifted, which is then added to the parent design variable.

Table 5.1: SMPM Design Parameters, Continuous Variables

Design Parameter	Symbol	Lower limit	Upper limit	Deviation	units
Rotor radius	r	.1	1.5	.7	m
Air-gap thickness	g	.1	10	5	cm
Magnet thickness	hm	1	50	25	cm
Rotor active length	l	.2	4	1.9	m
Stator tooth width	wt	1	10	5	cm
Slot depth ratio $\left(\frac{hs}{r}\right)$	fsd	.001	1	.5	

Table 5.2: SMPM Design Parameters, Integer Variables

Design Parameter	Symbol	Upper limit
Pole pairs	p	15
Slots per pole per phase	m	5
Slots short pitched	nsp	4
Turns per coil	nc	5
Number of phases	q	15

It should be noted that the design code does randomly generates a phase number q for the machine, allowing for a maximum of 15 phases. However, this feature is disabled for this thesis. Several difficulties arise in evaluating, comparing and ranking multiple motor designs with varying phase numbers. Some of the difficulties are:

- The size of the required controllers vary with the motor's phase number.

- The reliability of the motors is proportional to the complexity of the winding scheme.

- The possible degraded operating modes are affected by the number of phases that can be secured in a fault.

The ranking and evaluation scheme necessary to evaluate these differences is not developed in this thesis.

In order to eliminate the ambiguity between varying phase numbers and to maximize the degraded operating modes, 15 phases is chosen. This allows normal operation with 15 phases and

two degraded modes of operation with either 10 or 5 balanced phases in the event one or more phases fail. Setting the phase number to 15 also determines the required size of the power converter necessary to drive the motor (Chapter 8). Therefore, in the genetic variable generation and optimization code, NDA, of appendices G and H, the phase number is reassigned a value of 15 for every group of variables generated.

5.3 Constraints

Imposed physical constraints are given in Table 5.3. Those marked (*) are the actual levels used in the design.

Table 5.3: SMPM Constraints

Design constraint	Symbol	Value	Units
*Rotor speed	rpm	100	rpm
*Required minimum output power	Preq	21	MW
Maximum AC voltage applied	Vll	4160	ADC
*Copper conductivity	siga(σ)	5.917e7	1/(Ωm)
Max copper current density	Jalim	150	A/cm^2
*Max iron flux density	Bisat	1.2	T
*Magnet remanent flux density	Br	1.29	T
*Power factor	psi	1	

Additionally, several other design constraints are imposed throughout the design process to insure that the motor parts will actually fit together and material properties are not exceeded. If a design constraint is violated, the design loop is terminated and a new set of design parameters is generated. Constraints include:

1. The thickness of the stator teeth are checked to avoid magnetic saturation.

2. The circumference of the stator is verified to be not more than 60% magnetic steel teeth to insure adequate space factor for armature windings.

3. The resulting power output of the motor is checked to insure that at least the minimum required power is attained.

4. To insure adequate cooling to the stator coils, the slot packing factor, λ_a (lama in computer code) is limited to .60, and the allowed stator current density $Jalim$ is limited to 150 A/cm^2.

37

5. Although relatively slow speed motors are being evaluated, the tangential speed of the rotor magnets are verified below an a priori limit of 230 m/s to insure that special mounting, such as external strapping, is not required to retain the magnets to the rotor. By simply changing the constraint on rotor rpm, much faster, and thus smaller, motors could be evaluated.

6. The operating power factor is set to 1.0. This insures that the motor operates relatively close to the expected supply from a solid state power converter.

5.4 Generate Geometry

The majority of the geometry has been defined above. Some of the normally referenced values need to be calculated in order to use the classic synchronous machine equations given in Kirtley's lecture notes [27] and in Fitzgerald et al. [28]. For instance, the number of slots in the stator n_s is the product of phase number q slots per pole per phase m and number of poles $2p$. Other machine parameters determined are: n_a, the number of armature turns per phase (5.8); hs, the armature slot depth (5.9); $lamt$, the stator tooth fraction with respect to the annular stator area (5.10); and wst and wsb, the widths at the top and bottom of the slot, respectively (5.11,5.12).

$$n_s = 2qmp \tag{5.7}$$

$$n_a = 2mpnc \tag{5.8}$$

$$hs = f_{sd}r \tag{5.9}$$

$$lamt = \frac{n_s w_t}{2\pi(r + g + hd)} \tag{5.10}$$

$$wst = \frac{2\pi(r + g + hd)(1 - lamt)}{ns} \tag{5.11}$$

$$wsb = wst\frac{r + g + hd + hs}{r + g + hd} \tag{5.12}$$

5.5 Winding Factors

Shown in Figure 5-2 is part of a stator which has been laid out flat for ease of discussion. It is a three phase winding with twelve stator slots and two coils per each phase located in adjacent slots. This is a full pitch winding, so the slot spacing between the axial wraps of a given coil is six.
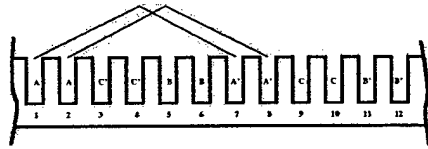
Figure 5-2: Full-pitched winding showing three phases in twelve slots. Each phase consists of two coils wrapped around six stator teeth.

Windings are not necessarily wound "full-pitched". This is for a variety of reasons including reduced harmonics and reduced end turn length. Shown in Figure 5-3 is a five-sixths-pitched winding in which the coils of each phase are staggered so that they span only five stator teeth instead of six, as in the full-pitched winding. This softens the normally square shape of the stator magnetic field, reducing the resulting harmonics. Also, since the end turns only wrap around five teeth, the overall end turn length is reduced.
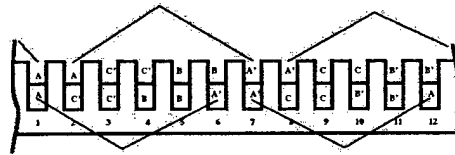
Figure 5-3: Five-sixths-pitched winding showing three phases in twelve slots. Each phase consists of four coils each wrapped around five stator teeth

The ratio of the actual flux linkage to that which could be obtained by a "full-pitched" winding is the winding factor:

$$k_w = \frac{\lambda_{actual}}{\lambda_{full-pitch}} \tag{5.13}$$

or, mathematically, as defined by Kirtley [27], using the product of two winding factors:

$$k_{wn} = k_{pn}k_{bn} \tag{5.14}$$

Where k_{pn} is the pitch factor which corrects for windings placed less than π electrical radians

39

apart as shown in Figure 5-4 and is given by equation 5.15, n is the Fourier series components that mathematically describe the square wave developed inside the stator.
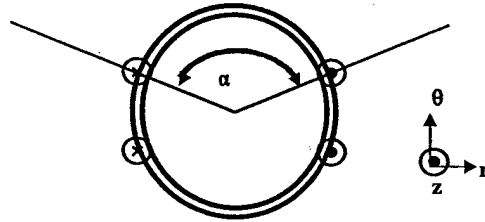
Figure 5-4: Short-pitched coils showing azimuthal angle extent, α, of individual coil which is less than the full pitched angle of π.

$$k_{pn} = \sin \frac{n\alpha}{2} \tag{5.15}$$

k_{bn} is the breadth factor which corrects for the fact that the armature windings are not spread uniformly along the circumference of the stator, but are placed in discrete coils inside stator slots as shown in Figure 5-5 and given by equation 5.16.
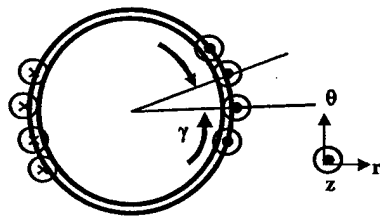
Figure 5-5: Distributed coils showing the physical angle, γ, between m adjacent coils.

$$k_{bn} = \frac{\sin \frac{nm\gamma}{2}}{m \sin \frac{n\gamma}{2}} \tag{5.16}$$

For the purposes of finding torque production and sizing of the motor, the space fundamental component is used to simplify the algebra ($n = 1$). Typically, the next harmonic torque magnitude

is only a small fraction of the fundamental. Although this will not significantly change the sizing of the motor, it will have a large effect on the noise and vibrations created by the machine and is discussed in more detail in chapters 8 and 9.

5.6 Magnetic Fields

The magnetic field at the surface of the magnetic gap is given by (5.17). This is a Fourier series representation of the magnetic field produced by discrete magnets on the surface of the rotor as defined by Kirtley's class notes [27].

$$B = \sum_{n=1,3,5,\dots}^{\infty} B_r \frac{4}{n\pi} \sin \frac{n p \theta_{wf}}{2} k_g \tag{5.17}$$

Where B_r is the permanent magnet's remanent flux density[3], θ_{wf} is the magnet angle and k_g is a factor that describes the magnet gap geometry given by equations 5.18 and 5.19. By choosing an electrical magnetic angle, $(\theta_{wfe} = p\theta_{wf})$, of $\frac{2\pi}{3}$, the third harmonic in this Fourier series is cancelled.

$$k_g = \frac{R_i^{p-1}}{R_s^{2p} - R_i^{2p}} \left(\frac{p}{p+1} \left(R_2^{p+1} - R_1^{p+1} \right) + \frac{p}{p-1} R_s^{2p} \left(R_1^{1-p} - R_2^{1-p} \right) \right) \quad , p \neq 1 \tag{5.18}$$

$$k_g = \frac{1}{R_s^2 - R_i^2} \left(\frac{1}{2} \left(R_2^2 - R_1^2 \right) + R_s^2 \log \frac{R_2}{R_1} \right) \quad , p = 1 \tag{5.19}$$

where R_s and R_i are the outer and inner magnetic boundaries, respectively, and R_2 and R_1 are the outer and inner boundaries of the magnets. Again, only the space fundamental component is used here. The required thickness of the flux return shield d_c can be calculated assuming operating at the designed maximum $B_{isat}(rms)$ value. (5.20)

$$d_c = \frac{B}{\sqrt{2}B_{isat}(rms)} \frac{r}{p} \tag{5.20}$$

---

[3]Assumed value of 1.29 Teslas is used. Current Neodymium-iron-boron magnets are approximately this strength. In the 2020 time frame, when electric drives in submarines will be a reality, this value will be readily available.

5.7 Flux Linkage and Internal Voltage

The space fundamental magnetic flux density, B_1, is used to find the magnitude of the sinusoidal flux linkage between the stator and the rotor utilizing

$$\lambda_f = \sum_{n=1,3,5,\dots}^{\infty} \frac{2RlB_nN_ak_{wn}}{p} \tag{5.21}$$

The magnitude of the speed voltage, or electromotive force, is the time derivative of flux linkage:

$$\begin{aligned} E_{af} &= \frac{d\lambda_f}{dt} = \omega\lambda_f \\ E_{afRMS} &= \frac{\omega\lambda_f}{\sqrt{2}} \end{aligned} \tag{5.22}$$

5.8 Estimation of End Turn Lengths

The stator wire must wrap around the ends of the stator laminations to complete each turn. The length of wire in the end turns will affect the total armature resistance as well as the overall size, weight and cost of the motor. The length of end turn wire is calculated with the assistance of an oblique view of the stator windings (Figure 5-6). The stator windings must cover a linear distance L_{az} from one stator slot to the next as shown in Figure 5-7. The winding area is assumed to remain constant as it departs and enters stator slots. However, the windings must also allow clearance for adjacent windings (Figure 5-8). The necessary winding departure angle is shown in Figure 5-9. The winding is estimated to follow this path for half of the linear distance between slots, it then mirrors the exit path into the next slot. The resulting increase in stator length l_{e1} as well as end turn length l_{e2} is given by equations 5.23 and 5.24 respectively.

$$\begin{aligned} le1 &= laz\tan(\theta) \end{aligned} \tag{5.23}$$

$$\begin{aligned} le2 &= laz/\cos(\theta) \end{aligned} \tag{5.24}$$
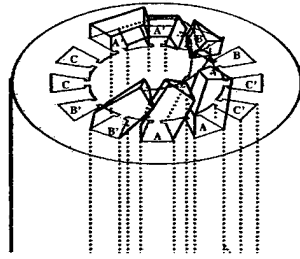
Figure 5-6: End turn winding arrangement. Showing angle of departure as windings move towards next slot opening and over adjacent windings.
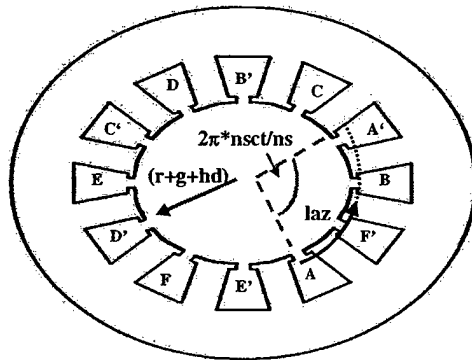
Figure 5-7: End turn required azimuthal traverse, l_{az}, slot to slot

5.9 Synchronous Reactance and Resistance

The synchronous reactance is comprised mostly of the air gap inductance and the slot leakage inductance. The inductance due to the end turns is neglected here. For this design, a round rotor design without saliency, the direct axis inductance is equal to the quadrature inductance, which is equal to the synchronous reactance. Thus;

$$X_s = \Omega(L_{ag} + L_{slot}) \tag{5.25}$$

Where the fundamental air gap inductance, L_{ag},(equation 5.26) is derived in Kirtley's 6.685 class notes [27].
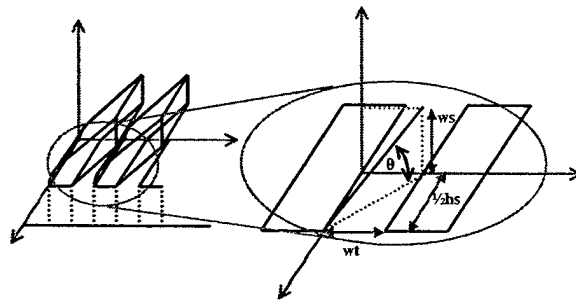
Figure 5-8: Armature winding departure path in slotted stator.
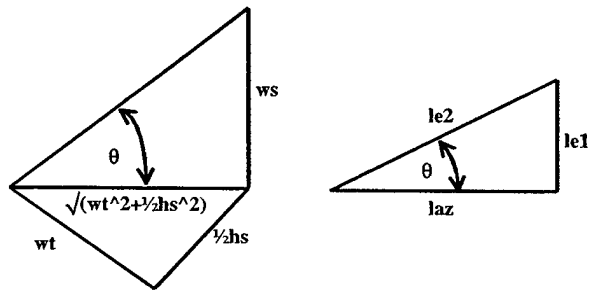
Figure 5-9: Armature winding departure angle in a slotted armature

$$L_{ag} = \sum_{n=1,5,7,\ldots}^{\infty} \frac{q}{2} \frac{4}{\pi} \frac{\mu_0 N^2 R l k_{wn}^2}{p^2(g+hm)} \tag{5.26}$$

The slot leakage is comprised of both the self and mutual inductance terms. These, too, are derived in [27].

$$L_{slot} = L_{as} + L_{am} \tag{5.27}$$

$$L_{as} = 2pl \left[(m - N_{sp}) (2N_c)^2 + 2N_{sp}N_c^2 \right] \tag{5.28}$$

44

$$L_{am} = 2plN_{sp}N_c^2 \tag{5.29}$$

Combining the slot self and mutual inductance and multiplying by the equivalent slot permeance per unit length yields the combined slot leakage equation 5.30. This equation holds true with two assumptions. The first is that the coil throw, or span between sides of a given coil, is $\frac{N_s}{2p} - N_{sp}$, where N_{sp} is the coil "short pitch" which describes the distribution of coils in the stator slots (Figure 5-3). Second, each phase belt overlaps no more than two other phases. This is true for a three phase machine, since there are at most two other phases, as well as for most other reasonable number of phases where the overlapped phases are simply the adjacent phases in sequence.

$$L_{slot} = 2pl\mathcal{P}N_c^2 \left(4m - N_{sp}\right) \tag{5.30}$$

$$\mathcal{P} = \mu_0 \left(\frac{1}{3}\frac{h_s}{w_s} + \frac{h_d}{w_d}\right) \tag{5.31}$$

where h_s , h_d , w_s and w_d are the slot dimensions for a simplified armature slot depicted in Figure 5-10.
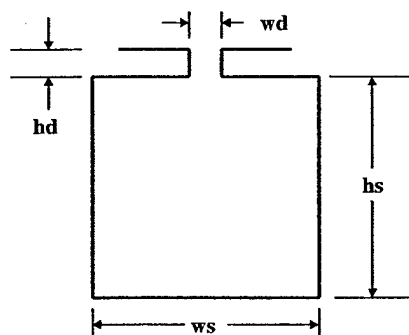
Figure 5-10: Single stator slot showing relative dimensions

The armature resistance is calculated using the total length of coil wire in the active section and in the end turns, along with the wire cross sectional area and the conductivity.

$$R_a = \frac{L_{ac}}{\sigma A_{ac}} \tag{5.32}$$

$$L_{ac} = 2N_a l + 2l_{e1} \tag{5.33}$$

$$Aac = \frac{A_{slot}\lambda_s}{2n_c} \tag{5.34}$$

5.10 Minimum Characteristics

There are a number of ways to determine the minimum output characteristics of a synchronous machine. One method, given a known minimum power, is to find the corresponding minimum armature current and the resulting terminal voltage and power factor. This method is described in section (5.10.1). Specifing the minimum current will converge on a motor solution, but leaves other variables in the total electrical system unconstrained, namely the terminal voltage and power factor. This method is better suited to solving the possible output voltage of a generator given a specified shaft power input. However, it is a quick way to determine the absolute minimum current required to generate a desired power and is used for a quick viability check of the motor.

A more constrained method in motor design is to specify a terminal voltage level and power factor, then determine the maximum output power. If a given motor design can generate at least a minimum output power requirement, then it is a viable design. This method leaves fewer variables unconstrained, enabling a more obvious comparison of machines. Further, given that output power is directly proportional to terminal voltage, this should converge faster on the most power dense machine. This method is described in section (5.10.2) and is the method utilized to determine the operating characteristics of the motor.

5.10.1 Minimum current for given power

The equation for power output in terms of armature current and rotor flux is given by equation 5.35, which is derived in chapter 4 of Kirtley [27].

$$P = -\frac{q}{2}p\omega\lambda_{af}I_a\sin(\delta_i) \tag{5.35}$$

The maximum output power for the minimum armature current occurs when the armature current is leading the rotor flux by 90°, as shown in Figure 5-11. In this situation, $\sin(\delta_i) = 0$, and

the armature current is entirely aligned with the quadrature or q axis. Thus, $\delta_i = -90°$.
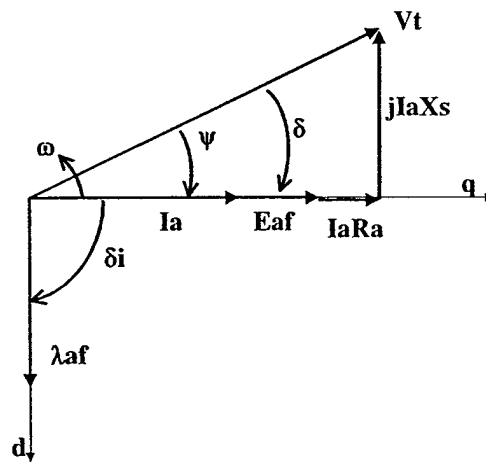
Figure 5-11: Synchronous phasor diagram at maximum power to current ratio. The armature current lays entirely on quadrature axis.

Rearranging equation 5.35 and solving for armature current yields (5.36).

$$I_a = \frac{2}{q}\frac{P}{p\omega\lambda_{af}} = I_q \qquad (5.36)$$

By Figure 5-11, the minimum required terminal voltage for required shaft power, including losses, can be solved for and thus compared to the available line voltage to determine if the motor is feasible.

$$V_t\angle\delta = E_{af}\angle 0° + I_a\angle 0°(R_a + jX_s) \qquad (5.37)$$

Of course, the power factor angle of this motor, $\cos(\psi)$, will not likely be the desired operating point. However, it does give some minimum criteria with which to simply evaluate the power characteristics of the given motor design. Regardless of what the actual torque angle or power factor is, equation 5.36 is the quadrature axis current required to develop the shaft power plus the non-electrical losses. This value will used again in equation 5.39.

5.10.2 Maximum power for given terminal voltage

The total real power drawn by the motor in Figures 5-12 and 5-13 is given by equation 5.38.

$$P = -\frac{q}{2}\frac{VtEaf}{Xd}\sin(\delta) \tag{5.38}$$

where q is the number of phases and E_{af} and V_t are peak values[4]. Rearranging (5.38) and solving
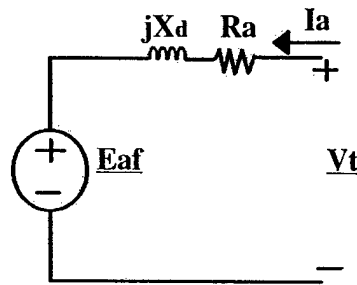
Figure 5-12: Equivalent circuit diagram for synchronous motor.
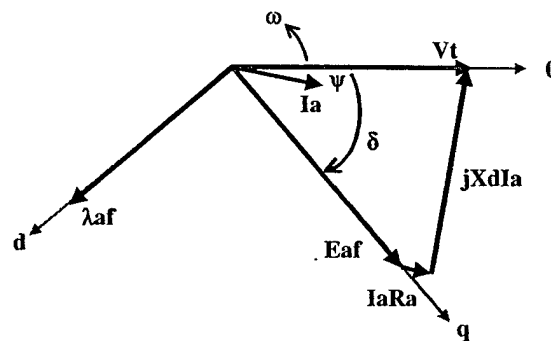
Figure 5-13: Synchronous motor phasor diagram, showing direct and quadrature axis and relative position of phasor quantities,

for the torque angle δ locates the relative angle of E_{af}. It also determines the angle between the armature current and generated voltage as $\delta - \psi$, where ψ is the desired operating power factor

---

[4]For a sinusoidal quantiy the rms value is $1/\sqrt{2}$ of the peak.

48

angle of the motor at its input terminals. Thus:

$$I_a = I_q / \cos(\delta - \psi) \tag{5.39}$$

As long as the resulting armature current density and the terminal voltage (5.40) remain below their respective set point, the motor is viable.

$$|V_t| = E_{af} \cos(\delta) + |I_a| R_a \tag{5.40}$$

5.11 Parameters at rated power

The required torque angle and armature current is determined in section 5.10.2. The motor's design parameters and operating armature current are used to determine the total losses and efficiency of the motor.

5.12 Losses

5.12.1 Windage Loss

The windage loss, although small in the slow speed, air cooled motor proposed here, is estimated using equation 5.41[27].

$$P_w = 2\pi R^4 \Omega^3 l \rho_{air} f \tag{5.41}$$

where f is the *friction factor* estimated as:

$$f = \frac{.0076}{R_n^{\frac{1}{4}}} \tag{5.42}$$

and R_n is the *Reynold's Number*:

$$R_n = \frac{\Omega R g}{\nu_{air}} \tag{5.43}$$

Although not analyzed in this design, the armature current density could be increased if the

49

cooling medium was water instead of air. The difference in the design program would be to use the specific heat capacity and density of water instead of air. This would of course increase the windage losses somewhat.

5.12.2 Ferromagnetic Losses

Hysteresis and eddy current losses in the back iron as well as the teeth are solved for semi-empirically using equation 5.44, determined in chapter 8 of Kirtley's class notes [27] and [29].

$$P_d = P_B \left(\frac{\omega_e}{\omega_B} \right)^{\epsilon_f} \left(\frac{B}{B_B} \right)^{\epsilon_b} \tag{5.44}$$

Where P_B is a base dissipation in watts per kilogram, ω_B and B_B are the base frequency and base flux, ϵ_f is the frequency exponent (varies from 1.3 to 1.6) and ϵ_b is the magnetic flux exponent (varies from 1.8 to 2.4).[5] The total iron mass in both the back iron and the teeth are determined, and the equation 5.44 is used to find the total core losses in the motor.

5.12.3 Joule Heating

The heating of the armature by joule heating losses is calculated using the armature current at maximum power for the motor. The so called I^2R loss is readily solved for given the armature current and total series resistance of the armature (5.32). The power loss due to joule heating is (5.45):

$$P_a = q I_a^2 R_a \tag{5.45}$$

5.12.4 Heat Removal

The losses derived thus far all contribute to heat production mechanisms internal to the motor.

$$P_{heat} = P_w + P_d + P_a \tag{5.46}$$

---

[5]For this design, utilizing M-19 steel, Kirtley [27][29]has determined these to be: P_B is 1.3 W/kg, ω_B is 60 Hz, B_B is 1, ϵ_f is 1.53 and ϵ_b is 1.88.

This heat must be removed in some way. The method of heat removal used is forced air blown through the air gap between the rotor and the armature. The required mass and volumetric flow rate of the fan is (5.47, 5.48):

$$\dot{m} = \frac{P_{heat}}{cp_{air}\Delta T} \tag{5.47}$$

$$Q = \frac{\dot{m}}{\rho_{air}} \tag{5.48}$$

The fan pressure and power are estimated (5.49, 5.50), based on an annulus flow approximation between inner and outer radii r_i and r_o for the air flow through the motor air gap from one end of the rotor to the other [6] [30].

$$\Delta P = \frac{8\mu_{air}l_{rot}Q}{\pi}[r_o^4 - r_i^4 - \frac{(r_o^2 - r_i^2)^2}{\ln(r_o/r_i)}]^{-1} \tag{5.49}$$

$$P_{fan} = \frac{\dot{m}\Delta P}{\rho_{air}\eta_{fan}} \tag{5.50}$$

The total losses are summed and the efficiency of the resulting motor calculated as

$$\eta = \frac{Pshaft}{Pshaft + Ploss} \tag{5.51}$$

5.13 Weights and cost

A simple weight based cost model is used to determine material cost only. No allowance for bearings, bearing supports or foundation material is included. Other manufacturing costs such as storage, shipping and overhead are not included. Labor rates are also neglected. Labor rates are usually based on material weight and would be subject to inaccuracies. Whatever the labor rate is, it will most likely be similar for all the motors. Therefore, this materials cost analysis will yield an accurate relative cost for the motors, but not an absolute acquisition cost.

---

[6] This is an incompressible fluid flow solution to the Navier-Stokes equations. Some error is introduced using compressible fluid (air). However, the velocity regime of the air is substantially below the Mach number of air so only slight compressible effects are expected.

Table 5.4: SMPM Material Cost

Material	Density kg/m^3	Cost $/kg
Magnet	7418	100
Copper conductor	8960	5
Magnetic steel	7800	2

5.14 Verification

The estimated size and volume of a 21 MW permanent magnet motor is 30 tonnes and 20m^3 [22][31]. These values correlate well with the output of the thesis design code (Table 5.5). However, the efficiency of the motors developed in this thesis are much higher. This discrepancy is attributed to limiting the torque and current analyses to the fundamental components only. Higher order harmonic currents circulating in the armature and magnetic steel flux paths will increase the losses in the motor above those calculated here. However, the analysis presented in this thesis is meant to be a first order comparison of overall characteristics of the three motor topologies and thus similar methods will be employed in all analyses.

5.15 Results

The optimized output obtained from the computer script is given in Appendix C. The quantitative attributes, (weight, length, diameter and efficiency) were equally weighted and evaluated by the OMOE script, described in 4.3, to find the dominant design. As expected, the lighter, smaller motors had the highest overall OMOE and the cheapest cost. The attributes and parameters of the motor with the highest OMOE are shown in Table 5.5.

Table 5.5: SMPM highest OMOE design

Design	#	24		Cost	M$	.41
OMOE	#	0.656		Pwr	MW	21.02
r	m	1.00		Mass	tonne	31.7
g	mm	77.57		Dia	m	3.09
hm	cm	243.46		L	m	1.03
l	m	1.025		eff	%	99.9
wt	mm	7.98		Inertia	kg/m^2	4.5
hs	mm	448.17		Ja	A/cm^2	110.52

Chapter 6

Superconducting Synchronous Motor (SCM)

6.1 Background

Since the discovery of superconductors, with their high current carrying capacity and minimal losses, engineers have been trying to utilize them in the pole pieces of alternating current machines in an effort to make compact, high power density and high efficiency AC motors [4] [32][33][3][34].

The superconducting synchronous motor (SCM) operates in much the same way as the surface mounted permanent magnet motor of chapter 5. However, the magnetic pole pieces are replaced with superconducting windings (see Figures 6-1 and 6-2). For this design, a High Temperature Superconducting (HTS) wire, such as BSCCO-2223 that is manufactured by American Superconductor[35], is assumed. This type of superconductor can operate at $77°K$[1], allowing the use of liquid Nitrogen (LN2) as the heat transfer medium instead of Helium, which is used with low temperature liquid cryogenic superconductors. Laboratory tests of BSCCO-2223 have demonstrated current density capacity well in excess of the of those used in this thesis[2].

Due to the relatively cold temperature environment required for the superconductors, a cryogenic thermal shield between the pole pieces and the heat producing elements of the rotor and stator will be necessary.

---

[1] Low temperature superconductors operate below $20°K$. The heat transfer medium is Helium.

[2] Superconducting current density assumed is $J_{sc} = 10$ kA/cm^2.

Since superconductor conducting properties diminish in the presence of alternating magnetic fields, a damper shield between the pole pieces and the armature is required to shield the superconducting pole pieces from the alternating fields produced by the armature.

Magnetic flux densities far in excess of the saturation flux density of magnetic steel will be realized. Thus, any magnetic steel within the motor will be useless in guiding flux and can be replaced with lighter structural materials. This includes the armature stator teeth, normally used to provide a low reluctance path for the magnetic flux lines into the back iron. Further, the size of the stator structure can be designed with only structural constraints. Thus, the armature area can be packed with more current carrying conductors to further increase the power output of the machine.

Another benefit of removing the stator teeth is the reduction in the cogging torque of the rotor. Magnetic poles of slotted synchronous machines tend to have a low reluctance when the poles are aligned with a stator tooth. This creates a cogging torque, a cyclic varying torque that increases the vibrational and electrical harmonic components of the motor. The air-core synchronous motor, however, will not have a cyclic reluctance torque since there is not a spacial varying reluctance path for the magnetic flux lines across the motor air gap.
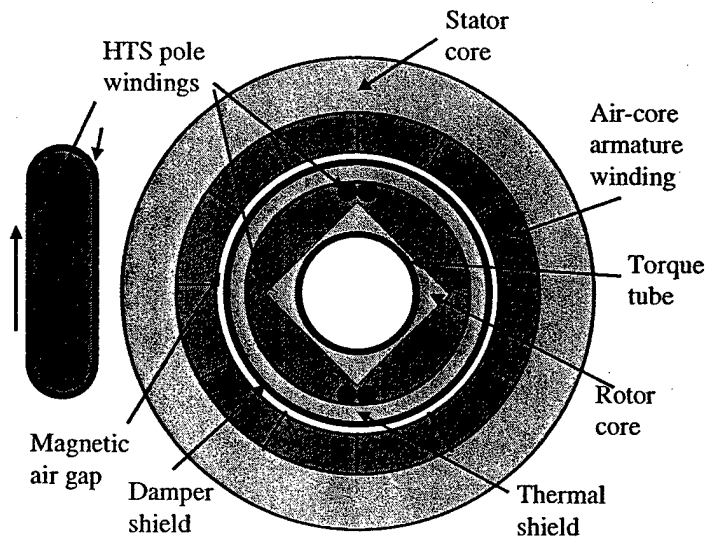
Figure 6-1: Air-Core synchronous machine with superconducting pole windings. Shown here is a four pole ($p = 2$) rotor.
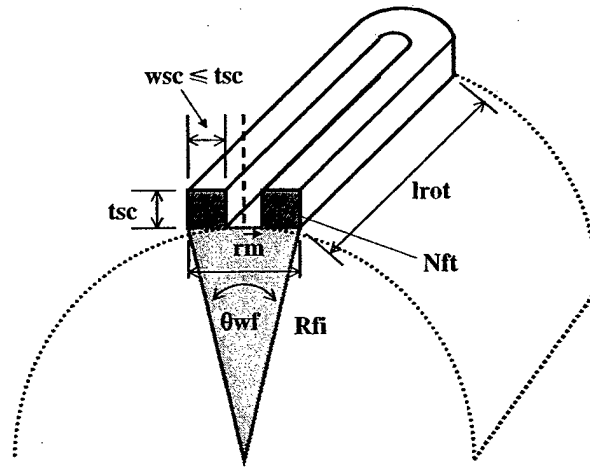
Figure 6-2: Superconducting pole head. Showing dimensions of field windings, minimum bend radius r_m, physical angle of extent θ_{wf}, number of field windings N_{ft} and radius of field.

6.2 Design Parameters

The variable design parameters used to generate an SC synchronous motor are given in tables 6.1 and 6.2. Table 6.1 gives the continuously varying inputs and table 6.2 gives the variables that vary by integer steps, just as in the permanent magnet motor of section 5.2.

Table 6.1: SCM Design Parameters, Continuous Variables

Design Parameter	Symbol	Lower limit	Upper limit	Deviation	units
Rotor radius	R_{fi}	.5	1.5	.5	m
Air-gap thickness	g	1	100	49.5	cm
SC coil thickness	t_{sc}	1	30	14.5	cm
Rotor active length	l	.2	3	1.4	m
Armature thickness	t_{arm}	1	500	249.5	cm

For the same reasons discussed in chapter, 5.2, the phase number q is reassigned to a value of 15 for every set of variables generated.

Table 6.2: SCM Design Parameters, Integer Variables

Design Parameter	Symbol	Upper limit
Pole pairs	p	20
Turns per coil	nc	40
Number of phases	q	15

6.3 Constraints

Imposed physical constraints are given in table 6.3. Those marked (*) are the actual levels used in the design.

Table 6.3: SCM Constraints

Design constraint	Symbol	Value	Units
*Field coil current density	Jc	10000	A/cm^2
*max rotor speed	rpm	100	rpm
*Minimum required output power	Preq	21	MW
Maximum AC voltage applied	Vll	4160	VAC
*Copper conductivity	siga(σ)	5.917e7	$1/(\Omega m)$
Max copper current density	Jalim	150	A/cm^2
Max iron flux density	Bisat	1.2	T
*Required power factor	psi	1	

Several design constraints are imposed throughout the design process to insure that the motor parts will actually fit together and material properties are not exceeded. As in the preceding chapter, if a design constraint is violated, the design loop is terminated and a new set of design parameters are generated. Constraints include:

1. The resulting power output of the motor is checked to insure that at least the minimum required power is attained.

2. To insure adequate cooling to the stator coils, the slot packing factor λ_a (*lama* in computer code appendix H) is limited to .35, and the allowed stator current density $Jalim$ is limited to 150 A/cm^2.

3. The armature space factors, or the amount of space available for conductors, for the straight section and the end turns are given as $\lambda_c = .6$ and $\lambda_e = .8$, respectively.

4. Although relatively slow speed motors are being evaluated, the tangential speed of the field coils are verified below an a priori limit of 230 m/s to insure their mounting will hold. By simply changing the constraint on rotor rpm, much faster smaller motors could be evaluated.

5. The operating power factor is forced to unity. This is to insure proper impedance matching with a predicted power converter operating at unity power factor.

6. The operating power factor is set to 1.0 This insures that the motor operates relatively close to the expected supply from a solid state power converter.

6.4 Generate Geometry

The outer radius of the field poles is (6.1).

$$R_{fo} = R_{fi} + t_{sc} \tag{6.1}$$

The thickness t_k of the damper shield system must be large enough to suppress the alternating magnetic field produced by the armature but, more limiting, it must also withstand the high torque and crushing loads produced by a terminal short as the now stationary magnetic field of the stator combines with the continually rotating field of the rotor and must be compressed within the small air gap. The determination of the exact thickness necessary is complex and would be computer time intensive. A deterministic method to evaluate the required thickness of the damper shielding is presented in a masters thesis by Furuyama [36]. For simplicity, the damper shield design calculated for the much larger rating machines of [36] will be used. This is a three section damper system. The inner primary shield is 2 mm of copper at 20°K, and primarily shields the pole pieces from thermal conduction. A thick secondary damper shield support, 11 cm of structural steel, is next followed by a thin 6 mm secondary damper shield of room temperature copper. Both secondary shield elements control the large torque and crushing loads during an unlikely three phase short terminal fault.

$$t_k = (.002 + .11 + .006) \text{ m} = .118 \text{ m} \tag{6.2}$$

The inner radius of the armature coils is (6.3).

$$R_{ai} = R_{fo} + t_k + g \tag{6.3}$$

Adding on the thickness of the armature, t_{arm}, gives the outer armature radius (6.4)

$$R_{ao} = R_{ai} + t_{arm} \tag{6.4}$$

The inner radius of the flux return shield is assumed at the outer radius of the armature coils.

$$R_s = R_{ao} \tag{6.5}$$

The air-core stator, assuming it is fully utilized, has an angular extent of each phase belt given by equation 6.6.

$$\theta_{wa} = \frac{\pi}{pq} \tag{6.6}$$

The electrical angle of the field pole is set at $\theta_{wfe} = 2\pi/3$. This cancels the third harmonic components in the Fourier series of a square wave and thus the third harmonic torque component of the machine. The physical angle of extent of the field poles is (6.7):

$$\theta_{wf} = \theta_{wfe}/p \tag{6.7}$$

The total width of a given superconducting wound pole is thus given as (6.8)

$$w_p = R_{fi}\theta_{wf} \tag{6.8}$$

The pole piece thickness t_{sc}, is given as a random variable. A typical HTS superconductor cross sectional area A_{wire} is 0.82 mm^2[35]. Assuming a field coil winding width not greater than the thickness and a minimum bend radius r_m, then the total cross section area of the field coil winding

is (6.9) (See Figure 6-2).

$$A_{coil} = t_{sc}w_{sc} \tag{6.9}$$

Allowing very close packing, the possible number of turns in each pole is given as (6.10)

$$N_{ft} = \frac{A_{coil}}{A_{wire}} \tag{6.10}$$

6.5   Estimate End Turn Lengths

Unlike the slotted armature of the permanent magnet motor, it is more difficult to find geometric solutions to the winding patterns for the air-core stator. Kirtley[37], estimated the half cone length as 6.12. The rotor length build up is estimated as the thickness of one phase belt (6.11).

$$l_{e1} = l_{az}\frac{1}{\tan\theta_e} \tag{6.11}$$

$$l_{e2} = l_{az}\frac{1}{\tan\theta_e} \tag{6.12}$$

$$l_{az} = \frac{\alpha R_{ai}}{2p} \tag{6.13}$$

$$\cos\theta_e = \frac{\lambda_c}{\lambda_e} \tag{6.14}$$

where λ_c and λ_e[3] are the space packing factors for the armature windings and end turns respectively, l_{az} (6.13) is half of the total azimuthal traverse of the end turn, where $\alpha = \pi$, or the electrical angle of the phase windings, assuming no short pitched windings, and θ_{wa} is shown in Figure 6-3.

6.6   Field and Armature Currents

Integrating radially and azimuthally enclosing one armature phase belt, (phase a), results in the phase current given in equation 6.15.

$$I_a = \frac{J_a\theta_{wae}R_{ao}^2(1-x^2)}{2N_{at}} \tag{6.15}$$

---

[3]λ_e is assumed to be .8 as in [37].
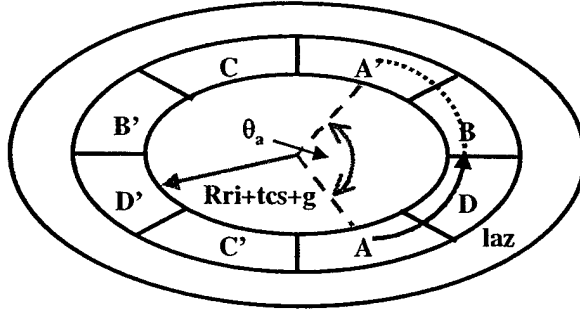
Figure 6-3: End turns required azimuthal traverse, l_{az}, belt to belt.

A similar integration in one pole piece yields the field current, equation 6.16

$$I_f = \frac{J_f \theta_{wfe} R_{fo}^2 (1 - y^2)}{2N_{ft}} \tag{6.16}$$

Where x and y are ratios of the respective inner and outer radii.

$$x = \frac{R_{ai}}{R_{ao}} \qquad y = \frac{R_{fi}}{R_{fo}} \tag{6.17}$$

6.7 Winding Factors

The windings on both the stator and rotor are without slots. Therefore, the conventional definitions for winding factor need to be modified. Assuming a phase belt of windings occupy an angular extent of θ_{wa}, the equivalent winding factor is (6.18). The field coils are actually full pitched concentrated windings. Therefore, referring to section 5.14, they link full flux.

$$k_{wa} = \sum_{n=1,5,7,\ldots}^{\infty} \frac{\sin pn\frac{\theta_{wa}}{2}}{pn\frac{\theta_{wa}}{2}} \tag{6.18}$$

$$k_{wf} = 1 \tag{6.19}$$

6.8 Magnetic Fields

The radial magnetic intensity that must be guided by the flux return shield is (6.20).

$$H_s = - \sum_{n=1,5,7,\ldots}^{\infty} \frac{2J_f \sin \frac{n\theta_{we}}{2} \sin np(\delta)}{n(2+np)} R_s (\frac{R_{fo}}{R_s})^{np+2} 2(1-y^{np+2}) \tag{6.20}$$

By multiplying by the permeability of free space μ_o, the magnetic flux seen at the shield is found. The required thickness of the shield is then determined as in the permanent magnet motor chapter with equation 5.20

6.9 Mutual Inductance

From the above winding factor, the mutual inductance can be determined from equation 6.21. The derivation of which can be found in [4].

$$M_a = \sum_{n=1,5,7,\ldots}^{\infty} M_n \cos np\phi \tag{6.21}$$

where

$$M_n = \frac{8l_m \mu_o N_{at} N_{ft}(1-y^{np+2})}{np\pi(1-y^2)(1-x^2)} k_{wa} k_{wf} C_{mn} \tag{6.22}$$

$$C_{mn} = \frac{1}{n(4-n^2p^2)}(\frac{R_{fo}}{R_{ao}})^{np}$$

$$\times [1 - x^{2-np} + \frac{2-np}{2+np}(1-x^{2+np})(\frac{R_{ao}}{R_s})^{2np}] \tag{6.23}$$

for $pn \neq 2$. For $p=2$ C_{m1} is given by:

$$C_{m1} = \frac{1}{8}(-\ln x + \frac{1-x^2}{4}(\frac{R_{ao}}{R_s})^4) \quad , p=2 \tag{6.24}$$

where l_m is the effective length of the armature for field-to-armature mutual inductance calculations. Kirtley [4] determined this length (6.25) experimentally on a similar superconducting motor.

$$l_m = l \tag{6.25}$$

61

6.10 Internal Voltage

$$\vec{E}_{af} = \frac{d\vec{\lambda}_{af}}{dt} \tag{6.26}$$

where

$$\vec{\lambda}_{af} = M_a I_f e^{j\delta} \tag{6.27}$$

with δ equal to the angle between the field pole and its corresponding armature winding. Thus, the speed voltage, or electromotive force, can be found from the time derivative of flux linkage or (6.28):

$$\vec{E}_{af} = j\omega M_a I_f e^{j\delta} \tag{6.28}$$

Rearranging equation 6.16 to solve for amp-turns $N_{ft}I_f$, yields (6.29).

$$N_{ft}I_f = \frac{J_f}{2}\theta_{wfe}R_{fo}^2(1-y^2) \tag{6.29}$$

Thus the magnitude of E_{af} can be found as (6.30).

$$|E_{af}| = j\omega\frac{M_a}{N_{ft}}N_{ft}I_f \tag{6.30}$$

Thus, given the superconductor rated current density J_f, the actual number of field pole turns need not be solved for explicitly.

6.11 Synchronous Reactance and Resistance

The synchronous reactance is determined by the self (6.31) and mutual (6.32) inductance of an armature phase and is given by equation 6.36.

$$L_a = \sum_{n=1,5,7,\ldots}^{\infty} \frac{4l_{oa}\mu_o N_{at}^2}{np\pi(1-x^2)^2}k_{wa}^2 C_{sn} \tag{6.31}$$

$$L_{ab} = \sum_{n=1,5,7,\ldots}^{\infty} \frac{4l_{ab}\mu_o N_{at}^2 \cos\left(\frac{2n\pi}{3}\right)}{np\pi(1-x^2)^2} k_{wa}^2 C_{sn} \tag{6.32}$$

$$C_{sn} = \frac{1}{(n^2 p^2 - 4)}[(np-2) + 4x^{np+2} - (np+2)x^4 \tag{6.33}$$

$$+2(\frac{np-2}{np+2})(1 - x^{np+2})^2(\frac{R_{ao}}{R_s})^{2np}] \tag{6.34}$$

for $pn \neq 2$. For $p = 2$ C_s is given by:

$$C_{s1} = (x^4 \ln x + \frac{1-x^4}{4} + \frac{(1-x^4)^2}{8}(\frac{Rao}{Rs})^4 \tag{6.35}$$

$$X_s = \Omega(L_a - L_{ab}) \tag{6.36}$$

where loa and lab are the affective length of the armature for self and mutual inductance calculations. Kirtley [4] determined these values from an experimental superconducting motor to be:

$$loa = l + 2.6\Delta l \tag{6.37}$$

$$lab = l + 1.2\Delta l \tag{6.38}$$

$$\Delta l = R_{ao} + R_{ai} \tag{6.39}$$

The armature resistance (6.40) is determined by the total length of wire in a given phase; including the end turn length.

$$R_a = \frac{L_{ac}}{\sigma A_{ac}} \tag{6.40}$$

63

$$L_{ac} = 2N_{at}(l + 2l_{e1}) \tag{6.41}$$

6.12 Minimum Characteristics

Now that the SCM electrical parameters have been determined, the minimum power characteristics can be determined just as in chapter 5.10, the SMPM design.

6.13 Parameters at Rated Power

This analysis is also the same as in chapter 5.11, and is not repeated here.

6.14 Losses

Eddy current and hysteresis losses in the back iron are computed as in the SMPM using equation 5.44. Losses here should be less than in the slotted armature motor since the iron losses in the stator teeth are absent. An additional loss here is in the cryogenic cooling requirements. An estimate derived from data for a superconducting motor designed by American Superconductor is[3]:

$$Pcryo = .3\% P_{GEN} \tag{6.42}$$

6.15 Weights and Cost

The same weight based cost model for materials only from 5.13 is used. Again, no allowance is given for bearings, bearing supports or foundations material. In addition, other manufacturing costs such as storage, shipping and overhead are not included. The cost of HTS is a DOE[4] estimate supplied by [38].

---

[4]Department of Energy estimate for 2020 time frame.

64

Table 6.4: SCM Material Cost

Material	Density kg/m^3	Cost $/kg
Superconductor	10510	100
Copper conductor	8960	5
Magnetic steel	7800	2

6.16 Verification

A proposed 25 MW air-core superconducting motor under development at American Superconductor Corporation (AMSC) *HTS Superdrive* [3] summarized in Table 6.5 is used to compare the output of the design program. The designs are relatively the same size for the given torque output. The lower efficiency of the AMSC design is due to the much higher joule heating losses in the armature. This could be attributed to their more exact Fourier harmonic analysis instead of the fundamental component analysis used in this thesis.

Table 6.5: American Superconductor's HTS SuperDrive

Pwr	MW	25.1
Speed	rpm	120
phases	q	3
Vll	VAC(rms)	6600
poles	p	6
eff	%	97
Dia	m	2.65
L	m	2.08

6.17 Results

The SC synchronous motor with the highest OMOE is shown in Table 6.6. The data and Pareto chart can be found in Appendix D.

Table 6.6: SCM highest OMOE design

Design	#	6
OMOE	#	0.629
Rfi	m	0.51
g	mm	14.15
tsc	mm	26.38
$lrot$	m	0.56
$tarm$	mm	469.5
p	#	3
nc	#	23
q	#	15

Cost	M$	0.05
Pwr	MW	21.06
Mass	tonne	19.4
Dia	m	2.419
L	m	0.961
eff	%	99.6
Inertia	kg/m^2	2.6
Ja	A/cm^2	119.51

Chapter 7

Homopolar Motor (HPM)

7.1 Theory of Operation

The homopolar motor (HPM), sometimes called an acyclic motor, utilizes the Lorentz force (7.1) directly. (see Figure ??).

$$\vec{F} = \vec{J} \times \vec{\beta} \tag{7.1}$$

A non-varying magnetic field, in space and time, interacts with the steady DC current carried by a conductive copper drum resulting in a torque imparted on the drum. It should be noted that since the magnetic field and the armature current are both constant in time and space, smooth rotational torque is developed without pulsations or structural excitations. Thus, the acoustic signature of this machine is expected to be extremely low. Several different papers on this type of motor have been published [5][39][40].

The resulting induced voltage E_{af} of this arrangement is found from Faraday's law (7.2) and is on the order of 40 VDC. For a propulsion motor on the order of 21 MW, this results in supply current on the order of 500 kA. This current is prohibitively large for modern sliding contacts. In the early days of HPM design, the current collection scheme employed was liquid metals such as mercury. However, the use of hazardous liquid metals on board a submarine would not be readily accepted.

Shown in Figure 7-2 is a multi-drum HPM in which the induced voltage, from Faraday's law
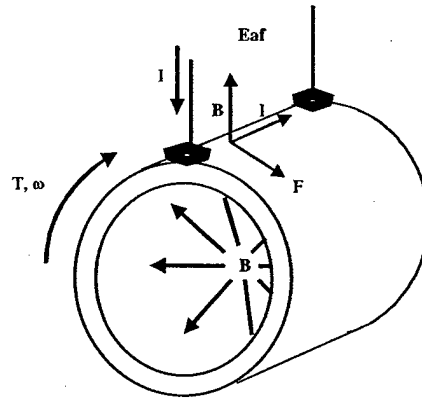
Figure 7-1: Single turn homopolar motor.

(7.2), of each drum is added in series in order to raise the motor induced voltage Eaf to the order of 400 VDC. For a propulsion motor on the order of 21 MW, this results in supply current on the order of 50 kA. This current is in the accepted range of newer technology copper fiber brushes being developed by Noesis, inc. and HipPerCon l.l.c [41]-[43]. These fiber brushes are currently undergoing performance testing at the LBES in Philadelphia [44] with promising results.
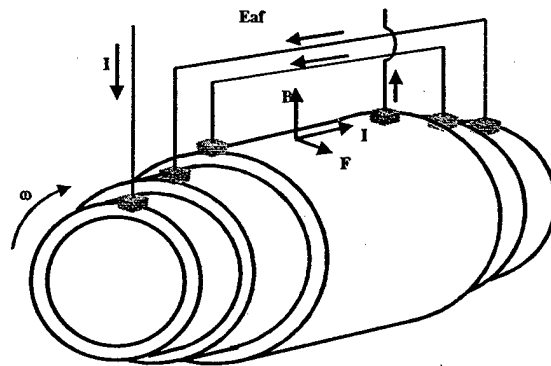
Figure 7-2: Multi-drum homopolar motor cartoon. The generated voltage of each drum is added in series to raise the total induced voltage to a reasonable level.

$$\vec{E} = \vec{v} \times \vec{\beta} \qquad (7.2)$$

68

7.2 Design Overview

The HPM motor design utilized here is one proposed by Mike Heiberger, formally of General Atomics and now at SatCon. It is a drum type machine which also incorporates radial risers. The conductive cooling superconducting field coils[45] at each end of the drum are oriented such that the resulting fields oppose each other. This forces the magnetic flux lines to cross the axial portion of the drum mostly perpendicularly. The radial drum risers also interact with the remaining axial flux lines to increase the torque output. (see Figure 7-3).
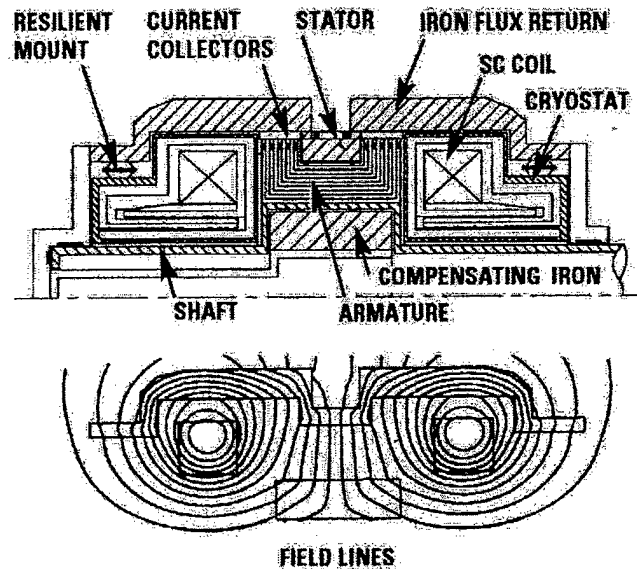
Figure 7-3: HPM cross section with flux path (courtesy of General Atomics)

In order to bring the terminal voltage of the machine to a reasonable level, multiple drums are used and connected electrically in series. The voltages induced along each drum are thus summed together.

Between each of the current carrying drums is a layer of high electrical insulation with high thermal conductivity. To remove the joule heat loss in the rotor, forced CO_2 cooling is utilized around the outside of the rotor drums along with water cooling around the periphery of the inner most drum. No allowance for conductive cooling from the current collector brushes is used.

The current carrying drum assembly is mounted onto a composite rotor to transmit the resulting

69

torque to the propeller shaft.

Copper fiber brushes are used as sliding current collectors along the periphery of the riser sections. They cover less than 2/3 of the total surface area of the rim (60%), as recommended by the designer [46].

A ferrous flux return shield surrounds the drum and field coils in order to guide, contain and provide a low reluctance return path for the magnetic flux lines.

7.3 Design Parameters

For the HPM, a less conventional set of design parameters was defined. Normally, with a rotating machine the number of pole pairs, number of parallel windings and input electrical phases, etc., are defined. Since the HPM is a true DC machine, however, it will be fed by a DC source, with a single phase. Also, by definition, it has only one pole and, instead of stator windings, it has opposing field coils at each end of the rotor. The relative dimensions of these field coils is defined and a nominal current density is assigned to the coil area. It is assumed that subsequent detailed analysis of the optimized machine will solve for the actual number of field turns and field current necessary to generate the required design current density. The design parameters used, along with their boundary values and standard deviations are given in Table 7.1.

Table 7.1: HPM Design Parameters, Continuous Variables

Design Parameter	Symbol	Lower limit	Upper limit	Deviation	units
Rotor length	$Lrot$	.5	4	.25	m
Composite rotor radius	Rri	.5	4	.25	m
Drum thickness	$trot$	.1	10	.3	cm
Drum spacing	$tins$	.1	10	.1	cm
Field coil radius	Rc	.3	5	.3	m
Field coil thickness	tc	2	100	2	cm
Field coil width	wc	5	100	5	cm

7.4 Constraints

Physical constraints and constants imposed are given in Table 7.2. Those marked (*) are the actual levels used in the design.

Table 7.2: HPM Constraints

Design constraint	Symbol	Value	Units
*Field coil current density	Jc	10000	A/cm^2
*Max rotor speed	rpm	100	rpm
Min required output power	Preq	21	MW
*Applied terminal DC voltage	Vll	1100	VDC
*Copper conductivity	siga(σ)	5.917e7	$1/(\Omega m)$
Max copper current density	Jalim	150	A/cm^2
*Max iron flux density	Bisat	2	T
Max copper brush current density	Jmax	150	A/cm^2

Several design constraints are imposed throughout the design process to insure that the motor components will actually fit together and material properties are not exceeded. If a design constraint is violated, the design loop is terminated and a new set of design parameters are generated. Constraints include:

1. Insuring that both rotor drums turn and that the field coils will fit inside the flux shield.

2. The resulting power output of the motor is checked to insure that at least the minimum required power is attained.

3. The required operating current is checked against the two current density constraints, one for the smallest cross sectional area occurring in the inner most drum and the other at the copper fiber brush contacts.

7.5 Derivation of Field Strength

Since the motor is symmetrical, both along its axis of rotation and from front to back, only half of the rotor is modeled and the resulting torque is doubled. A cross section of one quarter of the motor is shown in Figure 7-4.

Shown is the upper portion of a field coil and several drum turns. The motor will be analyzed axisymmetric and in 2-dimensions. In solving for the magnetic flux, a finite element analysis

71
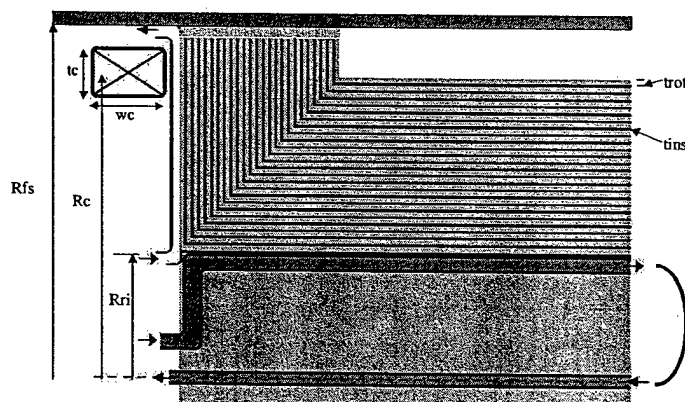
Figure 7-4: Cross section of 1/4 of hybrid HPM showing water cooling in inner drum and wetted C02 cooling on outer side of drum turns. Rri - inner drum radius, trot - drum thickness, tins - spacing between drums, Rfs - inner radius of flux shield, Rc - Coil mean radius, tc/wc - coil thickness and width.

method could have been utilized. However, in an effort to develop a quick solving routine, a macro-element analysis is used instead. Thus, the solving routine could be executed several thousand times and a set of non-dominated motors could be extracted.

The area of the drum turns, or armature, is segmented axially and radially into a uniform grid, or array. The magnetic flux, and later the resulting torque, is solved for in the center of each array element. The field coil is also segmented axially and radially to insure an accurate flux distribution calculation. Each field coil is a uniform circular conductor which will produce toroidal shaped flux lines. In the 2-dimensional analysis utilized, flux loops are generated as shown in Figure 7-5.

The flux due to a field coil element, at each array point, is solved for using the Biot-Savart law applied around a circular loop, as shown in Figure 7-6. Bumby [47] has solved the Biot-Savart equation in terms of the axial and radial components using elliptical integrals.

$$B_r = \frac{\mu_o I}{2\pi} \frac{z}{r\{(a+r)^2 + z^2\}^{1/2}} \{-K + \frac{a^2 + r^2 + z^2}{(a-r)^2 + z^2} E\} \tag{7.3}$$

$$B_z = \frac{\mu_o I}{2\pi} \frac{1}{r\{(a+r)^2 + z^2\}^{1/2}} \{K + \frac{a^2 - r^2 - z^2}{(a-r)^2 + z^2} E\} \tag{7.4}$$

where K and E are the complete elliptical integrals of the first and second kind, respectively, with

72
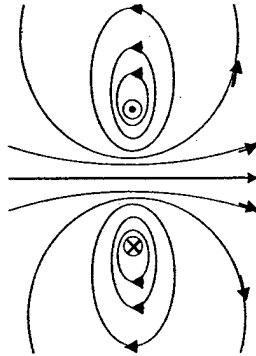
Figure 7-5: Flux lines induced by circular current

an input argument, or modules, of:

$$k = \sqrt{\frac{4ar}{(a+r)^2 + z^2}} \qquad (7.5)$$

The flux induced by each field coil element at each array element is solved in this way and the resulting flux contributions are summed together.

7.5.1 Flux Shield Boundary Condition

At the inner surface of the flux shield, all the magnetic lines must be perpendicular to the surface and thus entering the ferrous flux shield. From (7.6), the magnetic flux density β is defined as the product of permeability μ and magnetic intensity H.

$$\beta = \mu * H \qquad (7.6)$$

The permeability of the flux shield is assumed infinite. Thus, since β can not be infinite, H must be nearly zero. The closed integral form of ampere's law (7.7) is taken around an infinitesimally

73
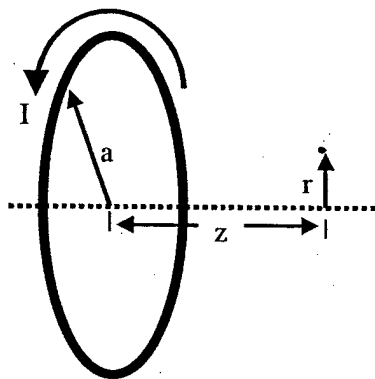
Figure 7-6: Circular current carrying coil

thin loop enclosing the flux shield inner surface (see Figure 7-7).

$$\oint H \cdot dl = K \tag{7.7}$$

Noting no actual surface current K, the summation of the axially directed H around the loop must be zero. Therefore, the axially directed H just outside the flux shield is zero. To mathematically
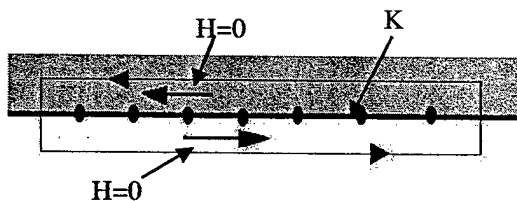
Figure 7-7: Ampere's law around flux shield boundary, K is an amperian current sheet and H is the magnetic field intensity.

impose this boundary condition an amperian current[1] is assumed at the surface of the flux shield. The amperian current induces a counter magnetic flux which cancels the axial component of flux due to the field coil, as in Figure 7-8. The magnetic field of the amperian currents is then superimposed onto the magnetic field due to the field coil itself. This results in the net radial and axial magnetic

---

[1]An *amperian current* is a term used in conjunction with permanent magnets to relate their inherent magnetization to an equivalent electrical current producing the same amount of magnetization.

flux at the center point of each array element with the proper boundary condition (zero field parallel to the surface of the flux shield).
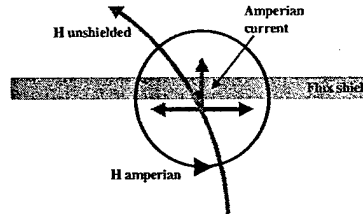
Figure 7-8: Flux shield boundary condition. Amperian current H field parallel to flux shield cancels the un-shielded field due to coil.

7.6 Induced Voltage and Maximum Current

The machine voltage rating, Eaf, is solved using Faradays equation 7.8

$$Eaf = \int (\nu \times \beta) \cdot dl \qquad (7.8)$$

where ν is simply the tangential velocity and β is the magnetic flux. The riser sections are symmetric and have equal yet opposite magnetic flux cutting them. The voltage induced on one end will cancel the voltage induced on the other. Therefore, only the voltage induced on the axially directed drum sections is calculated.

The maximum available current can now be determined based on the ohms law and the assumed terminal voltage.

$$Imax = \frac{Vll - Eaf}{R_a} \qquad (7.9)$$

7.6.1 Armature Resistance

The armature resistance R_a is the sum of all the series components of the multi-turn drum motor. This includes the copper losses in the drums themselves as well as the resistance of the copper fiber

brushes utilized in the current collectors[2]. Since all the current has to pass through the drums, the total copper cross-sectional area is determined and the normal means of calculating resistance in a conductor is used.

$$R = \frac{l}{\sigma A} \tag{7.10}$$

The brush resistance R_B is determined by Kuhlmann-Wilsdorf [43] as the sum of three parts.

$$R_B = R_0 + R_F + R_C \tag{7.11}$$

where R_0 is the resistance of the brush body, R_F is the surface film resistance and R_C is the "constriction resistance." For very thin copper fiber brushes under light pressure and elastic contact with the sliding surface, R_0 and R_C are negligible. Thus R_B is simply R_F (7.12):

$$R_F = \sigma_F(elp_C/P_B) \tag{7.12}$$

where σ_F is the measured film resistivity of clean metal fiber brushes, P_B is the brush pressure, elp_C is the average contact pressure (7.13).

$$elp_C \approx 0.004\beta^{1/3}E \tag{7.13}$$

$$\beta < 1 \tag{7.14}$$

where E is the *Youngs* modulus of copper[3].

7.7 Torque

The Lorentz force, equation 7.1, in its integral form is used to calculate the force per ampere of current in the drum section. Boolean arrays, one corresponding to axial magnetic flux component and the other to radial flux component, are created. An element is assigned a value of one if the

---

[2]Copper fiber brushes are being produced by Neosis, inc. and HiPerCon l.l.c.. Performance testing and validation is currently being conducted at the NAVSSES Land-based Engineering Site (LBES) on a 1000 HP HPM, and on a 500 kW motor generator on-board an operational submarine.

[3]$\sigma_F \approx 10^{-12}\Omega m^2$ $P_B = 5N$ and $E = 11 \times 10^{10} N/m^2$

armature turns are perpendicular to the corresponding magnetic flux. Otherwise the array element is assigned a value of zero. This will allow a simple matrix multiplication to solve for the force associated with each discreet element of magnetic flux. Now for each array element it is a simple matter of taking the product of axial length, number of drum turns contained and the magnetic field strength, along with the boolean array, to find force per ampere. Then multiply by radial distance from the center line for each element and sum them together to obtain the total torque per ampere for half of the machine.

Using torque per ampere multiplied by the maximum current already solved for, the maximum output power can be found and compared to the minimum required shaft power. If the machine can't deliver at least the minimum shaft power, the program terminates and starts over with a new set of design parameters.

7.8 Operating Current

An iterative loop is used at this time to converge on the operating current of the machine. A first guess at the operating current is established as that necessary in an ideal, lossless machine. Namely,

$$I = Preq/Eaf \qquad (7.15)$$

A temporary current is defined as

$$Itemp = \frac{Preq + I^2 R_a}{Eaf} \qquad (7.16)$$

The difference between the two currents is compared to a tolerance specification. If out-of-tolerance, the operating current is set to a value midway between the two currents and the loop is repeated until the difference between the operating current and the temporary current is within tolerance.

7.9 Losses

This is a very efficient motor concept. Since the magnetic flux is non-rotating and non-varying, there are no eddy current losses in this design. The rotating armature, being a large copper drum, is smooth and uniform, leading to low air rotational resistance. The armature resistance is relatively low when compared to similarly rated synchronous machines.

7.9.1 Windage and Joule Heating

Both the windage losses and the joule heating losses are calculated in the same way as in the SMPM design.

7.10 Cooling

The armature drum assembly will be conductive cooled from water channels inside the composite rotor and by wetted CO_2 at the drum ends. Conductive cooling at the rotor-brush interface is expected to remove the joule and friction heat created at the brush contact.

60% of the surface area of the composite rotor is assumed available for conducting heat out of the drums. The required volumetric flow rate of water is determined from the combined loss, joule heating and windage, assuming the coolant water removes the entire heat losses. The coolant channels are approximated as a ring of square tubes along the outer surface of the composite rotor, each half as tall as they are wide. An assumed 50 coolant channels thus extend 4.32° degrees each. The width of each channel is therefore calculated as the chord length of its inscribed arc and the height of the channel is assumed 1/2 the width.

$$ arc = \frac{6}{10}360°/50 \tag{7.17} $$

$$ wchan = 2Rri\sin arc/2 \tag{7.18} $$

$$ hchan = wchan/2 \tag{7.19} $$

The total channel area is determined and the resulting flow velocity v is verified less than 10 m/s to avoid excess flow noise. The hydraulic diameter D_H is found with equation 7.20. The corresponding Reynolds number is solved for and the flow is verified laminar. The friction factor

is given by (7.22)[30].

$$D_H = 4\frac{A}{P} \tag{7.20}$$

$$\mathrm{Re}\,n = \frac{\rho v D_H}{\mu} \tag{7.21}$$

$$f = 62.2/\mathrm{Re}\,n \tag{7.22}$$

A simple calculation yields the required differential pressure for the forced water cooling. The required pump power is then added to the input power for the motor in the efficiency calculation of the entire motor.

The wetted carbon dioxide cooling on the drum ends, as well as along the outside of the drum, is expected to make up for neglecting the conductive heat flow within the drum itself.

7.11 Weights and cost

The same weight based cost model for materials only from 5.13 is used. Again, no allowance is given for bearings, bearing supports or foundations material. In addition, other manufacturing costs such as storage, shipping and overhead are not included. The cost of HTS is a DOE[4] estimate supplied by [38].

Table 7.3: HPM Material Cost

Material	Density kg/m³	Cost $/kg
Superconductor	10501	100
Copper conductor	8960	5
Magnetic steel	7800	2

7.12 Verification

Both the power per unit mass and volume correlate closely to detailed conceptual designs developed by Heiberger [48]. His design is summarized in Table 7.4. The average flux densities B_{rot} calculated in this thesis were nearly twice those used in the GA design which would account for the larger size

---

[4]Department of Energy estimate for 2020 time frame.

of the GA design necessary to generate the 21 MW of shaft power. Thus the output, the design process and programs are deemed correct.

Table 7.4: Genaral Atomics estimate for 21 MW HPM

Pwr	MW	21
eff	%	99
Turns	#	18
B_{rot}	T	3
Dia	m	2.22
L	m	3.4
Mass	tonne	50

7.13 Results

The optimized output obtained from the computer script of Appendix I is given in Table 7.5. The data and Pareto chart can be found in Appendix E.

Table 7.5: HPM highest OMOE design

Design	#	8		Cost	M$	0.08
OMOE	#	0.598		Pwr	MW	21.1
$Lrot$	m	1.22		Mass	tonne	30.0
Rri	m	1.16		Dia	m	2.850
$trot$	mm	5		L	m	1.659
$tins$	mm	8		eff	%	99.5
Rc	m	0.84		Inertia	kg/m^2	7.6
tc	cm	54.8		Ja	A/cm^2	115.23
wc	cm	17.1				
$Nturns$	#	17				

The actual efficiency of this motor is expected to be very close to what is calculated above. Unlike the two synchronous motors, no higher order harmonic currents are present in this design. Therefore, the majority of the loss mechanisms have been accounted for.

Chapter 8

Power Converters

In chapters 5 through 7, the detailed design procedure for three different motor configurations has been presented. Each of these motors was designed with the assumption that a specific power supply was available at their terminal inputs. The two synchronous motors, SMPM and SCM, assumed that 4160 VA(rms) at variable frequency ($0-100$ rpm translates to $0-\frac{np}{120}$ Hz) was available at their inputs. The HPM motor assumed that 1100 VDC was available. These assumptions will have a large impact on the submarine. For instance, will the main supply for electrical power be alternating current (AC) or direct current (DC)[1]?

Also, it would be beneficial if the power converter was bi-directional, meaning it could either supply or absorb power. When absorbing power, it would raise the propulsion bus voltage and relieve the load on the main propulsion generators or charge large kinetic energy storage devices. This would mitigate the need to have large braking resistors to absorb the power produced by the propulsion motor as the speed of the motor is slowed and reversed.

In this chapter, the current power conversion technology is investigated and evaluated.

8.1 Variable Frequency Supply

There are several widely accepted AC/AC converter topologies being used in industry and some newer topologies are emerging [23]. Each has its own advantages and disadvantages.

---

[1]Several papers have been published on this topic [9]-[12].

8.1.1 Pulse Width Modulated (PWM)

The PWM converter is a staple of most industrial drives. It is also the power converter used in the Land-based Engineering Site (LBES) in NAVSEA Ship Surface Engineering Station (NAVSSES) as part of the Full Scale Advanced Development (FSAD) hardware to support the integration of all electric power into the Zumwalt-class (DD-21) land-attack destroyer.

This particular design is a 3 phase input-15 phase output converter; the output phases are made up of 3 blocks of 5 phases each. Each block of 5 phases is fed by the three phase input voltage rectified via a six-pulse SCR-based rectifier bridge and a DC link [49][16]. Each of the 5 phase groups is then inverted by a H-Bridge inverter (see Figure 8-1). The DC link voltage is unregulated and varies from $5.6 - 6$ kV. Therefore, eight 1600 V insulated gate bi-polar transistors (IGBT) per switch are used in series to block the DC link voltage. This allows for an $n + 1$ component rating[2]. The size and weight of this 19 MW converter is shown in Table 8.1[3]. Also in Table 8.1 is the estimated reduction in size of the converter, assuming the 8 series 1600 V IGBT's are replaced by 4 higher voltage 3300 V IGBT's[4]. Although it is rated at 2 MW less than needed for the motors in this thesis, it is expected that the switches and DC link can be upgraded to handle the increased current without an increase in volume or weight. Thus, this is the size and weight of the controller used to supply both synchronous motor designs of Chapters 5 and 6. The third controller assumes the replacement of the IGBT's with IGCT's discussed in section 8.3. They have considereably less conduction losses in about the same size package. The last column in Table 8.1 lists the conversion efficiencies of the switches themselves[51][5]. The overall efficiency of large power converters is typically over 99%[52].

Recent noise testing of this system at LBES resulted in high structure born noise being created by the 2 kHz switching frequency of the PWM inverters [53]. This can be mitigated by assuming a multi-level converter PWM configuration or possibly an active feedback method, each discussed anon.

---

[2]Component IGBT's are assumed to operate at half their individual rating with one failed.

[3]Data from Mr. Jeff Buckley of Alstom [50].

[4]60% of the weight and volume is assumed fixed in the DC link and rectifier. The remaining 40% is reduce by a factor of 2.

[5]Using expected 640 amp supply, with conduction voltage drops of: 4 V for the 1600V IGBT's, 2.2 V for the 3300V IGBT's and 1.4 V for the IGCT's.
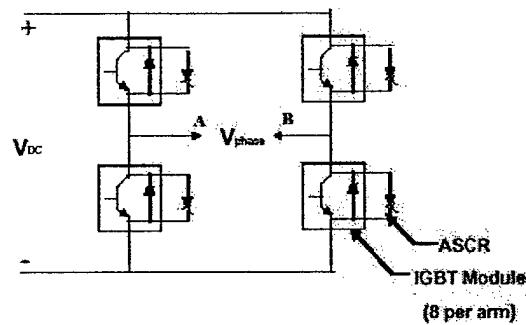
Figure 8-1: H-Bridge inverter used in 19 MW PWM AC/AC converter at the LBES

Table 8.1: 15 Phase, 21 MW PWM Converter Sizing

	units	**1600V**	**3300V**	**IGCT**
Length	m	5.6	4.47	4.47
Width	m	2.135	2.135	2.135
Height	m	2	2	2
Volume	m^3	23.9	19.1	19.1
Weight	tonne	17	13.6	13.6
switching eff	%	97.2	99.2	99.5

8.1.2 Multi-Level Inverters

In the multi-level inverter design, instead of blocking the full input DC link voltage with power semiconductor devices in series, the DC link input voltage is divided into independent voltage steps (see Figure 8-2) [23]. Thus, each semiconductor blocks and supplies a portion of the DC link voltage directly to the output. The result is an output with more voltage steps which more closely approaches the desired sine wave output. Simulations of this inverter show a significant reduction in the switching frequency harmonics from that of the single level H-Bridge inverter [54],[55], a major contribution being that not all devices are switched at each cycle. Rather, the switches on a given H-bridge arm are switched on sequentially as the voltage is stair stepped up and then switched off sequentially as the voltage is stair stepped down. Further, the resulting electromagnetic interference (EMI), which is caused by the dv/dt as switches change state, is reduced considerably, since switching Δv has been reduced by n (where n is the number of levels).

Published results for a multi-level converter design study sponsored by the Office of Naval Research (ONR) for a scalable low distortion drive resulted in the converter of Table 8.2 [56].
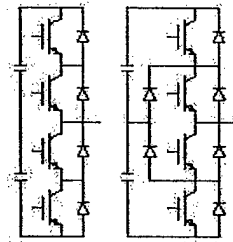
Figure 8-2: Multi-level simplified circuits (2-level series and a 3-level neutral-point-clamped circuit).

Table 8.2: ONR Sponsered 50MVA Multi-level Converter

	units	Rectifier	DC Link	Inverter	Total
Cost	$/kVA	18.52	13.17	20.22	51.91
@ 21MVA	M$	.389	.277	.425	1.090
Losses	kW/kVA	.0078	.0079	.0095	.0252
@ 21MVA	kW	164	166	200	530
Power Density	MVA/m^3	1.718	2.646	1.718	.649
@ 21MVA	m^3	12.22	7.94	12.22	32.38
Utilisation	MVA/tonne	1.078	3.055	2.071	.575
@ 21MVA	tonne	19.487	6.875	10.139	36.501

These numbers are significantly larger than on the unit in operation at LBES. The author attributes the difference to the flexible architecture of this multi-level converter design, which allows for scaleablity from $5-50$ MVA and voltages from $4160-13,800$ VAC. The PWM H-Bridge design above should be able to be implemented in a multi-level strategy without a large increase in size or voltage from the LBES converter. However, reliability will be lost since a failure of any single IGBT will cause an imbalance in the output waveform that may not be controllable

8.1.3 Cycloconverter

The topology of the cycloconverter is shown in Figure 8-3[23]. It is an AC/AC regenerative converter which directly feeds, for each switching cycle, whichever input phase is closer to the desired wave form of the output. The result is a sine wave with ripples. As the output frequency drops below about 35% of the input frequency, the harmonics caused by the voltage ripple is too large. Thus, given a 60 Hz input, the cycloconverter can generate from $0-20$ Hz output relatively cleanly. For the slow rpm of a submarine propeller, 3 pole pair machines and up can run off

of a cycloconverter. However, no designs of sufficient rating are known to the author. This is the power converter employed in the Coast Guard Ice Breaker "Healy", which is a twin shafted ship. Each propulsion motor is rated at 11.2 MW and fed by two cycloconverters each. Thus, each cycloconverter supplies roughly 5.8 MW. The size of the required cycloconverter for 21 MW (Table 8.3) is prohibitively large compared to other converters [23][57].

Table 8.3: Cycloconverter Attributes

	units	Cycloconverter
Power density	kW/m^3	455
@ 21MVA	m^3	46.154
Utilisation	kW/tonne	1240
@ 21MVA	tonne	16.93
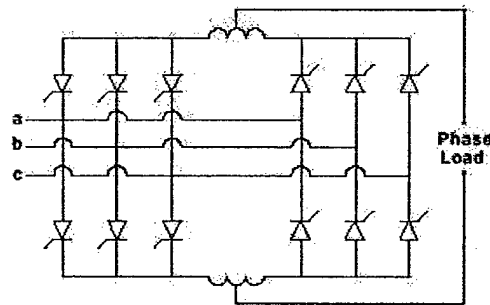
Figure 8-3: Cycloconverter simplified circuit.

8.1.4 Synchroconverter

The synchroconverter (Figure 8-4) is widely used in the cruise ship industry because of its low component count, ease of inserting redundant components, high power density [W/m3] and high power utilization [W/kg]. However, the thyristors in the inverter section rely on the load inductance for natural commutation and thus the load must be operated with a leading power factor. Further, due to the high inductance in the switching circuits, high switching currents are generated that contribute to large torque harmonics and EMI. Thus the Synchroconverter is not suitable for submarine use [23].

85
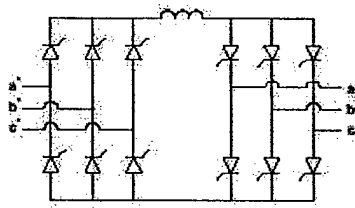
Figure 8-4: Synchroconverter simplified circuit [23].

8.1.5   Matrix Converter

The matrix converter (Figure 8-5) is a re-emerging converter design that converts AC/AC directly without the use of reactive storage elements. It relies on high power bidirectional switches, however, which are just beginning to be developed. There is some research in implementing lower power bidirectional switches in a matrix converter topology [58][59].
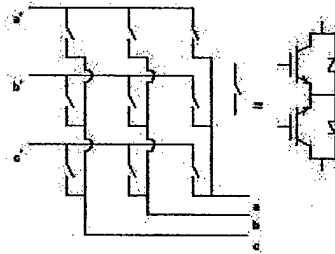
Figure 8-5: Matrix converter simplified circuit.[23]
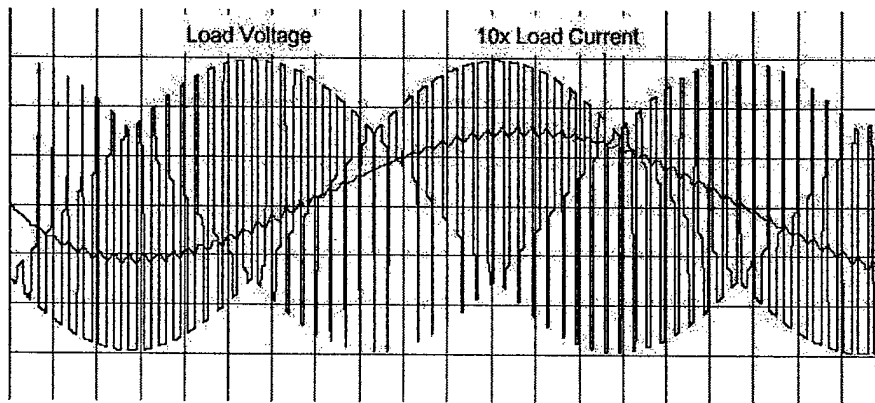
Matrix converter output waveform.

8.1.6 Active Feedback

Active feedback is not a power converter in itself, but is rather a means to mitigate the torque and vibration harmonics caused by the power converter as well as by the propulsion motor, shafting bearings, propeller etc.. Reference [60] outlines an active feedback control scheme utilizing microelectromechanical-based sensors (MEMS) to regulate the amplitude of the phase voltages supplied to the stator of a synchronous motor. Another control scheme involves active feedback control utilizing the actual current harmonics sensed at the input to the motor stator and through a feedback loop adjusting the switching times to cancel the estimated undesired torque harmonics in the motor [61]-[63]. These are promising technologies for submarine electric propulsion drives, and are worth mentioning here.

8.2 DC Supply

Direct current supplies are typically boost and buck converters, each having two switches and a DC filter (see Figure 8-6).
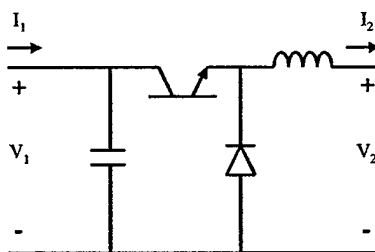
Figure 8-6: Buck converter simplified circuit.

The HPM outlined in Chapter 7 utilizes a DC source of relatively low voltage and high current. The design program (appendix I) assumes that a supply of 1100 VDC is available at the terminals of the motor. The converter should vary the supply current to the motor in order to control motor torque and thus speed. A Thyristor based (SCR) rectifier integrated into the propulsion turbine generators and buck converter/motor controller is employed (see Figure 8-6). The estimated attributes are in Table 8.4[48] (see Appendix F)[6]. For the purpose of comparing the different

---

[6]The capacitor and inductor dominate the weight and volume of the converter. The sizing is estimated as the

converters, the SCR rectifier is assumed to be part of the power generation system and is not included in the propulsion system.

Table 8.4: Thyristor (SCR) rectifier

	units	SCR rectifier
length	m	2.13
width	m	1.5
height	m	1.8
volume	m^3	5.8
weight	tonne	5.4
Switch eff	%	99.8

Table 8.5: Thyristor (SCR) Buck Converter

	units	Buck converter
length	m	2.19
width	m	1.5
height	m	1.8
volume	m^3	5.9
weight	tonne	3.2
Switch eff	%	99.8

The buck capacitor and inductor will of course have to be extremely high power devices to handle the AC ripple voltage and current. The estimated component values to maintain less than 5% ripple current at full power are on the order of 3 μH and 9 μF (see Appendix F). These component reactances are given simply as a reference; the actual component size and weights are estimated by similar DC link reactive components. Several different design and control strategies for a buck converter are discussed in Ciezki and Ashton[19].

8.3   Solid State Power Switching Technology

The increased interest in high power switching power converters has also sparked an interest in industry to develop better switching devices. Integrated Gate Commutated Thyristor (IGCT) have been developed which can block much higher voltages than IGBT's when off and conduct current low resistance, similar to a thyristor, when on[51]. These devices have been utilized in prototype

---

DC link portion of the converter utilized at LBES. The efficiency is based on 6, 4500 V IGCT's, each conducting 3.3 kA of current with 2.5 V voltage drop across them[51].

power conversion systems developed by Asea Brown Boveri (ABB) [64][65]. The resulting power converter topologies should result in even fewer component counts and a corresponding increase in reliability, with an increased power conversion efficiency and decreased heat removal requirements.

Silicon Carbide (SiC) based switching devices are also being developed which could bring similar increased performance to power conversion devices[66].

These technologies, however, are still immature and not evaluated. In the future they are expected to decrease the power conversion system's overall weight and size as well as increased efficiency and reliability.

Chapter 9

Analyses and Conclusions

9.1 Quantitative Attributes

In this chapter, the three motor topologies, superconducting homopolar (HPM), surface mount permanent magnet synchronous (SMPM) and superconducting synchronous (SCM), are compared and contrasted. The quantifiable attributes from Chapter 3, overall length, diameter, weight, volume and efficiency are used, as well as the qualitative attributes.

9.1.1 Length, Weight and Volume

The weight and volume of the mechanical drive system, a 21 MW double reduction locked-train reduction gear set, two mechanically coupled propulsion turbines and two electrical coupled turbines, are given in Table 2.2 (see Appendix B). Comparing the mechanical drive train system weight and volume summarized in Table 9.1 to that of the three motor designs with the highest OMOEs, the necessary power converters analyzed in chapter 8 and necessary electrical turbine generator sets summarized in Table 9.2[1] (see Appendix B) yields the potential weight and volume benefits within the baseline submarine design given in Table 9.3.

The weight of the HPM was higher than expected, compared to that of the SMPM. This can be attributed to the increased amount of copper, especially for the HPM's multiple copper drums. In addition, the higher magnetic fields generated in both of the superconducting motors necessitated

---

[1]Utilizes a pair of superconducting generators developed in Smith et al. [32]

Table 9.1: Summary of Baseline Mechanical Drive Train

	units	Reduction gear	Propulsion turbines (2)	Electrical turbines (2)	Electrical generators (2)
Weight	tonnes	90.7	41.7	33.8	27.2
Diameter	m	3.8	1.5	1.2	1.2
Length	m	2.6	3.7	2.4	1.8
Volume	m^3	28.8	13.3	5.7	5.4

Table 9.2: Summary of Electrical Propulsion Drive Train

	units	Propulsion turbines (2)	Electrical generators (2)
Weight	tonnes	45.6	15
Diameter	m	1.5	1
Length	m	4.3	1.5
Volume	m^3	15.6	2.4

a thicker flux return shield around the outer periphery of the motors.

The volumes, however, were related as expected. AC motors are able to produce higher torque and power than DC motors for the same size. Of the AC motors, the SCM outperforms the SMPM due to its much higher magnetic flux strength interacting with a stator carrying an increased current density.

Regardless of the electric motor, a definite weight and volume reduction is obtained with an electric motor propulsion system.

9.1.2 Efficiency

The efficiencies of the mechanical and electrical propulsion systems are summarized in Table 9.4. The efficiency of the propulsion turbines for either system at 60% load is 70.3%[20]. The efficiency of a single turbine, de-coupled from the propulsion motor and operating at rated load, is 72.4% (see Appendix A). The efficiencies of all the motors were at or above 99%[2]. The efficiency of each respective converter is also estimated at 99% (see Chapter 8 and [52]). The efficiency of the propulsion generators are 98.7%[32]. Lastly, the efficiency of the reduction gear is estimated at 90% [24].

---

[2]However, the actual efficiency of the two synchronous motors can be expected to be less than what was calculated in these designs due to the higher order harmonic losses that were not accounted for. For this reason the HPM should have a superior efficiency over the two synchronous motors.

Table 9.3: Mechanical vs Electrical Propulsion Drive Train

	units	Mechanical system	Electrical system	SMPM	SCM	HPM
Weight	tonne	193.4	60.6	31.7	21.6	30
Volume	m^3	53.3	17.9	7.7	4.4	10.6
Power Converter/Motor Controller						
Weight	tonne			13.6	13.6	8.6
Volume	m^3			19.1	19.1	11.7
Overall Comparison to Mechanical Drive Train						
Weight	Δtonnes			−87.5	−97.6	−94.2
Weight	%ch			−45.2%	−50.5%	−48.7%
Volume	Δm^3			−8.5	−11.8	−13.1
Volume	%ch			−16%	−22.2%	−24.6%

Table 9.4: Efficiency Summary at 60 Percent Rated Load

	Mechanical	Electrical
Steam Turbine	70.3%	72.4%
Generator	−	98.7%
Converter	−	99%
ReductionGear/Motor	99%	99%
Combined	69.6%	70%

The combined efficiency of the electric drive propulsion system is 70%, which is slightly higher than the combined efficiency of the mechanical drive propulsion system at 69.6%. Therefore, some improvement in efficiency is obtained with an electric propulsion drive train when operating at 60% of maximum speed.

9.2 Qualitative Attributes

For the remaining attributes a qualitative analysis is used.

9.2.1 Harmonics

The SMPM design is expected to have relatively high harmonic torque pulses which will be transmitted through the propulsion drive train and induced in the stator backing iron and structural support. This is due to the low reluctance air gap paths provided by the iron stator winding teeth. Rotor and stator skew can mitigate these harmonic torques to a large degree, but will also reduce

the overall torque output of the motor, resulting in a larger motor to achieve the same torque without skew. Active power converter feedback schemes, such as those discussed in section 8.1.6, can also be utilized to reduce these harmonics.

The SCM, with an air-core stator and rotor, removes the low reluctance harmonic torques which are produced in an iron stator motor. Therefore, complicated and detrimental rotor and winding skew is not necessary. There will still be some harmonic torque components due to the discrete variations in the stator and rotor magnetic field strength azimuthally. These, however, are not expected to be large, and with further analysis and design may be dampened out by the mechanical dynamics of the rotating drive train components (the rotor, shafting and propeller).

The HPM has no spacial or time varying magnetic fields in its design and therefore will have no harmonic torques delivered to the propulsion drive train. The lack of harmonic vibrations should allow the HPM to be hard mounted to the submarine hull without the use of complicated sound isolation mounts[40][3].

9.2.2 Converter Aspects

Both AC motors, the SCM and SMPM, require an AC converter capable of delivering a constant volts/Hz output in order to maintain sufficient torque to the shaft at all speeds. They also require multiple solid state switching elements in series and in parallel to block the supply voltage when they are in the off state and to supply rated current when switched on. They are very complex in construction, control and operation. As discussed in chapter 8, the largest PWM converter known to the author is the 19 MW unit installed at the LBES. From interviews with personnel on site, it is apparent that the installation of this converter was difficult at best. Noise test results indicate switching harmonics carried into the load, causing vibrational noise as well as increased heating of the reactive portions of the load[53]. The prospects of using the much simpler DC buck converter with the HPM are appealing.

---

[3]Sound isolation mounts are frequently used between machinery and the submarine's hull in order to filter the vibrational harmonics. For large propulsion machinery these sound mounts are very heavy and expensive.

9.2.3 Reliability

Determining the reliability of propulsion motors that have yet to be built is difficult. A measure of reliability can be made by the apparent complexity in the engineering of each motor. The SCM appears to be the more complex design, having more components that could possibly fail and thus the lowest reliability. The HPM appears to have the least components and thus the higher reliability. The SMPM lies somewhere in between.

9.2.4 Degradation

Neglecting the yet to be overcome risks for the three motor topologies, all have about equal degraded operation modes. In regard to the two AC motors, both stators are wound with 15 phases for versatility of control with one or more failed phases. If one phase fails, the corresponding symmetric phases can be disabled and the motor can continue balanced torque output at a decreased level. In the event of a loss of cooling to the superconducting pole pieces of the SCM, the motor can still operate as a normal wound rotor motor at a reduced torque output. However, redundant cryogenic coolers can be utilized to limit this possibility.

The third motor, the HPM, also has inherent redundancy in that the current collection brushes are dispersed around the periphery of each drum, and electrically connected in parallel. Failure of a few brush contacts will just reduce the current supplied to the drum turns, rather than disabling the motor. The HPM can also operate without cryogenic cooling to the field coils. Similar to the SCM, redundant cryogenic cooling would be utilized. Further, the HPM can be operated at about half rated torque output with a single superconducting field coil operating.

9.2.5 Torque

The motor design programs discussed in chapters 5 through 7 and given in appendices G through I only evaluate the motors at full power. However, for the synchronous AC motors, the torque characteristics can be controlled by varying the terminal voltage for a given frequency input. With proper voltage and frequency control input to a synchronous AC motor, a constant torque vs. speed output can be obtained. The HPM's torque does not vary with speed and is only a function of the applied current.

9.2.6 Risk

All three motor topologies have yet to be tested at full scale, as in the designs of this thesis. This in itself induces a great deal of risk for all the motors. The particular risks incurred by each motor are as follows:

SMPM

The manufacturing techniques needed to assemble and magnetize, not necessarily in that order, a multi-pole high remanent magnet strength permanent magnet rotor need to be developed. However, there is little doubt that this manufacturing concern will be solved.

SCM

The HTS material used in the superconducting wire of this design is composed of a ceramic, BSCCO-2223. No shock test data was available for this material. For a submarine installation, however, a high shock resilience is required. Therefore, the shock resilience of HTS material must be proven. American Superconductor, the major proponent of HTS synchronous motors, does have a contract with ONR to develop HTS motor technologies and continue proof of concept testing. This is undoubtedly one of the areas that American Superconductor, and other superconducting wire manufacturers are working on.

HPM

The risks that have been associated with HPM technology in the past have been mitigated somewhat, but proof of concept testing is still necessary to validate them.

These risks include:

1. Liquid cryogenics for low temperature superconductors (LTS) have been replaced with mechanical conductive cooled cryogenic units [5], [45].

2. High current density sliding contacts have been developed to replace the liquid metal current collectors previously used [5], [41], [42], [44].

3. Unlike ceramic based HTS wire, LTS have been proven shock resilient. LTS based mine hunting magnets, of suitable size and magnetic strength for a HPM, have been built and shock qualified[40][45].

4. No HPM's of comparable size have been successfully tested to date. However, General Atomics currently has an ONR contract to design and build a 5 kHP multi-drum HPM for proof of concept testing.

5. No data on a suitable DC converter design could be found in open resources. A relatively high power buck type DC/DC converter needs to be developed with low electrical harmonic content in order to utilize the HPM's inherent harmonic free design.

9.2.7 Summary

A qualitative analysis of all three motors is summarized in Table 9.5

Table 9.5: Motor Summary, Qualitative

	SMPM	SCM	HPM
Harmonics	-	+	++
Converter	0	0	+
Reliability	0	0	0
Degradation	0	0	0
Torque	+	+	++
Risk	++	-	-

9.3 Conclusions and Recommendations

If the risk was set aside, or future full scale testing verifies theory, the HPM would certainly be preferred over the SMPM and SCM. The HPM is competitive in size and volume with the other two and has superior torque characteristics. The HPM also has a much simplified controller scheme and its associated power converter has a lower component count with an easily managed current ripple (and associated torque/vibration harmonics) through DC reactive filter components.

Assuming risk, with current technologies, the SMPM should be selected. Several motor manufacturers are currently designing permanent magnet motors of similar topology to the one analyzed

in this work. Their designs are to be fielded on the DD-21. Their extensive research and development for the DD-21 could easily be inserted into a submarine propulsion system. However, additional complexity would need to be introduced in order to reduce the anticipated vibrational harmonics, which are produced by the necessary power converter inverter section (discussed in 8.1.1 and 8.1.6), to a level acceptable for a submarine installation.

The SCM, although much smaller and lighter than the other two designs analyzed, currently adds similar risk to the HPM and the same inverter harmonic problems as the SMPM. In addition, the ceramic based BSCCO-2223 superconductor utilized hasn't met navy shock testing requirements to date. This is a reliability issue, as a single pole piece losing its magnetic field due to an open circuit would cause the propulsion motor's torque characteristics to become unbalanced, resulting in noisy operation and possible further damage. However, future proof of concept research and testing on the SCM motor and its associated power converter, along with the development of more shock resilient HTS materials, may result in a very small and light propulsion system.

9.4 Submarine Arrangements Impact

Shown in Figure 9-1 is a notional arrangements schematic for an electric drive submarine engine room. It utilizes two high speed steam turbines coupled to a pair of high power density generators, permanent magnet or superconducting, such as those described in [22] or [32]. The design of these high speed generators was not developed further in this thesis. However, the weight and volume of a superconducting generator developed in [32] were used in the electrical system data of Table 9.3 and for the efficiencies listed in Table 9.4.

The increased volume and weight allowance in the submarine's engine room can either be filled with additional payloads, such as a pulsed alternator to store high energy electrical energy for use in another system, or the size of the submarine itself could be reduced and rebalanced. Either alternative is now available to the submarine designer and program manager.

9.5 Further work

1. Incorporate higher order harmonics to evaluate numerically the harmonic torque of the electric motors and determine losses associated with the electrical harmonics in the stators and

shielding elements. Having a quantitative value for the harmonic torques would help in determining the motors' OMOE more accurately.

2. Develop a dynamic model for the motors. The individual motor's rotational inertia was calculated in anticipation of incorporating a dynamic model of the shafting and propeller as well as the ship itself. This will enable an evaluation of the dynamic vibrations induced on the shaft line component due to dynamic load and speed changes and enable another OMOE input.

3. Incorporate routines in the computer codes to evaluate generators as well as motors. This will enable an evaluation of the high speed generators that would be used for the power generation portion of the electric drive submarine.

4. Develope a better cost model for the motor analysis which includes stator and rotor fabrication, machining of the various components, assembly, etc.

5. Incorporate electric drive weight and volume impacts into the computer algorithms used in developing the baseline submarine. Parametric engine room data from historical submarine designs is currently used to determine the necessary weight and volume of a submarine's engine room based on the required horsepower. The weight and volume reductions resulting from the use of an electric propulsion motor will reduce these parametric values.
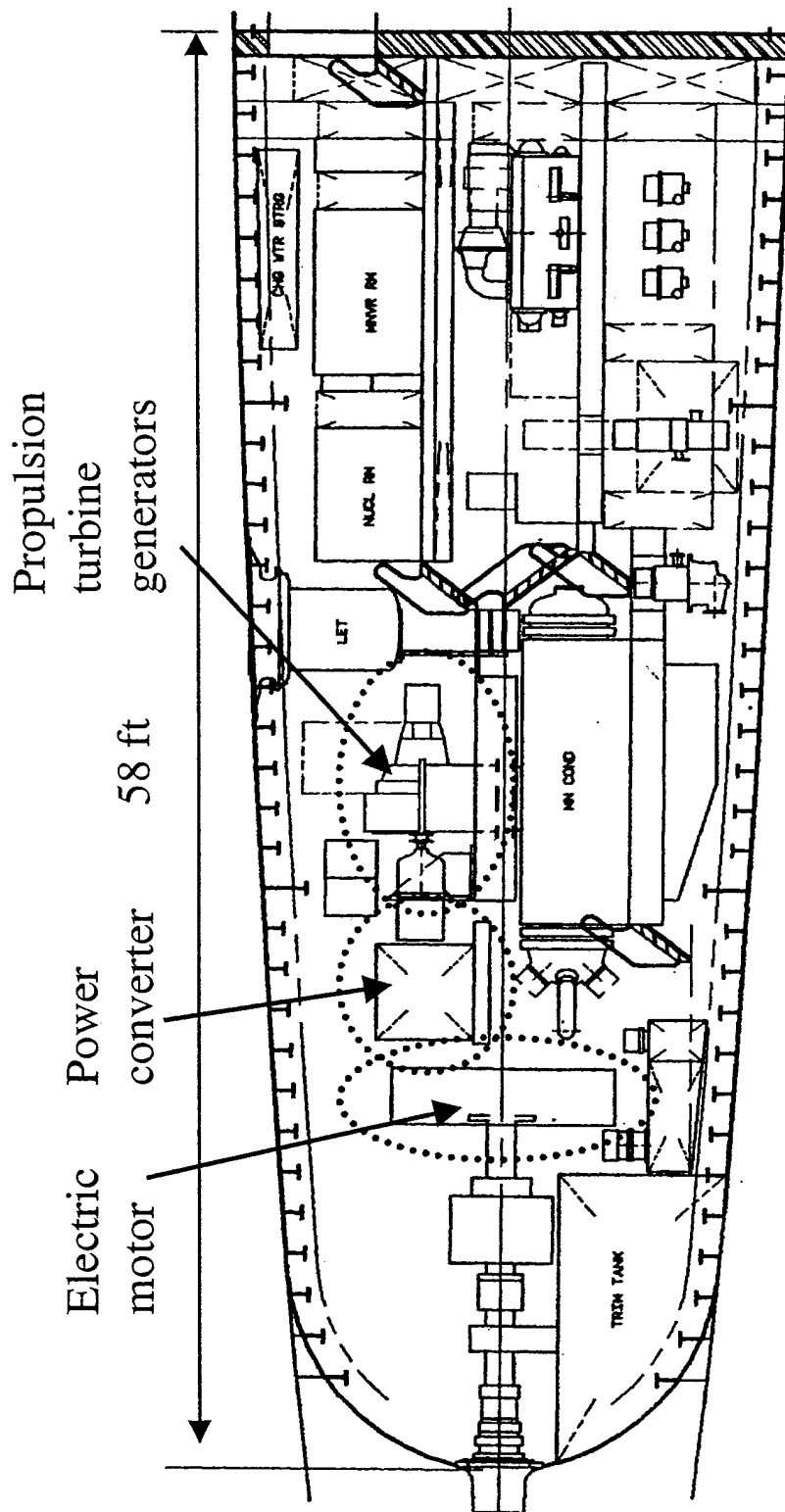
Figure 9-1: Engine room, electric propulsion. Scanned image from [22].

Bibliography

[1] "Naval Systems Update: Navy Ship and Submarine Systems Integration and Program News", Vol. 4, Number 20, November 30, 2000.

[2] Ronald O'Rourke, "Electric-Drive Propulsion for U.S. Navy Ships: Background and Issues for Congress" Congressional Research Services, RL30622, July 31, 2000.

[3] S. Kalsi, B. Gamble, N. Henderson, S. Karon, M. Mulholland, G. Snitchler, R. Howard, W. Sand, P. Winn, C. Gold, "Status of the Navy HTS Superdrive Motor for Ship Propulsion Development" Proceedings Third Naval Symposium on Electric Machines, December 4-7, 2000.

[4] James L. Kirtley Jr, "Design and Construction of an Armature for an Alternator With a Superconducting Field Winding", Doctoral Thesis, E.E., Massachusetts Institute of Technology, 1971.

[5] M. Heiberger, M. Reed, W. P. Creedon, B. J. O'Hea, "Superconducting DC Homopolar Motors for Ship Propulsion", Proceedings Third Naval Symposium on Electric Machines, December 4-7, 2000.

[6] J. A. Moses, J. L. Kirtley Jr., J. H. Lang, R. D. Tabors and F. De Cuadra, "A Computer-Based Design Assistant for Induction Motors", IEEE Industry Applications Society Conference, September 30, 1991.

[7] Wood, Geoffrey. "Electric Propulsion In Warships Then and Now". Naval Forces, No. 3, 1995: 20.

[8] ADM Frank L. "Skip" Bowman, "An Integrated Electric Power System: The Next Step", Undersea Warfare, "U.S. Submarines...Because Stealth Matters", Fall 2000,pp. 2-5.

[9] LCDR J. V. Amy Jr, D. H. Clayton, R. O. Kotacka, "Shipboard Electrical Power Distribution: AC verses DC is not the Issue, Rather How Much of Each is the Issue" Proceedings All Electric Ship: Developing Benefits for Maritime Applications, 29-30 September 1998.

[10] R. Beridge, S. Rigg, G. N. Bishop, "AC or DC for Electricity Distribution to Ships Services?" Proceedings All Electric Ship: Developing Benefits for Maritime Applications, 29-30 September 1998.

[11] J. J. A. Van Der Burgt, R. P. Dill, P. Van Gelder, "Comparison of an AC and a DC Integrated Electrical Distribution System for an All Electric Frigate", Proceedings of Third International Symposium on All Electric Ship, AES 2000, October 26-27, 2000.

[12] J. Courault, "Comparing the Stabilization of AC and DC Networks. Transient rates - Harmonic Pollution", Proceedings Third International Symposium on All Electric Ship, AES 2000, October 26-27, 2000.

[13] S. D. Sudhoff, D. H. Schmucker, R. A. Youngs, H. J. Hegner, "Stability Analysis of DC Distribution Systems Using Admittance space Constraints", Proceedings All Electric Ship: Developing Benefits for Maritime Applications, 29-30 September 1998.

[14] LCDR N. H. Doerry, LCDR J. C. Davis, "Integrated Power System for Marine Applications", Naval Engineers Journal, Vol. 106, May 1994. pp. 77-90.

[15] N. Doerry, H. Robey, J. Amy, "Powering the Future with the Integrated Power System", Engineers Journal, May 1996.

[16] M. Benatmane, T. McCoy, T. L. Cooper, "Electric Propulsion Full Scale Development on U.S. Navy Surface Ships", Proceedings Naval Symposium on Electric Machines, October 26-29, 1998, pp 125-134.

[17] H. Hegner, H. Robey, B. Desai, "Integrated Power System Full Scale Advanced Development Phase II Integration and Test at the US Navy's Land-Based engineering Site", Proceedings Third International Symposium on All Electric Ship, AES 2000, October 26-27, 2000.

[18] M. Benatmane, LCDR T. McCoy, T. Dalton, T. L. Cooper, "Electric Power Generation and Propulsion Motor Development for U.S. Navy Surface Ships", Proceedings All Electric Ship: Developing Benefits for Maritime Applications, 29-30 September 1998.

[19] J. G. Ciezki, R. W. Ashton, "A Technology Overview for a Proposed Navy Surface Combatant DC Zonal Electric Distribution System", Naval Engineers Journal, May 1999, pp. 59-69.

[20] E. A. Avallonem, T. Baumeister III, "Mark's Standard Handbook for Mechanical Enginers" Tenth Edition, McGraw-Hill Publishing, 1996, Chapter 9, pp. 69-71.

[21] C. J. Hanson, D. S. Hunt, M. Galvin, J. P Harbour, "The Next Generation Nuclear Submarine (NGSSN)", design project report, 13.114, Sring 2001.

[22] Thomas B. Dade, "Advanced Electric Propulsion, Power Generation, and Power Distribution", Naval Engineers Journal, March 1994, pp. 83-92.

[23] J. G. Ciezki, R. W. Ashton, "A Survey of AC Drive Propulsion Options", Proceedings Third Naval Symposium on Electric Machines, December 4-7, 2000.

[24] A. D. Carmichael, "Ship Power and Propulsion", Class notes from 13.21, Massachusetts Institute of Technology, Independent Activities Period January, 1999.

[25] H. A. Jackson, Capt. USN (Ret.), "MIT Professional Summer Submarine Design Trends", Class Notes, July 1999.

[26] C. A. Whitcomb. "Naval Ship Design Philosophy Implementation", Naval Engineers Journal, January 1998. pp. 49-63.

[27] James L Kirtley Jr, "Electric Machines", Class notes from 6.685, Massachusetts Institute of Technology, Spring 2000.

[28] A. E. Fitzgerald, C. Kingsley Jr., S. D. Umans, "Electric Machines-Fifth Edition", McGraw-Hill, inc, 1990.

[29] Correspondence with James L. Kirtley Jr., Ph.D., Professor of Electrical Engineering, Massachusetts Institute of Technology, September 2000-June 2001.

[30] B. R. Munson, D. F. Young, T. H. Okiishi, "Fluid Mechanics", John Wiley & Sons, Inc, 1990.

[31] Correspondence with Thomas B. Dade, Senior Technology Engineer, Newport News Shipbuilding, October 2000.

[32] J. L. Smith Jr., J. L. Kirtley Jr., F. C, Rumore, "Superconducting AC Machines for Ship Propulsion", paper presented at the Society of Naval Architects and Marine Engineers Spring Meeting/STAR Symposium, April 26-29, 1978.

[33] "American Superconductor and Rockwell Automation Successfully Operate World's First Commercial-Scale HTS Motor 1,000 Horsepower Motor a Key Milestone in Commercialization of HTS Motors and Generators", Press release, American Superconductor, July 19, 2000.

[34] "American Superconductor Announces New Contract from U.S. Navy for Development of HTS Propulsion Motors", Press release, American Superconductor, November 27, 2000.

[35] N. Kelley, M. Nassi, L. Masur, "Application of HTS Wire and Cables to Power Transmission: State of the Art and Opportunities", Preliminary paper submitted to IEEE Power Engineering Society, Winter Power Meeting, January, 2001.

[36] M. Furuyama, "A Design of a Damper Shield of a Superconducting Alternator", Masters Thesis, M.E., Massachusetts Institute of Technology, 1974.

[37] J. L. Kirtley, "Air-Core Armature Shape: A Comparison of Helical and Straight-With-End-Turns Winding", Electric Machines and Power Systems, V. 23, No 3, 1995, pp 263-278.

[38] Correspondence with Nathan Kelley, Senior Technology Engineer, Pirelli Cables and Systems, January 2001.

[39] J. D. Walters, N. Sondergaard, D. J. Waltman, "Liquid Cryogen Free, Increased Voltage, Homopolar Motor for Propulsion", Proceedings Naval Symposium on Electric Machines, July 28-31, 1997, pp 57-65.

[40] J. D. Walters, N. A. Sondergaard, J. Levedahl, D. J. Waltman, E. M. Golda, T. H. Fikse, "Re-examination os Superconductive Homopolar Motors for Propulsion", Naval Engineers Journal, January 1998, pp. 107-116.

[41] A Versatile Electrical Fiber Brush and Method of Making", D. Kuhlmann-Wilsdorf, November 9, 1982, U.S. Patent #4,358,699.

[42] Doris Kuhlmann-Wilsdorf, "Electric Fiber Brushes-Theory and Observations", IEEE Trans. On Components, Packaging, and Manufacturing Technology-Part A, Vol., 19, NO. 3, September 1996.

[43] Doris Kuhlmann-Wilsdorf, "Metal Fiber Brushes", Chapter 20 of: P. G. Slade, "Electrical Contacts-Principles and Applications", Marcell Dekker, inc, 1999.

[44] L. J. Petersen, et al. "A Study of the Magnetic Field Effects Upon Metal Fiber Current Collectors in a High Critical Temperature Superconducting Homopolar Motor", Proceedings Third Naval Symposium on Electric Machines, December 4-7, 2000.

[45] M. Heiberger, et-all, "Design, Fabrication and Testing of the ALISS Superconducting Mine Countermeasures Magnet", Advances in Cryogenic Engineering, Vol43A, Plenum Press, 1998. pp 77-90, May 1994.

[46] Correspondence with Dr. Doris Kuhlmann-Wilsdorf, University of Virginia and HiPerCon l.l.c., March 2001.

[47] Bumby, J. R,, "Superconducting rotating electrical machines", Oxford Clarendon Press, 1983.

[48] Correspondence with Mike Heiberger, General Atomics September 2000-February 2001.

[49] Dr. M. Benatmane, LCDR T. McCoy, "Development of a 19 MW PWM Converter for U.S. Navy Surfacer Ships", ElecShip '98: International Conference on Electric Ship, September 1 1998.

[50] Correspondence with Jeff Buckley, Alstom, November 2000.

[51] Prof. Alex Q. Huang, "Current and Future High-Power Semiconductor Devices", All Electric Power Symposium October 4, 2000.

[52] J. G. Kassakian, M. F. Schlecht, G. C. Verghese, "Principles of Power Electronics", Addison-Wesley Publishing Company, Inc, 1992.

[53] T. Dalton, CDR T. McCoy, T. Calvert, "Noise Test Results of a PWM Powered 19 MW Advanced Induction Motor Design", Proceedings Third Naval Symposium on Electric Machines, December 4-7, 2000.

[54] K. A. Corzine, S. D. Sudhoff, E. A. Lewis, D. H Schmucker, R. A. Youngs, H. J. Hegner, "Use of Multi-Level Converters in Ship Propulsion Drives", Proceedings All Electric Ship: Developing Benefits for Maritime Applications, 29-30 September 1998.

[55] K. A. Corzine, "Use of Multi-Level Inverters to Reduce High-Frequency Effects in Induction Motor Drives", Proceedings Third Naval Symposium on Electric Machines, December 4-7, 2000.

[56] Gary E. Baumgart, "Advanced Propulsion Motor Controls for Navy Submarine and Surface Vessels", Proceedings Third International Symposium on All Electric Ship, AES 2000, October 26-27, 2000.

[57] A. S. Kallah, B. Hall, V. E. Watson, "Power, Propulsion and Control Systems for the U.S. Coast Guard Polar Icebreaker Healy", American Society of Naval Engineers, 1994 Technology Innovation Symposium, 7-9 September 1994.

[58] K. G. Kerris, P. W. Wheeler, J. C. Clare, L. Empringham, "Implementation of a Matrix Converter using P-Channel Mos-Controlled Thyristors", Power Electronics and Variable Speed Drives, 18-19 September 2000, Conference Publication No. 475.

[59] K. Kerris, T. Podlesak, J. Raftery, "Matrix Converter Research at the Army Research Laboratory: A PEBB Success Story", Presentation at AEPS Program Review - October 2000.

[60] S. E. Lyshevski, A. Menozzi, "Vibration Modeling and Attenuation in Stealth-Technology Electric Drives", Proceedings Third Naval Symposium on Electric Machines, December 4-7, 2000.

[61] P. L. Chapman, S. D. Sudhoff, "A Multiple Reference Frame Synchronous Estimator/Regulator", IEEE Transactions on Energy Conversion, Vol. 15, No. 2, June 2000, pp 197-202.

[62] P. L. Chapman, S. D. Sudhoff, C. A. Whitcomb, "Optimum Current Control Strategies for Non-Sinusoidal Permanent-Magnet Synchronous Machine Drives", IEEE Transactions on Energy Conversion, Vol. 14, No. 3, December 1999, pp 1043-1050.

[63] Victor Donescu of Kaman Aerospace Corp., "Sensorless Control Methods With Regard to PM Machine Propulsion Applications", Proceedings Third Naval Symposium on Electric Machines, December 4-7, 2000.

[64] Dr. P. K. Steimer, "Very High Power PEBB Developments", Presentation at AEPS Program Review - October 2000.

[65] P. Steimer, O. Apledoorn, E. Carroll, "IGCT Devices - Applications and Future Opperturnities", IEEE archives (0-7803-6420-1/00).

[66] G. J. Campisi., "The Status and Future of Silicon Carbide", Proceedings Third International Symposium on All Electric Ship, AES 2000, October 26-27, 2000.

Appendix A

Steam Turbine Efficiency

rated load=	20000	eff at superheated/saturated steam with inlet press of:					
	percent	@ 500 F	@ sat.	@ 650 F	@ sat.	@ 750 F	@ sat.
load	load	250psi	0.96	400psi	0.94	600psi	0.905
875	0.04	63.00%	60.48%	63.00%	59.22%	62.00%	56.11%
1875	0.09	76.00%	72.96%	67.00%	62.98%	66.00%	59.73%
2500	0.13	69.00%	66.24%	69.00%	64.86%	68.00%	61.54%
5000	0.25			74.00%	69.56%	73.00%	66.07%
7500	0.38			76.00%	71.44%	75.00%	67.88%
12500	0.63			78.00%	73.32%	78.00%	70.59%
15625	0.78			79.00%	74.26%	79.00%	71.50%
20000	1.00			79.00%	74.26%	80.00%	72.40%
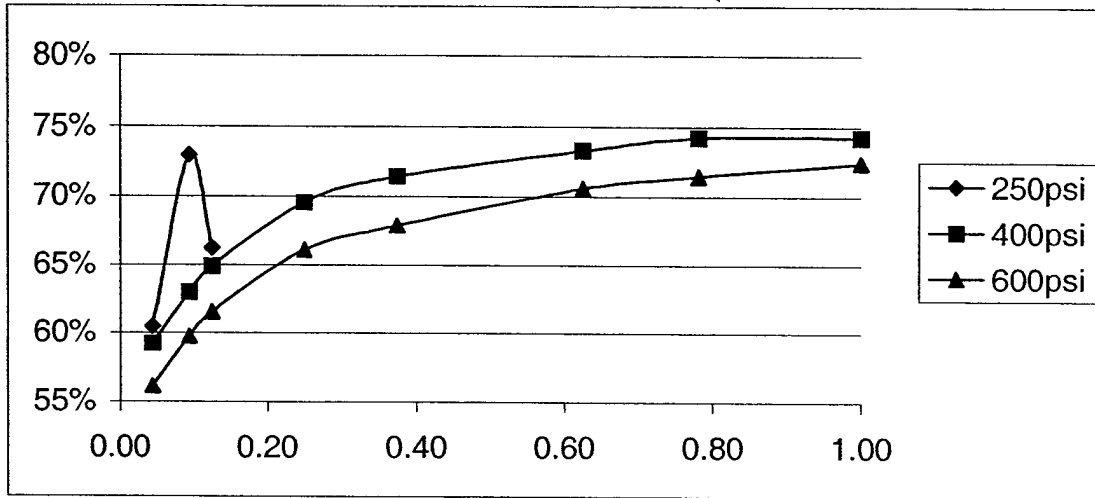
Using 600 psi saturated steam, a 2% reduction in efficiency is noted when the steam turbine is operated at 60% of its rated power. (Data derived from [20]).

Appendix B

Submarine Propulsion Plant Sizing

data from MIT MATHCAD model for
conventional steam turbine, reduction gear
and SSTGs

$$\text{Iton} := 2240 \cdot \text{lb}$$

$$\text{Wold} := \begin{pmatrix} 3538.126 \\ 950.715 \\ 360 \\ 339.837 \\ 529.5 \\ 340.393 \\ 1505.714 \end{pmatrix} \text{lton}$$

The Baseline submarine was designed for 140 shaft RPM

$$\text{SHP} := 28000\text{hp} \quad \text{RPM} := 140 \cdot \text{min}^{-1}$$

from CAPT Harry Jackson's notes pg. 3-12

T.w = width of exhaust trunk, T.L = Length of turbine

$$W_T(T_w, T_L) := 7.5 \frac{\text{lb}}{\text{in}^2}(T_w \cdot T_L) + 20000\text{lb}$$

$$W_{Tp} := 2 \cdot W_T(2 \cdot \text{ft}, 12 \cdot \text{ft}) \qquad W_{Tsstg} := 2 \cdot W_T(2 \cdot \text{ft}, 8 \cdot \text{ft})$$

$$W_{Tp} = 41\,\text{lton} \qquad\qquad W_{Tsstg} = 33.3\,\text{lton}$$

$$W_{Tp} = 41.7\,\text{tonne} \qquad\quad W_{Tsstg} = 33.8\,\text{tonne}$$

2 Propulsion + 2 SSTG's

$$W_{2T} := W_{Tp} + W_{Tsstg}$$

$$W_{2T} = 74.3\,\text{lton} \quad W_{2T} = 75.5\,\text{tonne}$$

Weight of reduction gears

$$K_{rg} := 1000\frac{\text{lb}}{\text{hp} \cdot \text{min}}, 1100\frac{\text{lb}}{\text{hp} \cdot \text{min}} .. 1200 \cdot \frac{\text{lb}}{\text{hp} \cdot \text{min}}$$

$$W_{rg}(K_{rg}) := K_{rg} \cdot \frac{\text{SHP}}{\text{RPM}}$$

$$W_{rg}(K_{rg}) = \qquad \text{use lightest}$$

89	lton
98	
107	

$$W_{2rg} := W_{rg}\left(1000\frac{\text{lb}}{\text{hp} \cdot \text{min}}\right)$$

$$W_{2rg} = 89.3\,\text{lton}$$

$$W_{2rg} = 90.7\,\text{tonne}$$

Volume of steam turbines are estimated using a
cylindrical appoximation

$$V_{Tp} := 2 \cdot \left[12 \cdot \text{ft} \cdot \frac{\pi}{4} \cdot [5 \cdot (\text{ft})]^2 \right] \quad V_{Tsstg} := 2 \cdot \left[8 \cdot \text{ft} \cdot \frac{\pi}{4} \cdot [4 \cdot (\text{ft})]^2 \right]$$

$$V_{Tp} = 471.2\,\text{ft}^3 \quad V_{2T} := V_{Tp} + V_{Tsstg} \quad V_{Tsstg} = 201.1\,\text{ft}^3$$

$$V_{Tp} = 13.3\,\text{m}^3 \qquad V_{2T} = 19\,\text{m}^3 \qquad V_{Tsstg} = 5.7\,\text{m}^3$$

Propeller size and weight
estimate

$$D_p := 12\text{ft} \qquad k := 623\frac{\text{lb}}{\text{ft}^3}$$

7 blades

$$W_p(k, D_p) := k \cdot D_p^3 \cdot .315 \cdot .035$$

$$W_{2P} := W_p(k, D_p)$$

$$W_{2P} = 5.3\,\text{lton}$$

n := 1,2 .. 4   Parametric breakdown of SWPS group 2

$$\text{Wold}_{2frac} := \begin{pmatrix} .33 \\ .2 \\ .25 \\ .22 \end{pmatrix} \begin{matrix} \text{Steam generation} \\ \text{Shielding} \\ \text{Electric + Auxiliaries} \\ \text{Propulsion Machinery} \end{matrix}$$

$$W_{tot} := \sum_n \text{Wold}_{2frac_n} \quad W_{tot} = 1$$

Estimate weight and volume of baseline
electric generators:

$$\rho_{gen} := 5000\text{kg} \cdot \text{m}^{-3} \quad \text{an engineering approx}$$

$$V_{2gen} := 2 \cdot (6\text{ft} \cdot 4\text{ft} \cdot 4\text{ft}) \quad V_{2gen} = 5.4\,\text{m}^3$$

$$W_{2gen} := V_{2gen} \cdot \rho_{gen} \qquad W_{2gen} = 26.8\,\text{lton}$$

$$W_{2gen} = 27.2\,\text{tonne}$$

$W_{2prop} := Wold_2 \cdot Wold_{2frac_4}$

$W_{2prop} = 209.2\,lton$

$W_{2shaft} := W_{2prop} - \left(W_{2T} + W_{2rg} + W_{2P}\right)$

$W_{2T} = 74.3\,lton$

$W_{2rg} = 89.3\,lton$

$W_{2P} = 5.3\,lton$

$W_{2shaft} = 40.3\,lton$

$W_{2steam} := Wold_2 \cdot Wold_{2frac_1}$

$W_{2steam} = 313.7\,lton$

can reduce this some since prime movers can now be placed closer to RC.

Reduction gear size and volume calculations based on 13.21 class notes
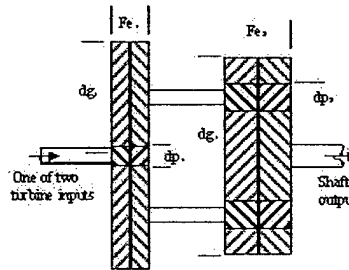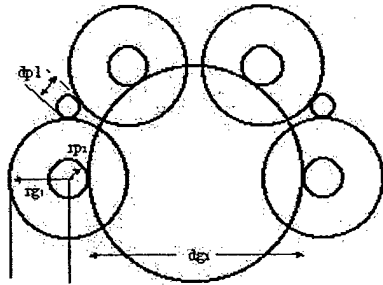
Volume Calculation

$RPM_t := 3600 \cdot min^{-1}$

$C_t := 2.5$

$K_t := 2500$

Ct is face width per pinion diameter, parametric value, class notes 13.21 (1.5 to 2.5, 2.5 for lock train)

use a relatively aggressive gear strength to reduce the size

Kt is measure of gear strength as determined by manufacture (689.5 to 3447.5 kN/m^2)

$dp(PWR,R,rps) := \left[\dfrac{PWR \cdot (R+1)}{\pi \cdot rps \cdot C_t \cdot K_t \cdot R}\right]^{\frac{1}{3}} m$

$dg(dp,R) := R \cdot dp$ PWR in kW

$R_t := \dfrac{RPM_t}{RPM}$ $R_t = 25.7$

Navy standard for double reduction gearing, total reduction is equally split on each stage.

$R_1 := \sqrt{R_t}$ $R_2 := R_1$ $R_1 = 5.1$

$RPM_t = 60\,Hz$

SHP $= 20880\,kW$

drive pinion and first gear

$dp_1 := dp\left(10440, R_1, 60\right)$ $dp_1 = 0.2\,m$

$dg_1 := dg\left(dp_1, R_1\right)$ $dg_1 = 1.1\,m$

$Fe_1 := C_t \cdot dp_1$ $Fe_1 = 0.5\,m$

$\dfrac{SHP}{2} = 10440\,kW$

pinion off of first gear and Bull gear

$dp_2 := dp\left(10440, R_2, \dfrac{60}{R_1}\right)$ $dp_2 = 0.4\,m$

$dg_2 := dg\left(dp_2, R_2\right)$ $dg_2 = 1.9\,m$

$Fe_2 := C_t \cdot dp_2$ $Fe_2 = 0.9\,m$

minimum reduction gear radius is:

need a structural case and clearance for motion

$t_{clr} := 1in$ $t_{case} := 6in$

$r_t := \dfrac{dg_2}{2} + \left(\dfrac{dp_2}{2} + \dfrac{dg_1}{2}\right) + t_{clr} + t_{case}$

$r_t = 1.9\,m$ $d_t := 2 \cdot r_t$ $d_t = 3.8\,m$ $d_t = 12.3\,ft$

111

minimum reduction gear stack length is:

$L_{Quill} := Fe_1 \cdot 2$

Articulated quill shaft couples first gear to second pinion. Assume twice as long as face of first pinion/gear set.

$SL_{rg} := Fe_1 + Fe_2 + L_{Quill}$

weight check $\quad \rho_s := 7800 \text{kg} \cdot \text{m}^{-3}$

$SL_{rg} = 2.6 \, \text{m} \quad SL_{rg} = 8.5 \, \text{ft}$

$Vol_{rg} := \pi \cdot r_t^2 \cdot SL_{rg}$

$W_{rd} := Vol_{rg} \cdot .4 \cdot \rho_s \quad 40\% \text{ steel}$

$Vol_{rg} = 28.8 \, \text{m}^3 \quad Vol_{rg} = 1017.2 \, \text{ft}^3$

$W_{rd} = 89.9 \, \text{tonne}$

Volume and weight comparisons of each electrical system to the baseline mechanical system

Estimate electrical propulsion plant steam turbine and generator weight and size.

Turbine weight

$W_{Tep} := 2 \cdot W_T(2 \cdot \text{ft}, 14 \cdot \text{ft})$

$W_{Tep} = 44.9 \, \text{lton}$

$W_{Tep} = 45.6 \, \text{tonne}$

Turbine volume

$V_{Tep} := 2 \cdot \left[14 \cdot \text{ft} \cdot \frac{\pi}{4} \cdot [5 \cdot (\text{ft})]^2 \right]$

$V_{Tep} = 549.8 \, \text{ft}^3$

$V_{Tep} = 15.6 \, \text{m}^3$

Generator weight and volume

$V_{Pgen} := 2 \cdot \left[1.5 \text{m} \cdot \frac{\pi}{4} \cdot (1\text{m})^2 \right]$

$W_{Pgen} := 2 \cdot 7500 \text{kg} \quad V_{Pgen} = 83.2 \, \text{ft}^3$

$W_{Pgen} = 14.8 \, \text{lton} \quad V_{Pgen} = 2.4 \, \text{m}^3$

$W_{Pgen} = 15 \, \text{tonne}$

Summation of mechanical drive train components

$W_{2mech} := W_{2rg} + W_{2T} + W_{2gen}$

$W_{2mech} = 190.3 \, \text{lton}$

$W_{2mech} = 193.4 \, \text{tonne}$

$Vol_{2mech} := Vol_{rg} + V_{2T} + V_{2gen}$

$Vol_{2mech} = 1.9 \times 10^3 \, \text{ft}^3$

$Vol_{2mech} = 53.3 \, \text{m}^3$

Summation of electrical drive train components excluding motor specific components

$W_{Telec} := W_{Tep} + W_{Pgen}$

$V_{Telec} := V_{Tep} + V_{Pgen}$

$W_{Telec} = 59.6 \, \text{lton} \quad V_{Telec} = 633 \, \text{ft}^3$

$W_{Telec} = 60.6 \, \text{tonne} \quad V_{Telec} = 17.9 \, \text{m}^3$

Percent change formula

$W_{div}(W) := \left(\dfrac{W - W_{2mech}}{W_{2mech}} \right) \quad V_{div}(V) := \left(\dfrac{V - Vol_{2mech}}{Vol_{2mech}} \right)$

Surface Mount Permanent magnet   Assumes 60Hz, three phase 4160 V input

IPS 19MW PWM converter with 1600V IGBT's. Assume 40% weight and volume is fixed in reactive components. Thus if use 3300V IGBT's, the converters weight is reduced by:

$V_{1600} := 5.6\text{m} \cdot 2\text{m} \cdot 2.135\text{m} \qquad W_{1600} := 17 \text{tonne}$

$V_{3300} := V_{1600} \left(\dfrac{.4}{2} + .6 \right) \qquad W_{3300} := W_{1600} \left(\dfrac{.4}{2} + .6 \right)$

$W_{SMPMc} := W_{3300} \qquad\qquad Vol_{SMPMc} := V_{3300}$

$W_{SMPMc} = 13.6 \, \text{tonne} \qquad Vol_{SMPMc} = 19.1 \, \text{m}^3$

$Vol_{SMPM} := \dfrac{\pi}{4} \cdot [3.087 \cdot (\text{m})]^2 \cdot 1.030\text{m}$

$W_{SMPM} := 31.7 \text{tonne} \qquad Vol_{SMPM} = 7.7 \, \text{m}^3$

112

Summation of all SMPM components

$$W_{SMPMt} := W_{SMPM} + W_{SMPMc} + W_{Telec}$$

$$Vol_{SMPMt} := Vol_{SMPM} + Vol_{SMPMc} + V_{Telec}$$

$$W_{SMPMt} = 105.9\,\text{tonne} \quad W_{div}(W_{SMPMt}) = -45.2\,\%$$

$$Vol_{SMPMt} = 44.8\,\text{m}^3 \quad V_{div}(Vol_{SMPMt}) = -16\,\%$$

$$W_{2mech} - W_{SMPMt} = 86.1\,\text{lton}$$

$$W_{2mech} - W_{SMPMt} = 87.5\,\text{tonne}$$

$$Vol_{2mech} - Vol_{SMPMt} = 8.5\,\text{m}^3$$

$$Vol_{2mech} - Vol_{SMPMt} = 300.7\,\text{ft}^3$$

Super conducing AC synch   Assumes 60Hz, three phase 4160 V input
same PWM as above

$$Vol_{SCM} := \frac{\pi}{4} \cdot [2.419 \cdot (m)]^2 \cdot 0.961m$$

$$W_{SCMc} := W_{3300} \qquad Vol_{SCMc} := V_{3300}$$

$$W_{SCMc} = 13.6\,\text{tonne} \qquad Vol_{SCMc} = 19.1\,\text{m}^3$$

$$W_{SCM} := 21.6\,\text{tonne}$$

$$Vol_{SCM} = 4.4\,\text{m}^3$$

Summation of all SCM components

$$W_{SCMt} := W_{SCM} + W_{SCMc} + W_{Telec}$$

$$Vol_{SCMt} := Vol_{SCM} + Vol_{SCMc} + V_{Telec}$$

$$W_{SCMt} = 95.8\,\text{tonne} \qquad W_{div}(W_{SCMt}) = -50.5\,\%$$

$$Vol_{SCMt} = 41.5\,\text{m}^3 \qquad V_{div}(Vol_{SCMt}) = -22.2\,\%$$

$$W_{2mech} - W_{SCMt} = 96.1\,\text{lton}$$

$$W_{2mech} - W_{SCMt} = 97.6\,\text{tonne}$$

$$Vol_{2mech} - Vol_{SCMt} = 11.8\,\text{m}^3$$

$$Vol_{2mech} - Vol_{SCMt} = 417\,\text{ft}^3$$

Homopolar   Assumes 1100 V DC input

Buck and SCR rectifier $\quad W_{HPMc} := 3.2\,\text{tonne} + 5.4\,\text{tonne}$

$$Vol_{HPMc} := (2.19m \cdot 1.5m \cdot 1.8m) + (2.13m \cdot 1.5m \cdot 1.8m)$$

$$Vol_{HPM} := \frac{\pi}{4} \cdot [2.85 \cdot (m)]^2 \cdot 1.659m$$

$$W_{HPMc} = 8.6\,\text{tonne} \qquad Vol_{HPMc} = 11.7\,\text{m}^3$$

$$W_{HPM} := 30\,\text{tonne} \qquad Vol_{HPM} = 10.6\,\text{m}^3$$

Summation of all HPM components

$$W_{HPMt} := W_{HPM} + W_{HPMc} + W_{Telec}$$

$$Vol_{HPMt} := Vol_{HPM} + Vol_{HPMc} + V_{Telec}$$

$$W_{HPMt} = 99.2\,\text{tonne} \qquad W_{div}(W_{HPMt}) = -48.7\,\%$$

$$Vol_{HPMt} = 40.2\,\text{m}^3 \qquad V_{div}(Vol_{HPMt}) = -24.6\,\%$$

$$W_{2mech} - W_{HPMt} = 92.7\,\text{lton}$$

$$W_{2mech} - W_{HPMt} = 94.2\,\text{tonne}$$

$$Vol_{2mech} - Vol_{HPMt} = 13.1\,\text{m}^3$$

$$Vol_{2mech} - Vol_{HPMt} = 462.8\,\text{ft}^3$$

Appendix C

SMPM Non-Dominated Design Space

```
Summary SMPM Motor Attribute  29-Apr-2001
Number of viable candidates optimized     1822
 #   Pwr    Cost   Mass    Dia    Length  Gen     Inerti    JA
     MW     M$     tonne   m      m       Eff     Mg/m^2    A/cm^2
 1   21.02  1.16    51.8   2.956  1.929   0.999     8.0      57.09
 2   21.01  0.69    54.0   3.848  1.346   0.999    27.8      30.56
 3   21.01  1.04    66.6   3.704  1.691   0.999    33.7      45.74
 4   21.02  0.50    41.3   2.662  1.902   0.999     8.9     108.39
 5   21.02  0.56    34.4   2.501  1.976   0.999    10.0     123.09
 6   21.05  0.65    36.7   3.083  1.172   0.998     3.9     145.50
 7   21.02  0.88    43.1   2.711  1.828   0.999     4.7      76.31
 8   21.01  1.29    68.3   4.036  1.547   0.999    48.6      51.23
 9   21.01  1.17    45.7   3.194  1.559   0.999    12.8      79.38
10   21.01  1.32    86.4   3.725  2.407   0.999    47.6      33.86
11   21.02  0.49    39.3   3.093  1.450   0.999    15.7     109.19
12   21.02  0.24    46.9   2.801  1.875   0.999     7.7      72.45
13   21.01  1.10    76.1   4.266  1.520   0.999    34.2      37.99
14   21.02  0.94    37.3   2.789  1.966   0.999    12.8      68.86
15   21.02  0.37    44.6   3.171  1.462   0.999    11.0      67.32
16   21.01  0.74    36.2   3.185  1.178   0.999     9.8      82.66
17   21.02  1.19    52.2   3.307  1.641   0.999    14.3      59.41
18   21.03  0.74    39.3   2.809  1.520   0.998     3.5     116.07
19   21.02  0.95    43.0   3.094  1.522   0.999     7.0      61.80
20   21.01  1.33    53.5   3.937  1.381   0.999    29.2      58.44
21   21.02  0.66    47.2   2.771  2.049   0.999     7.3      85.68
22   21.02  0.39    42.6   3.074  1.661   0.999    20.2      72.70
23   21.02  0.39    35.6   3.282  1.111   0.999    10.8      53.57
24   21.02  0.41    31.7   3.087  1.030   0.999     4.5     110.52
25   21.02  0.95    31.9   2.875  1.449   0.999    10.3     143.60
26   21.03  1.04    39.0   3.066  1.763   0.999    16.6     119.34
27   21.02  0.39    41.2   3.007  1.806   0.999    15.5      99.48
28   21.02  0.74    36.6   3.138  1.404   0.999    14.7     115.64
29   21.02  1.62    42.7   2.849  2.321   0.999    18.4      95.61
30   21.01  1.28    82.5   4.168  1.653   0.999    24.2      34.12

Summary SMPM geometry
 #   Rr     air-gap  hm      lact   wt      hs       p   m  nsp nc q
     m      mm       mm      m      mm      mm
 1  1.01   76.07    458.99   1.90   10.72   347.67   10   1   1   1  15
 2  1.46  105.29    209.85   1.33    4.62   341.13   20   1   3   2  15
 3  1.44  104.27    278.59   1.66   13.05   258.16   13   1   2   1  15
 4  1.00   59.61    159.48   1.89    7.82   246.87   17   1   1   1  15
 5  1.02   58.07    179.81   1.96    7.07   144.43   18   1   2   1  15
 6  0.96  107.33    431.60   1.14   17.25   418.52    7   1   2   3  15
 7  0.89   57.15    404.19   1.82    9.63   366.79   12   1   3   1  15
 8  1.63  114.33    349.60   1.52   12.52   233.46   16   1   1   3  15
 9  1.19   88.78    476.20   1.55   10.07   289.18   16   1   2   1  15
10  1.45  131.03    241.28   2.39    7.18   264.60   18   1   3   1  15
11  1.23   83.20    170.63   1.44    4.27   207.02   16   2   4   2  15
12  0.95   63.78     54.25   1.87    6.63   370.66   17   1   3   1  15
13  1.50  179.83    301.63   1.49   10.09   423.20   13   1   3   3  15
14  1.11   82.37    304.25   1.95    3.04   183.61   20   1   3   2  15
15  1.12   85.45    119.74   1.45    7.12   360.35   17   1   3   2  15
16  1.18   74.49    379.87   1.16   11.19   293.03   13   1   3   2  15
17  1.21   95.97    446.17   1.61   11.42   304.46   11   1   1   3  15
18  0.87   85.96    425.17   1.50    6.82   392.00    7   2   5   1  15
19  1.03   77.01    446.22   1.51    6.09   408.81   14   1   1   2  15
```

```
20 1.50 174.82    465.82    1.35    4.68    257.30    12  2  3  1  15
21 0.94  94.14    212.89    2.04    4.52    317.99    11  2  5  1  15
22 1.26  77.91    109.06    1.64    6.26    177.07    18  1  1  2  15
23 1.20  66.82    167.20    1.11    2.48    350.37    20  2  3  1  15
24 1.00  77.57    243.46    1.03    7.98    448.17    17  1  3  1  15
25 1.15  83.30    433.79    1.44    4.66    179.48    15  2  5  2  15
26 1.22 126.46    346.23    1.75    2.87    166.87    17  2  5  1  15
27 1.16 125.03    106.17    1.77    5.38    200.04    14  1  2  2  15
28 1.24 104.89    289.03    1.39    2.86    195.33    15  3  4  1  15
29 1.18  99.28    461.00    2.30    2.27    123.26    17  2  2  1  15
30 1.36 149.08    360.95    1.64    7.35    555.22    16  1  3  2  15
```

```
D  =     r        g       hm       l        wt       fsd
DU = 2.5000   0.5000   0.5000   4.0000   0.1000   1.0000
DM = 1.1130   0.0824   0.3042   1.9493   0.0030   0.1650
DL = 0.1000   0.0001   0.0100   0.2000   0.0001   0.0010
DS = 1.1928   0.2485   0.2435   1.8886   0.0497   0.4965
DIN =   pmax    mmax  nspmax  ncmax  qmax
DIN =    20       5      5      5      3
```


SMPM

Design # 24 dominates with OMOE = 0.656128

Appendix D

SCM Non-Dominated Design Space

Summary SC Motor Attribute   29-Apr-2001
Number of viable candidates optimized   1924

#	Pwr MW	Cost M$	Mass tonne	Dia m	Length m	Gen Eff	Inerti Mg/m^2	JA A/cm^2
1	21.09	0.05	28.8	2.154	1.657	0.996	5.2	120.09
2	21.07	0.08	39.5	2.647	1.775	0.997	15.7	44.62
3	21.08	0.07	33.0	2.721	1.135	0.996	5.9	85.95
4	21.08	0.04	23.6	2.383	1.335	0.996	7.8	101.03
5	21.09	0.06	28.8	2.752	0.958	0.996	10.8	120.62
6	21.08	0.05	21.6	2.419	0.961	0.996	2.6	119.51
7	21.07	0.06	34.9	2.272	1.809	0.997	11.5	70.14
8	21.07	0.09	40.8	3.229	1.497	0.997	28.0	43.65
9	21.08	0.06	24.4	2.548	1.353	0.996	5.1	84.33
10	21.09	0.06	26.4	2.314	1.218	0.996	3.9	128.16
11	21.09	0.06	24.0	2.515	0.964	0.996	2.9	144.48
12	21.07	0.09	40.8	2.965	1.296	0.996	7.2	68.05
13	21.08	0.04	24.8	2.371	1.470	0.996	8.7	105.52
14	21.09	0.05	21.5	2.397	1.023	0.996	2.8	131.89
15	21.08	0.08	37.3	2.797	1.146	0.996	11.1	95.54
16	21.08	0.06	29.4	2.457	1.173	0.996	5.1	113.95
17	21.07	0.08	35.0	2.461	1.893	0.997	8.6	45.48
18	21.09	0.09	45.4	2.504	1.892	0.996	10.5	93.89
19	21.08	0.12	57.5	2.580	2.068	0.996	22.1	69.56
20	21.07	0.10	42.1	2.516	1.641	0.997	6.8	46.31
21	21.07	0.11	68.1	2.858	2.089	0.997	37.9	29.67
22	21.08	0.11	55.5	2.932	1.026	0.996	7.3	119.14
23	21.08	0.09	42.5	2.856	1.185	0.996	9.6	81.01
24	21.08	0.05	58.8	1.999	3.205	0.996	26.0	112.53
25	21.07	0.11	52.8	2.880	1.319	0.997	9.7	68.14
26	21.11	0.08	35.6	2.393	1.661	0.995	8.0	134.32
27	21.07	0.07	47.9	2.192	2.503	0.997	17.3	53.17
28	21.07	0.07	31.5	2.429	1.818	0.997	7.6	56.21
29	21.09	0.06	30.0	2.530	1.165	0.996	5.5	115.39
30	21.07	0.10	55.3	2.438	2.333	0.997	13.0	47.91

Summary SC synch geometry

#	Rfi m	air-gap mm	tsc mm	lrot m	tarm mm	p	nc	q
1	0.53	34.23	5.36	1.04	321.19	2	14	15
2	0.72	52.40	1.70	0.96	394.66	2	8	15
3	0.61	32.86	22.81	0.66	486.65	3	19	15
4	0.68	3.13	1.80	0.61	351.28	2	14	15
5	0.72	1.95	28.13	0.64	470.22	5	10	15
6	0.51	14.15	26.38	0.56	469.50	3	23	15
7	0.64	3.57	2.15	1.12	327.19	2	11	15
8	1.04	25.23	1.06	0.42	373.96	2	2	15
9	0.60	62.68	3.02	0.65	459.81	2	16	15
10	0.51	19.93	22.07	0.81	405.53	3	19	15
11	0.53	56.20	29.61	0.52	430.85	3	11	15
12	0.69	48.36	8.18	0.51	484.83	2	3	15
13	0.67	56.46	1.60	0.70	301.04	2	8	15
14	0.51	23.95	23.15	0.62	465.05	3	24	15
15	0.69	29.50	28.44	0.75	451.94	4	21	15
16	0.57	7.59	19.86	0.74	426.23	3	11	15
17	0.58	37.89	1.07	1.23	486.87	2	9	15
18	0.58	60.86	15.27	1.42	416.36	3	4	15
19	0.67	11.97	23.88	1.77	444.98	5	9	15

118

```
20   0.53   15.12     27.05   1.22   484.61     3    8  15
21   0.86   14.51      2.58   1.19   333.24     2    4  15
22   0.69   15.78     28.35   0.51   341.33     3    7  15
23   0.69   12.11     19.35   0.68   461.33     3    2  15
24   0.64   70.41      1.56   2.45   110.95     2    6  15
25   0.66   49.12     28.27   0.80   412.77     3    1  15
26   0.55   69.67     27.71   1.32   400.09     4    2  15
27   0.63   27.37      1.56   1.80   288.09     2    4  15
28   0.57   66.54      1.15   1.13   446.39     2   11  15
29   0.59   19.19     19.24   0.72   437.88     3   18  15
30   0.60   50.39      6.04   1.64   355.78     2    2  15

DM  =     Rfi       g       tsc      lrot    tarm
DU  = 1.5000   0.1000   0.0300   3.0000   0.5000
DM  = 0.6650   0.0120   0.0239   1.7714   0.4450
DL  = 0.5000   0.0010   0.0010   0.2000   0.0010
DS  = 0.4828   0.0478   0.0140   1.3518   0.2409
DIN =    pmax   ncmax  qmax
DIN =     20      40     15
```


Design # 6 dominates with OMOE = 0.629248

119

Appendix E

HPM Non-Dominated Design Space

Summary HPM Motor Attribute   24-Apr-2001
Number of viable candidates optimized   1236

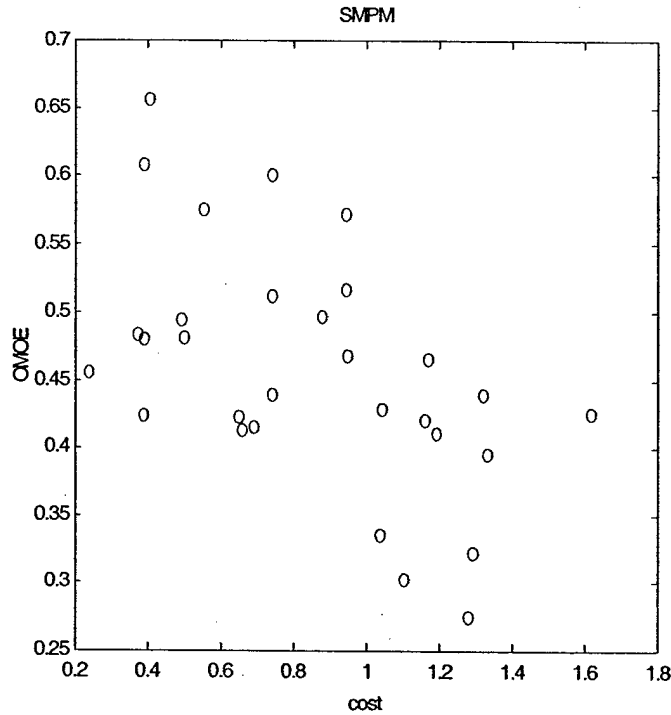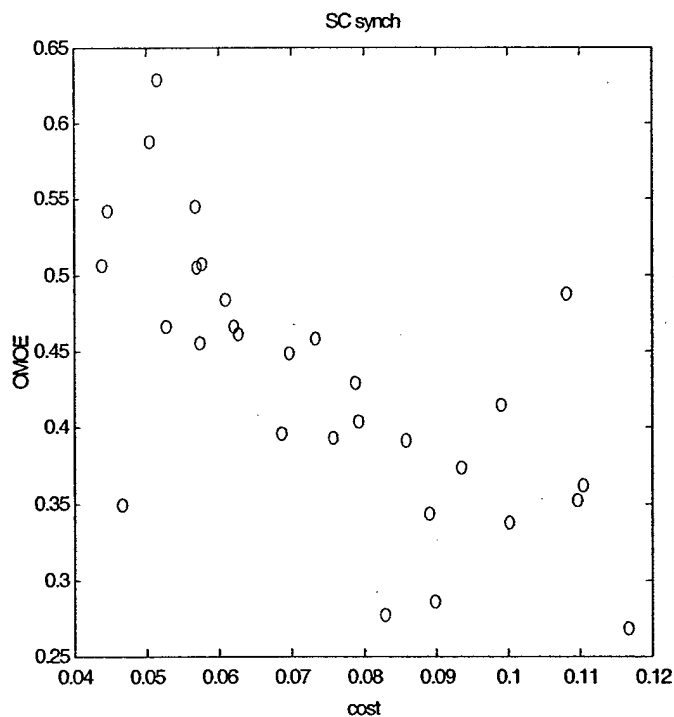| #	Pwr MW	Cost M$	Mass tonne	Dia m	Length m	Gen Eff	Inerti Mg/m^2	Ja A/cm^2
1	21.09	0.15	45.0	3.462	1.296	0.996	18.9	22.70643
2	21.11	0.09	41.7	3.768	1.562	0.995	16.7	67.47105
3	21.27	0.10	37.2	3.517	1.327	0.987	17.9	46.88799
4	21.14	0.30	76.2	4.001	1.487	0.993	56.3	35.31176
5	21.09	0.14	62.8	1.864	2.476	0.996	1.2	103.59831
6	21.17	0.12	33.4	1.990	2.005	0.992	4.2	81.77263
7	21.16	0.12	46.2	2.629	1.634	0.993	6.2	30.51131
8	21.10	0.08	30.0	2.850	1.659	0.995	7.6	115.23440
9	21.16	0.08	50.2	3.884	2.507	0.992	30.8	128.22000
10	21.13	0.21	68.7	3.386	1.705	0.994	24.5	12.36429
11	21.09	0.10	36.6	2.334	1.906	0.996	4.1	73.30967
12	21.20	0.14	67.5	3.357	1.970	0.990	14.6	23.07652
13	21.08	0.08	75.5	5.176	2.134	0.996	100.9	76.92336
14	21.10	0.20	76.8	3.395	1.579	0.995	18.2	8.30469
15	21.13	0.13	44.3	3.142	2.094	0.994	16.0	67.54394
16	21.09	0.14	69.2	2.174	2.303	0.996	2.3	47.13380
17	21.16	0.12	83.2	3.729	2.261	0.992	14.5	30.54293
18	21.13	0.26	61.3	2.743	2.076	0.994	26.3	31.44602
19	21.14	0.15	55.5	3.058	2.546	0.993	15.4	45.05367
20	21.10	0.32	87.3	2.530	2.645	0.995	26.5	21.10257
21	21.10	0.10	65.2	4.020	2.041	0.995	49.0	60.14484
22	21.23	0.07	44.5	3.890	2.045	0.989	26.2	110.97289
23	21.10	0.23	67.7	4.163	1.583	0.995	50.9	35.17711
24	21.10	0.18	69.6	1.870	2.647	0.995	4.6	66.14367
25	21.12	0.14	46.6	1.933	2.860	0.994	3.5	89.42201
26	21.12	0.10	60.4	4.222	1.863	0.994	38.2	93.80158
27	21.11	0.24	63.6	2.208	2.817	0.995	16.2	37.32889
28	21.15	0.15	76.2	3.195	2.148	0.993	7.9	27.41795
29	21.12	0.19	76.9	2.924	2.274	0.994	11.6	16.66837
30	21.09	0.14	63.4	3.793	2.422	0.996	42.6	56.57868

Summary HPM Motor geometry

#	Lrot m	Rri m	trot m	tins m	Rc m	tc m	wc m	Nturns
1	0.99	1.38	0.019	0.004	1.34	0.530	0.107	13
2	0.74	1.58	0.008	0.004	0.94	0.639	0.380	20
3	1.03	1.55	0.025	0.005	1.56	0.267	0.103	5
4	1.14	1.43	0.018	0.002	1.79	0.179	0.134	25
5	0.81	0.68	0.007	0.004	0.64	0.392	0.580	17
6	1.56	0.70	0.018	0.001	0.54	0.564	0.147	12
7	0.93	1.00	0.035	0.009	0.76	0.898	0.252	6
8	1.22	1.16	0.005	0.008	0.84	0.548	0.171	17
9	1.15	1.80	0.006	0.004	0.78	0.458	0.640	9
10	1.32	1.32	0.055	0.010	1.20	0.921	0.119	5
11	1.24	0.85	0.008	0.009	0.58	0.834	0.238	16
12	0.99	1.48	0.044	0.003	1.06	0.658	0.388	3
13	1.16	2.43	0.003	0.006	1.28	0.645	0.452	12
14	0.87	1.30	0.062	0.006	1.23	0.915	0.242	5
15	1.49	1.31	0.011	0.005	0.83	0.374	0.262	13
16	0.87	0.85	0.013	0.005	0.59	0.844	0.498	10
17	0.63	1.70	0.026	0.002	1.04	0.801	0.721	4
18	1.65	0.74	0.027	0.009	0.92	0.336	0.160	16
19	1.57	1.29	0.018	0.005	0.90	0.268	0.421	8

```
20  1.82 0.63   0.031 0.005  0.87  0.336  0.287  16
21  1.52 1.90   0.006 0.003  1.47  0.527  0.194   6
22  0.94 1.82   0.009 0.001  0.91  0.468  0.516   7
23  1.25 1.66   0.011 0.003  1.13  0.560  0.144  26
24  1.07 0.35   0.014 0.008  0.55  0.475  0.550  24
25  1.70 0.69   0.012 0.003  0.38  0.567  0.457  15
26  0.97 2.00   0.005 0.007  1.88  0.197  0.366   5
27  1.54 0.47   0.023 0.002  0.47  0.397  0.541  23
28  0.65 1.40   0.031 0.004  1.26  0.382  0.594   4
29  1.18 1.15   0.044 0.007  0.88  0.632  0.415   5
30  1.99 1.65   0.007 0.008  1.10  0.487  0.174  13
```

DM =	Lrot	Rri	trot	tins	Rc	tc	wc
DU =	4.0000	4.0000	0.1000	0.0100	5.0000	1.0000	1.0000
DM =	0.9934	1.3834	0.0186	0.0038	1.3400	0.5298	0.1066
DL =	0.5000	0.2500	0.0010	0.0010	0.2500	0.0200	0.0500
DS =	1.7500	1.8750	0.0495	0.0045	2.3750	0.4900	0.4750

```
DIN =  Nturns
DIN =    30
```
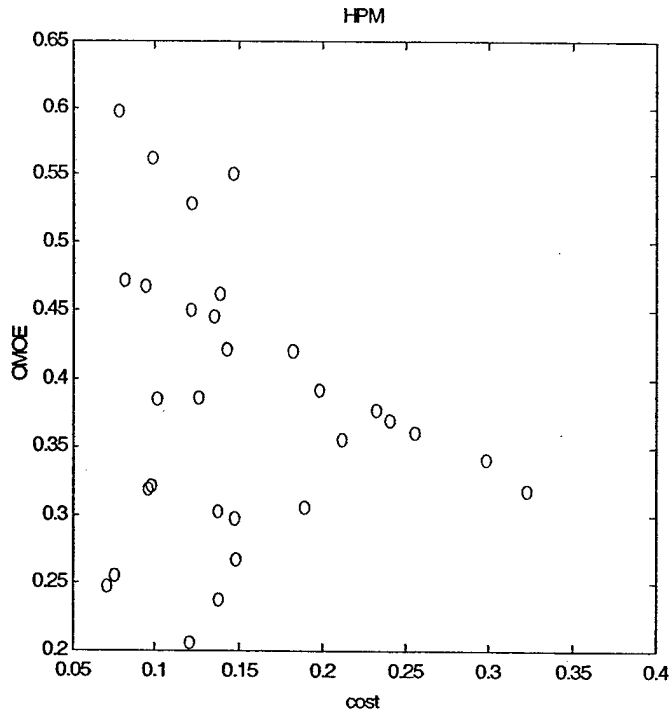

Design # 8 dominates with OMOE=0.597782

Appendix F

Buck Converter Reactive Component Values

Calculation of buck converter inductor and capacitor values
From Principles of Power Electronics
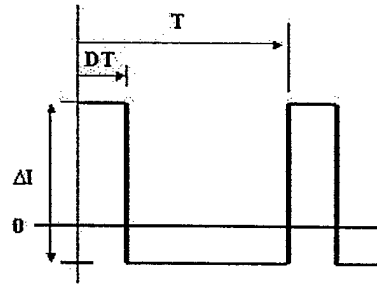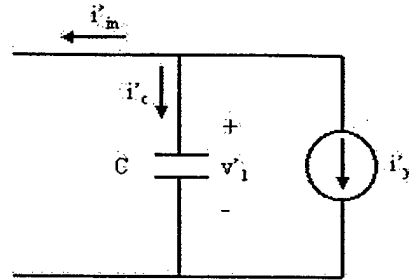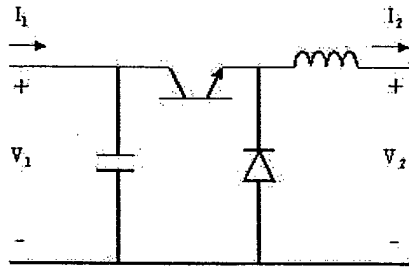
$MW := 1 \cdot 10^6 W$

$f_{sw} := 50 kHz$

$pwr := 21 MW$

$i_{rip} := 5\%$

$V_1 := 1100 V$

$R_{in} := 1\Omega$

$V_2 := 841 V$

$T_{sw} := \dfrac{1}{f_{sw}}$　　　$T_{sw} = 20 \times 10^{-6} s$

$I_2 := \dfrac{pwr}{V_2}$　　$I_2 = 24.97 \times 10^3 A$

$D := \dfrac{V_2}{V_1}$　　　$D = 764.545 \times 10^{-3}$

$I_1 := I_2 \cdot D$　　　$I_1 = 19.091 \times 10^3 A$

$\Delta v_1 := i_{rip} \cdot I_1 \cdot R_{in}$　　$\Delta v_1 = 954.545 \times 10^0 V$

$L_{out} := \dfrac{V_2 \cdot (1 - D) \cdot T_{sw}}{i_{rip} \cdot I_2}$　　　$L_{out} = 3.172 \times 10^{-6} H$

$C_{out} := \dfrac{(1 - D) I_2 \cdot D \cdot T_{sw}}{\Delta v_1}$　　　$C_{out} = 94.182 \times 10^{-6} F$

Appendix G

SMPM MATLAB™ code

```
% Surface magnet script for propulsion motor for use with ndasm
% Stator defined as formed coils with lama=packing factor

clear               % Clean slate
NA = 8;             % attributes
NDE = 30;           % designs to keep
NITER = 10000;      % shots to try
DEBUG=1;            % 1=debug output, 2=screen output
                    % 3=attribute output, 4=std reduction optimization
DF=.999;            % Standard deviation reduction factor
viable=0;           % index of viable designs

% Variables Inputs:

% Lower Limit
r = .1;             % Rotor radius
g = .0001;          % Air-gap
hm = .01;           % Magnet Thickness
l = .2;             % Active Length
wt = .0001;           % tooth width
fsd = .001;          % Slot depth to bottom ratio
% Lower limir vector
DL = [r g hm l wt fsd];

% Upper Limit
r = 2.5;            % Rotor radius
g = .5;             % Air-gap
hm = .5;            % Magnet Thickness
l = 4;              % Active Length
wt = .1;            % tooth width
fsd = 1;            % Slot depth to bottom ratio
% Upper limit vector
DU = [r g hm l wt fsd];

ND = size(DL,2);        % continuous design space
DM=(DL+DU)/2;           % Mean value array
DS=(DU-DL)/2;           % initial standard normal multplier vector

% Limits of integer variables
pmax = 20;              % Pole Pairs
mmax = 5;               % Slots per pole per phase
nspmax = 5;             % Slots short pitched
ncmax =5;               % Turns per coil
qmax = 3;               % number of phases
% Integer upper limit vector
DIN = [pmax mmax nspmax ncmax qmax];

% fixed inputs
rpm = 100;       % Rotational speed
Preq = 21*10^6;% Required power
Vll = 4160;      % line-line voltage
Br = 1.9;        % Magnet Remanent Flux Density
thme = 2*pi/3;   % Magnet Electrical Angle
siga = 5e7;      % Stator Conductivity
P0=1.3;           % Iron Model: Base Dissipation
F0=60;           % Base Frequency
B0=1;            % Base Flux Density
```

```
epb=1.88;        % Flux Exponent
epf=1.53;        % Frequency Exponent
rhos=7800;       % Steel Density
rhom=7418;       % Magnet Density
rhoc=8960;       % Conductor Density
Jalim = 1.5e6;   % armature current density limit [A/m2]
Pmag = 100;      % magnet price: $/kg
Pcu = 5;         % copper price: $/kg
Pfe = 2;         % iron price: $/kg
Btsat = 1.3;     % maximum tooth flux density
Bisat = 1.3;     % maximum iron flux density
vtip = 230;      % max tip speed m/s
etamin = .4;     % min efficiency
hd = .002;       % Slot depression depth
wd = .005;       % Slot depression width
pf = 1;          % Required power factor (+ => lag)
lama=.4;         % armature packing factor
Dmax=5;          % maximum overall diameter allowed
Mmax=100;        % Maximum overall mass allowed
DoverLmax=3;     % aspect ratio limit

B = [rpm Preq Vll Br thme siga P0 F0 B0 epb epf rhos rhom rhoc Jalim
Pmag...
   Pcu Pfe Btsat Bisat vtip etamin hd wd pf lama Dmax Mmax DoverLmax];

% Here are the matrices that NDA will fill out

MA = zeros(NDE, NA);        % design attributes across rows
MD = zeros(NDE, ND);        % design variables (continuous)
NI = length(DIN);           % number of integer variables
MDI = zeros(NDE, NI);       % design variables (integers)
DI = zeros(size(DIN));      % space for integer variables

MAOpt = zeros(NDE, NA);     % scratchpad for optimized machine
MDOpt = zeros(NDE, ND);     % ditto

% run ndasm or runsm
```

```
%
% ***************************************************************** %
%                                                                 %
%              Novice Design Assistant Surface mount PM           %
%                           ndasm                                 %
%                   by Joe Harbour 12/14/00                       %
%          Derived/coverted from J.L. Kirtley Jr. nda             %
%                    used with permision                          %
% ***************************************************************** %
%
% Requires an attribute generating function called this way:
% [A, g] = attribut(D, DI, B, Out)
% A is a vector of attributes of size NA
%   Attributes are all positive and goodness is increaseing
% g is a scalar that is 0 if a design is not viable and 1 if it is
% D is a vector of design variables that nda will manipulate
%   it is of size ND
% DI is a vector of integer variables to be varied randomly
%   it is of size NI
% B is a vector of design variables that will remain fixed
% Out = 1 will cause the thing to print
% DL, DU, DS and DM are starting points for the vector D
% DL and DU are lower and upper limit points
% DM is the median value to be used in generating D
% DS is a vector of standard deviation to be used in generating D
% DIN is the vector of ranges of the elements of DI
% NDE is the number of design points to be accumulated
% NITER is the total number of shots to be tried
% Output will be accumulated in two matrices
% MA [NA, NDE] holds the attributes of all designs
% MD [ND, NDE] holds the design variables
% These matrices are declared in the setup program, so
% that NDA can be run over again

if DEBUG==1,
    fprintf('DU= %6.4f %6.4f %6.4f %6.4f %6.4f %6.4f %6.4f\n',DU(:));
    fprintf('DM= %6.4f %6.4f %6.4f %6.4f %6.4f %6.4f %6.4f\n',DM(:));
    fprintf('DL= %6.4f %6.4f %6.4f %6.4f %6.4f %6.4f %6.4f\n',DL(:));
    fprintf('DS= %6.4f %6.4f %6.4f %6.4f %6.4f %6.4f %6.4f\n',DS(:));
end;
for i = 1:NITER,
    temp=randn(1, ND);
    D = DM + DS .* randn(1, ND);     % generate a random input

    if sum([DL>D]+[DU<D]) == 0,      % if design is in range, continue
        for ii = 1:NI,        % generate the integer random
            pt = randperm(DIN(ii));          % variables
            DI(ii) = pt(1);
        end

        DI(5)=15;    % set number of phases desired

        if DEBUG==1,
            fprintf('%3.3f design in range ',i/NITER);
        end

        [A, g] = attributsm(D, DI, B, DEBUG);  % generate design
```

```matlab
        if g ~= 0,              % if viable, do dominance check
            viable=viable+1;
            fprintf(' viable at %3.3f complete\n',i/NITER);
            for nd=1:NDE,            % dominance check against gross
dimensions in array
                % A=[Pmax 1/Cost 1/Mass 1/Dover 1/Lover eff 1/J 1/Ja] \n')
            if sum(A(3:NA-2)>MA(nd,3:NA-2))== NA-4,
                % every element of A is greater than stored element at
index nd.
                % Replace MA(nd) with A.
                MA(nd, :) = A;      % it goes here
                MD(nd, :) = D;      % save design too!
                MDI(nd, :) = DI;
                fprintf('Replacing Design %5.0f At %3.3f complete\n',
nd, i/NITER);
                if DEBUG==4,   % use as baseline design, refine Standard
deviation vector
                    DM=D;
                    Dtemp=DS*DF;
                    DS=Dtemp;
                end
                break;
            end % dominance check
        end % end storage array for loop
    end  % viable check
  end % design in range check
end % NITER

% run output program
% Msm
```

```
function[A, C] = attributsm(D, DI, B, DEBUG)
% ***************************************************************** %
%                                                                 %
%          Permanent Magnet Motor, Stator in Slots                %
%                       Surface Magnets                           %
%          Copyright 1995, 1997, 2000 James L. Kirtley Jr.        %
%                 converted/updated 12/10/00 by Joe Harbour       %
%                                                                 %
% ***************************************************************** %
% Requires input variables generated by nda:

% Here are the fixed variables, defined in B[]
rpm = B(1);         % Rotational speed
Preq = B(2);        % Required power
Vll = B(3);         % line-line voltage
Br = B(4);          % Magnet Remanent Flux Density
thme = B(5);        % Magnet Electrical Angle
siga = B(6);        % Stator Conductivity
P0 = B(7);          % Iron Model: Base Dissipation
F0 = B(8);          % Base Frequency
B0 = B(9);          % Base Flux Density
epb = B(10);        % Flux Exponent
epf = B(11);        % Frequency Exponent
rhos = B(12);       % Steel Density
rhom = B(13);       % Magnet Density
rhoc = B(14);       % Conductor Density
Jalim = B(15);      % armature current density limit
Pmag = B(16);       % magnet price: $/kg
Pcu = B(17);        % copper price: $/kg
Pfe = B(18);        % iron price: $/kg
Btsat = B(19);      % maximum tooth flux density
Bisat = B(20);      % maximum iron flux density
vtip = B(21);       % max tip speed m/s
etamin = B(22);     % min efficiency
hd = B(23);         % slot depression depth
wd = B(24);         % slot depression width
psi = B(25);        % Required power factor (+ => lag)
lama=B(26);         % armature packing factor
Dmax=B(27);         % maximum overall diameter allowed
Mmax=B(28);         % maximum overall mass allowed
DoverLmax=B(29);    % maximum aspect ratio allowed

% Here are the continuous variables to search, defined in D[]
r = D(1);           % rotor radius (rotor structure plus magnets)
g = D(2);           % air-gap
hm = D(3);          % magnet thickness
l = D(4);           % active length
wt = D(5);          % tooth width
fsd = D(6);         % slot depth to bottom ratio

% Here are the discrete variables to search, defined in DI[]
p = DI(1);          % number of pole pairs
m = DI(2);          % slots per pole per phase
nsp = DI(3);        % slots short-pitched
nc = DI(4);         % Turns per coil
q = DI(5);          % number of input phases
```

```
% Here are a few constants
muzero=pi*4e-7;            % free-space permeability
cpair = 1005.7;           % mass heat capacity of air
rhoair = 1.21;            % density of air
nuair = 1.79e-5;          % dynamic viscosity of air [N*s/m^2]
etf = .25;                % efficiency of fan
dtt = 50;                 % allowable temperature rise

% A=[1/Pmax 1/Cost 1/Mass 1/Dover 1/Lover eff 1/J 1/Ja];
A = [1 0 0 0 0 0 0 0];    % poor design but not an empty array
C=0;                      % not viable yet

% First, generate the rest of the geometry
ns = 2*q*m*p;                       % Number of stator slots
na = 2*m*p*nc;                      % Number of armature turns
hs = fsd*r;                         % slot depth
lamt = ns*wt/(2*pi*(r+g+hd));       % tooth fraction at slot top (gap side)
wst = 2*pi*(r+g+hd)*(1-lamt)/ns;    % slot top width
wsb = wst*(r+g+hd+hs)/(r+g+hd);     % slot bottom width

% check slot area sufficient:
if lamt > .6, % thus lams < .4; no room for armature
   C = 0;
   if DEBUG==1, fprintf('lamt= %g\n',lamt); end
   return;
end;

nsfp = ns/(2*p);          % full-pitched coil throw
nsct = nsfp - nsp;        % actual coil throw

% estimate of end cone length
tb=sqrt(wt^2+(hs/2)^2);             % coil departure run
thetae = atan(wst/tb);              % coil departure angle
laz = pi*(r+g+hd+.5*hs)*nsct/ns;    % azimuthal travel (half end)
le1 = laz*tan(thetae);              % end length (axial)
le2 = laz/cos(thetae);              % end length (half coil)

% Electrical frequency
f = p*rpm/60;
om = 2*pi*f;
stip = r*om/p;            % magnet speed

% check surface speed
if stip > vtip,
   C = 0;
   if DEBUG==1, fprintf('stip= %g\n',stip); end
   return;
end;

% Winding factor
gama = 2*pi*p/ns;
kb = sin(m*gama/2)/(m*sin(gama/2));
alfa = pi*nsct/nsfp;
kp = sin(alfa/2);
kw = kb * kp;

% Calculation of magnetic field
```

131

```
rmi=r-hm;
if rmi < 0,
   C = 0;
   if DEBUG==1, fprintf('hm > r, rmi= %g\n',rmi); end
   return;
end;
rs=r+g;
if p==1,
 kg = (.5*(r^2-rmi^2)+rmi^2*log(r/rmi))/(rs^2-rmi^2);
else
 kg = (rs^(p-1)/(rs^(2*p)-rmi^(2*p)))*...
      ( (p/(p+1))*(r^(p+1)-rmi^(p+1))+...
        (p/(p-1))*(rmi^(2*p)) * (rmi^(1-p)-r^(1-p)) );
end
B1 = (4/pi)*sin(thme/2)*Br*kg;

lambda = 2*rs*l*B1*na*kw/p;       % Calculation of internal voltage
Eaf = om*lambda/sqrt(2);          % RMS Internal Voltage:

% Supply voltage is assumed as a rectified AC signal of RMS value Vll.
The entire
% rectified voltage, or portions there of could be applied to any given
phase if needed.
Va=Vll;

if ((Eaf > Va) | (Eaf <= 0)),
   C = 0;
   if DEBUG==1, fprintf('Eaf = %g, Va= %g\n',Eaf,Va); end
   return;
end

% Calculation of reactances: only two count here!
% Air-gap inductance:
Lag = (q/2)*(4/pi)*muzero*na^2*kw^2*l*rs/(p^2*(g+hm));
% slot leakage
perm = muzero*l*(hd/wd+(1/3)*hs/wst);
Lslot = 2*p*l*nc^2*perm*(4*m-nsp);
% Above is true for 3 phase machine.  Also accurate for most reasonable
odd
% phase stator designs
if Lslot <= 0,
   C = 0;
   if DEBUG==1, fprintf('Negative slot leakage q= %g\n',q); end
   return;
end

% Synchronous Reactance (Ohms)
% round rotor thus Xd=Xq=Xs
Ls=Lag+Lslot;
Xs=om*Ls;

% Calculate Stator resistance
Lac = 2*na*(l+2*le2);       % Armature Conductor Length
Aslot=hs*.5*(wst+wsb);      % Armature Tooth Area
Aac = Aslot*lama/(2*nc);    % Armature Conductor Area
Ra = Lac/(siga*Aac);        % stator resistance
```

```
% Calculate magnetic flux in iron
Bt = B1/(sqrt(2)*lamt);        % Tooth Flux Density (RMS)
dc=(B1/(sqrt(2)*Bisat))*r/p;   % Back Iron minimum thickness (RMS value
of B1)
fbi=dc*p/r;                    % Back iron thicness ratio (comparison
term)
Bb = B1*r/(sqrt(2)*p*dc);      % Back iron Flux Density (RMS, should be
Bisat)
%check flux density limits
if Bt > Btsat,
   C = 0;
   if DEBUG==1, fprintf('Bt= %g, Btsat= %g\n',Bt,Btsat); end
   return;
end
dcinner=(B1/(sqrt(2)*Bisat))*rmi/p;   % rotor flux path thickness(RMS
value of B1)
% the rest of rotor can be lighter structural composit

% Misc. Lengths, Volumes and Weights
Lover = 1+2*le1;          % Overall machine length
rci = r+g+hd+hs;          % Core Inside Radius
rco = rci + dc;           % Core Outside Radius
Dover = 2*rco;            % Overall Diameter
if Dover > Dmax,
   C = 0;
   if DEBUG==1, fprintf('Dover too big = %g, Dmax= %g\n',Dover,Dmax);
end
   return;
end

DoverL=Dover/Lover;
if DoverL > DoverLmax,
   C = 0;
   if DEBUG==1, fprintf('D/L too big = %g, D/Lmax=
%g\n',DoverL,DoverLmax); end
   return;
end

Mcb = rhos*l*pi*(rco^2-rci^2);              % Back Iron
Mci = rhos*l*pi*(rmi^2-(rmi-dcinner)^2);    % inner flux return
Mct = rhos*l*(ns*wt*hs+2*pi*r*hd-ns*hd*wd); % Teeth

Ma = q*Lac*Aac*rhoc;                 % Mass of Armature Conductor:
Mm = 0.5*thme*(r^2-(r-hm)^2)*l*rhom; % Magnet Mass
Mrot = .4*rhos*l*pi*(rmi-dcinner)^2; % rotor structure 40% steel
Mfe = Mcb+Mct+Mci;                   % total magnentic steal
Mr=Mm+Mci+Mrot;                      % rotating mass
Mass=Mfe+Ma+Mm+Mrot;                 % total mass
if Mass/1000 > Mmax,
   C = 0;
   if DEBUG==1, fprintf('Mass too big = %g, Mmax= %g\n',Mass/1000,Mmax);
end
   return;
end

% Calculation of Losses
Pcb = (Mcb+Mci)*P0*abs(Bb/B0)^epb*abs(f/F0)^epf;      % Core Iron Loss
```

```
Pct = Mct*P0*abs(Bt/B0)^epb*abs(f/F0)^epf;          % Teeth
Pd = Pcb+Pct;


% Estimate of gap friction loss
omegam = om/p;                          % mechanical rotational speed
ren = omegam*r*g/nuair;                 % Reynold's Number in the gap
ff = .0076/ren^.25;                     % that gives a friction factor
Pwind = 2*pi*r^4*omegam^3*l*rhoair*ff;% windage loss


Pereq = Preq+Pwind+Pd;   % must be converted
Iq=2*Pereq/(q*p*Eaf);    % Required quadrature current for required
power


% For viability check assume Ia is inline with Eaf, (requiring a
lagging pf)
Iamax=sqrt(2)*Jalim*Aac;    % peak allowable armature current
if Iq > Iamax,
   C = 0;
   if DEBUG==1, fprintf('can not make min power, Iqmin = %g, Iamax=
%g\n',Iq,Iamax); end
   return;
end


% now assuming full line voltage applied at required pf (psi). The
required torque angle
% is determined as well as the this will also define the operating
current Ia
num=Pereq*Xs;
denom=q*Va*Eaf;
if num > denom,
   C = 0;
   if DEBUG==1, fprintf('can not make power, negative torque angle\n');
end
   return;
end
delt=asin((Pereq*Xs)/(q*Va*Eaf));
thetapf=acos(psi)*sign(psi);
Ia=Iq/cos(delt-thetapf);
if Ia > Iamax,
   C = 0;
   if DEBUG==1, fprintf('Ia = %g, Iamax= %g\n',Iq,Iamax); end
   return;
end


% assuming a forced air fan, required pumping power is:
Pa=Ia^2*Ra;
Paq=q*Pa;
mdot=(Pd+Paq+Pwind)/(cpair*dtt); % mass flow based on temperature rise
Qdot=mdot/rhoair;                       % volumetric flow rate
Agap=pi*(rs^2-r^2);                     % air gap area
Vel=Qdot/Agap;                          % flow velocity
Dh=2*(rs-r);                            % hydraulic diameter
Ren=rhoair*Dh*Vel/nuair;                % Reynolds number
deltap1=8/pi*nuair*l*Qdot;
deltap2=rs^4-r^4-(rs^2-r^2)^2/(log(rs/r));
deltap=deltap1/deltap2;                 % pressure drop across rotor
```

```
Pfan=mdot*deltap/(rhoair*etf);    % fan power is volume flow times
pressure drop

% Performance Characterization
Ploss=Pwind+Pd+Pfan+Paq;          % total losses
eff=Preq/(Preq+Ploss);            % efficiency

% Cost estimate
Costm = Pmag*Mm;
Costcu = Pcu*Ma;
Costfe = Pfe*Mfe;
Cost = Costm + Costcu +Costfe;    % Materials Cost

% check efficiency addequate
if etamin > eff,
   C = 0;
   if DEBUG==1, fprintf('eff= %g\n',eff); end
   return;
end;

Ja=Ia/Aac;
Vt=Eaf*cos(delt)+Ia*Ra;

if Vt > Va,
   C = 0;
   if DEBUG==1, fprintf('Vt required= %g\n',Vt); end
   return;
end;

% check current density, Redundant check but oh, well
if Ja > Jalim,
   C = 0;
   if DEBUG==1, fprintf('Ja required= %g\n',Ja); end
   return;
end;

% Some simple checks...
Torque = Preq/omegam;                     % required torque
shear1 = Torque/(2*pi*rs^2*l);            % required shear (stator
surf)
Ksubz = 1.5*na*sqrt(2)*2*Ia/(pi*rs);      % PEAK surface current
density
shear2 = .5 * Ksubz * B1 * cos(delt+psi); % another guess at shear
volts2 = 2*na*rs*l*omegam*kw*B1/sqrt(2);  % RMS voltage by blv...

% rotational inertia constant
Jrot = .5*Mrot*(rmi-dcinner)^2;   % Composite rotor moment of inertia
Jm = .5*Mm*(r^2+(r-hm)^2);        % magnet moment of inertia
Jci = .5*Mci*(rmi^2+(rmi-dcinner)^2); % flux return moment of inertia
J=Jrot+Jm+Jci;                    % total moment of inertia

C=1;
A = [Preq+Ploss 1/Cost 1/Mass 1/Dover 1/Lover eff 1/J 1/Ja ];
if DEBUG==3, fprintf('A= %6.4f %6.4f %6.4f %6.4f %6.4f %6.4f %6.4f
%6.4f \n',A(:));
    fprintf('A=[1/Pmax 1/Cost 1/Mass 1/Dover 1/Lover eff 1/J 1/Ja] \n');
```

```
    fprintf('inverse A= %6.4f %6.4f %6.4f %6.4f %6.4f %6.4f %6.4f %6.4f
\n',1./A(:));
end;




% OMOE calc data storage for SMPM
% needs number of designs
% needs an array of attributes all increasing goodness
% MA=[Preq+Ploss 1/Cost 1/Mass 1/Dover 1/Lover eff 1/J 1/Ja ];
% need to initialize a weighting factor array should sum to zero

fp=fopen('smomoe.dat','w');  % create/write over file

% wf=[Pwr Cost Mass Dover Lover eff J Ja]
WF=[0 0 1 1 1 1 0 0];  WFV=1; % relative weighting factors
% WFV is the relative weighting factor for volume
V=pi/4*(1./MA(:,4)).^2.*(1./MA(:,5));
Vin=1/V;    % Volume with increasing value good
te=sum(WF')+WFV
wf=WF/te;
wfv=WFV/te;
MAmin=min(MA);
MAmax=max(MA);
Vmin=min(Vin);
Vmax=max(Vin);
range=MAmax-MAmin;
rangev=Vmax-Vmin;
for ii=1:NDE;
    dif(ii,:)=MA(ii,:)-MAmin;
    difv(ii)=Vin(ii)-Vmin;
    OMOEvol(ii)=difv(ii)/rangev*wfv;
    OMOEv(ii,:)=dif(ii,:)./range.*wf;
    OMOEt(ii)=sum(OMOEv(ii,:)')+OMOEvol(ii);;
end
OMOE=OMOEt';    % make column vector

for rr = 1:NDE,
    cost=10^-6/MA(rr,2);
    omoe=OMOE(rr);
    omoedat(rr,:)=[rr cost omoe];
    fprintf('%3d %7.5g %7.5g\n',rr,cost,omoe);
    fprintf(fp,'%3d %7.5g %7.5g\n',rr,cost,omoe);
end
err=fclose(fp);
plot(omoedat(:,2),omoedat(:,3),'bo');
xlabel('cost');
ylabel('OMOE');
title('SMPM');
[OMOEmax,OMOEd] = max(OMOE);
fprintf('highest OMOE is design # %2d, OMOE= %4g\n',OMOEd,OMOEmax);
fprintf('wf= %5.4f %5.4f %5.4f %5.4f %5.4f %5.4f %5.4f %5.4f\n',wf);
```

```
% This script displays motor details for smpm
fp=fopen('smpm.dat','w');  % create/write over file pmsm.dat
fprintf('Summary SMPM Motor Attribute  %s\n',date);
fprintf('Number of viable candidates optimized %7g\n',viable);
fprintf(' #  Pwr       Cost Mass     Dia     Length Gen     Inerti
Ja\n');
fprintf('    MW        M$   tonne    m       m      Eff     Mg/m^2
A/cm^2\n');
fprintf(fp,'Summary SMPM Motor Attribute  %s\n',date);
fprintf(fp,'Number of viable candidates optimized %7g\n',viable);
fprintf(fp,' #  Pwr       Cost Mass     Dia     Length Gen     Inerti
JA\n');
fprintf(fp,'    MW        M$   tonne    m       m      Eff     Mg/m^2
A/cm^2\n');

for r = 1:NDE,
    if MD(r,1)==0   % Avoid division by 0
        MA(r,:)=1e-7;
        MDI(r,1)=1;
    end
  Pwr = 10^-6*MA(r,1);
  Cost = 10^-6/MA(r,2);
  Mass = 10^-3/MA(r,3);
  Dia = 1/MA(r,4);
  Len = 1/MA(r,5);
  Eff = MA(r,6);
  J = 10^-3/MA(r,7);
  Ja = 10^(-4)/MA(r,8);

    fprintf('%2g  %4.2f %7.2f %7.1f %7.3f %7.3f %7.3f %6.1f
%7.2f\n',...
              r,Pwr,Cost,Mass,Dia,Len,Eff,J,Ja);
    fprintf(fp,'%2g  %4.2f %7.2f %7.1f %7.3f %7.3f %7.3f %6.1f
%7.2f\n',...
              r,Pwr,Cost,Mass,Dia,Len,Eff,J,Ja);

end

% This script displays motor geometry for pmrs
fprintf('\nSummary SMPM geometry\n');
fprintf(' #  Rr    air-gap   hm    lact   wt      hs      p  m  nsp nc
q\n');
fprintf('    m     mm        mm    m      mm      mm        \n');
fprintf(fp,'\nSummary SMPM geometry\n');
fprintf(fp,' #  Rr    air-gap   hm    lact   wt      hs      p  m  nsp
nc q\n');
fprintf(fp,'    m     mm        mm    m      mm      mm        \n');

for r = 1:NDE,
  % MD = [r g hm l wt fsd];
  % MDI = [p m nsp nc q];
  p =MDI(r,1);
  m = MDI(r,2);
  nsp = MDI(r,3);
  nc = MDI(r,4);
  q = MDI(r,5);
  R = MD(r,1);
```

```
    g = 1000*MD(r,2);
    hm = 1000*MD(r,3);
    lact = MD(r,4);
    wt = 1000*MD(r,5);
    hs = 1000*MD(r,6)*R;
    % dc = 1000*MD(r,7)*R/p;


    fprintf('%2g %3.2f %6.2f    %6.2f %6.2f   %6.2f   %6.2f   %2d %2d %2d %2d
%2d\n',...
            r,R,g,hm,lact,wt,hs,p,m,nsp,nc,q);
    fprintf(fp,'%2g %3.2f %6.2f    %6.2f %6.2f   %6.2f   %6.2f   %2d %2d %2d
%2d %2d\n',...
        r,R,g,hm,lact,wt,hs,p,m,nsp,nc,q);


    end
    fprintf(fp,'\nD =     r          g        hm        l          wt
fsd\n');
    fprintf(fp,'DU = %6.4f   %6.4f   %6.4f   %6.4f   %6.4f   %6.4f\n',DU);
    fprintf(fp,'DM = %6.4f   %6.4f   %6.4f   %6.4f   %6.4f   %6.4f\n',DM);
    fprintf(fp,'DL = %6.4f   %6.4f   %6.4f   %6.4f   %6.4f   %6.4f\n',DL);
    fprintf(fp,'DS = %6.4f   %6.4f   %6.4f   %6.4f   %6.4f   %6.4f\n',DS);
    fprintf(fp,'DIN =  pmax   mmax nspmax  ncmax qmax\n');
    fprintf(fp,'DIN = %4d   %4d   %4d   %4d   %4d\n',DIN);


    fprintf('\nDM =      r          g        hm        l          wt        fsd\n');
    fprintf('DU = %6.4f   %6.4f   %6.4f   %6.4f   %6.4f   %6.4f\n',DU);
    fprintf('DM = %6.4f   %6.4f   %6.4f   %6.4f   %6.4f   %6.4f\n',DM);
    fprintf('DL = %6.4f   %6.4f   %6.4f   %6.4f   %6.4f   %6.4f\n',DL);
    fprintf('DS = %6.4f   %6.4f   %6.4f   %6.4f   %6.4f   %6.4f\n',DS);
    fprintf('DIN =  pmax   mmax nspmax ncmax qmax\n');
    fprintf('DIN = %4d   %4d   %4d   %4d   %4d\n',DIN);

err=fclose(fp);
```

```
% smdata
% saves design parameters to be read in manually for further analysis

fp=fopen('smdata.dat','w');  % create/write over file

fprintf(fp,'%7d  %7d\n',NDE,viable);
for rr = 1:NDE,
    % MD = [r g hm l wt fsd fbi];
    % MDI = [p m nsp nc q];;
  r = MD(rr,1);
  g = MD(rr,2);
  hm = MD(rr,3);
  l = MD(rr,4);
  wt = MD(rr,5);
  fsd = MD(rr,6);
  p = MDI(rr,1);
  m = MDI(rr,2);
  nsp = MDI(rr,3);
  nc = MDI(rr,4);
  q = MDI(rr,5);
  fprintf(fp,'%7.5f %7.5f %7.5f %7.5f %7.5f %7.5f ',...
     r,g,hm,l,wt,fsd);
  fprintf(fp,'%7d %7d %7d %7d %7d\n',p,m,nsp,nc,q);
end

err=fclose(fp);
```

```
% reads in data (should be dominate) and runs attribute for designs
% run SM setup first to initialize B and NA
smsetup;
DEBUG=4;

fp=fopen('smdata.dat','r');  % open file to read

NDEt=fscanf(fp,'%7d',1);
viable=fscanf(fp,'%7d',1);
first=0;
for rr = 1:NDEt,
   % Dt= [r g hm l wt fsd]
   % DIt = [p m nsp nc q];
   r = fscanf(fp,'%7g',1); Dt(rr,1) = r;
   g = fscanf(fp,'%7g',1); Dt(rr,2) = g;
   hm = fscanf(fp,'%7g',1);  Dt(rr,3) = hm;
   l = fscanf(fp,'%7g',1); Dt(rr,4) = l;
   wt = fscanf(fp,'%7g',1); Dt(rr,5) = wt;
   fsd = fscanf(fp,'%7g',1); Dt(rr,6) = fsd;
   p = fscanf(fp,'%7g',1); DIt(rr,1) = p;
   m = fscanf(fp,'%7g',1); DIt(rr,2) = m;
   nsp = fscanf(fp,'%7g',1); DIt(rr,3) = nsp;
   nc = fscanf(fp,'%7g',1); DIt(rr,4) = nc;
   q = fscanf(fp,'%7g',1); DIt(rr,5) = q;
   if r == 0,
       return
   end

   [A, gg] = attributsm(Dt(rr,:), DIt(rr,:), B, DEBUG);
   if gg ~= 0,
       fprintf(' motor %2d viable\n',rr);
       MA(rr, :) = A;       % if still viable it goes here
       MD(rr, :) = Dt(rr,:);    % save design too!
       MDI(rr, :) = DIt(rr,:);
       if first==0,
           DM=MD(rr,:); % set parent design
           first=1;
       end
    end % if

  DM=Dt(1,:);         % initialize mean variable vector to first
optimized design

end
err=fclose(fp);
```

Appendix H

SCM MATLAB™ code

```
% scsetup.m

clear
NA = 8;              % attributes
NDE = 30;            % designs to keep
NITER = 1000;        % shots to try
DEBUG=1;             % 1=debug output, 2=screen output
                     % 3=attribute output, 4=std reduction optimization
DF=.999;             % Standard deviation reduction factor
viable=0;            % index of viable designs

% Lower Limit
Rfi = .5;            % Rotor radius
g = .001;            % Air-gap
tsc = .001;          % Super-c coil Thickness
lrot = .2;           % Active Length
tarm = .001;         % armature thickness
% Lower limit vector
DL = [Rfi g tsc lrot tarm];

% Upper Limit
Rfi = 1.5;           % Rotor radius
g = .1;              % Air-gap
tsc = .03;           % Super-c coil thickness
lrot = 3;            % Active Length
tarm = .5;           % armature thickness
% Upper limit vector
DU = [Rfi g tsc lrot tarm];

ND = size(DL,2);     % continuous design space
DM=(DL+DU)/2;        % Mean value array
DS=(DU-DL)/2;        % initial standard normal multiplier vector

% Limits of integer variables
pmax = 20;           % Pole Pairs
ncmax =40;           % Turns per coil
qmax=15;             % number of phases
% Integer upper limit vector
DIN = [pmax ncmax qmax];

% fixed inputs
rpm = 100;       % Rotational speed
Preq = 21*10^6;% Required power
Vll = 4160;      % line-line voltage
thwfe = 2*pi/3;% Sc feild coil Electrical Angle
siga = 5e7;      % Stator Conductivity
P0=1.3;          % Iron Model: Base Dissipation
F0=60;           % Base Frequency
B0=1;            % Base Flux Density
epb=1.88;        % Flux Exponent
epf=1.53;        % Frequency Exponent
rhos=7800;       % Steel Density
rhosc=10510;     % SC (silver) Density
rhoc=8960;       % Conductor (copper) Density
rhocs=.4*rhos;   % 40% steel structure
Jalim = 1.5e6;   % armature current density limit [A/m2]
Psc = 100;       % Superconductor: $/kg
```

```
Pcu = 5;          % copper price: $/kg
Pfe = 2;          % iron price: $/kg
Bisat = 1.3;      % maximum iron flux density
vtip = 230;       % max tip speed m/s
etamin = .95;     % min efficiency
psi = 1;          % Required power factor angle
lamf=.9;          % field packing factor
lama=.35;         % armature packing factor
Dmax=6;           % maximum overall diameter allowed
Mmax=100;         % Maximum overall mass allowed
DoverLmax=3;      % aspect ratio limit
rm=.01;           % minimum bend radius for SC tape
lamc=.4;          % straight section space factor
lame=.8;          % end turn space packing factor
Jsc=1e8;          % SC current density [A/m^2]
rhoss=7800;       % density of secondary support structure

B=[rpm Preq Vll thwfe siga P0 F0 B0 epb epf rhos rhosc rhoc rhosc Jalim
Psc Pcu ...
   Pfe Bisat vtip etamin psi lamf lama Dmax Mmax DoverLmax rm lamc lame
Jsc rhoss];

% Here are the matrices that NDA will fill out

MA = zeros(NDE, NA);     % design attributes across rows
MD = zeros(NDE, ND);     % design variables (continuous)
NI = length(DIN);        % number of integer variables
MDI = zeros(NDE, NI);    % design variables (integers)
DI = zeros(size(DIN));   % space for integer variables

MAOpt = zeros(NDE, NA);  % scratchpad for optimized machine
MDOpt = zeros(NDE, ND);  % ditto
```

```
%
% ******************************************************** %
%                                                         %
%          Novice Design Assistant SC AC Synchronous      %
%                        ndaSC                            %
%                 by Joe Harbour 01/23/01                 %
%          Derived/coverted from J.L. Kirtley Jr. nda     %
%                  used with permision                    %
% ******************************************************** %
%
% Requires an attribute generating function called this way:
% [A, g] = attribut(D, DI, B, Out)
% A is a vector of attributes of size NA
%   Attributes are all positive and goodness is increaseing
% g is a scalar that is 0 if a design is not viable and 1 if it is
% D is a vector of design variables that nda will manipulate
%   it is of size ND
% DI is a vector of integer variables to be varied randomly
%   it is of size NI
% B is a vector of design variables that will remain fixed
% Out = 1 will cause the thing to print
% DL, DU, DS and DM are starting points for the vector D
% DL and DU are lower and upper limit points
% DM is the median value to be used in generating D
% DS is a vector of standard deviation to be used in generating D
% DIN is the vector of ranges of the elements of DI
% NDE is the number of design points to be accumulated
% NITER is the total number of shots to be tried
% Output will be accumulated in two matrices
% MA [NA, NDE] holds the attributes of all designs
% MD [ND, NDE] holds the design variables
% These matrices are declared in the setup program, so
% that NDA can be run over again

if DEBUG==1,
    fprintf('DU= %6.4f %6.4f %6.4f %6.4f %6.4f\n',DU(:));
    fprintf('DM= %6.4f %6.4f %6.4f %6.4f %6.4f\n',DM(:));
    fprintf('DL= %6.4f %6.4f %6.4f %6.4f %6.4f\n',DL(:));
    fprintf('DS= %6.4f %6.4f %6.4f %6.4f %6.4f\n',DS(:));
end;
for i = 1:NITER,
    temp=randn(1, ND);
    D = DM + DS .* randn(1, ND);     % generate a random input

    if sum([DL>D]+[DU<D]) == 0,     % if design is in range, continue
        for ii = 1:NI,        % generate the integer random
            pt = randperm(DIN(ii));          % variables
            DI(ii) = pt(1);
        end

        DI(3)=15;  % design for three phase only

        if DEBUG==1,
            fprintf('%3.3f design in range ',i/NITER);
        end

        [A, g] = attributsc(D, DI, B, DEBUG);  % generate design
```

144

```
        if g ~= 0,                % if viable, do dominance check
            viable=viable+1;
            fprintf(' viable at %3.3f complete\n',i/NITER);
            for nd=1:NDE,          % dominance check against gross
dimensions in array
                % A=[Pmax 1/Cost 1/Mass 1/Dover 1/Lover eff 1/J 1/Ja] \n')
            if sum(A(3:NA-2)>MA(nd,3:NA-2))== NA-4,
                % every element of A is greater than stored element at
index nd.
                % Replace MA(nd) with A.
                MA(nd, :) = A;     % it goes here
                MD(nd, :) = D;     % save design too!
                MDI(nd, :) = DI;
                fprintf('Replacing Design %5.0f At %3.3f complete\n',
nd, i/NITER);
                if DEBUG==4,   % use as baseline design, refine Standard
deviation vector
                    DM=D;
                    Dtemp=DS*DF;
                    DS=Dtemp;
                end
                break;
            end % dominance check
        end % end storage array for loop
    end  % viable check
    end % design in range check
end % NITER

% run output program
%Msc
```

```
% scattribut.     Joe Harbour 01/23/01
% used in conjunction with scsetup to find
% solution to an air core superconducting AC synchronous motor
%
% uses following variables previously initialized

function[A,C] = attributsc(D,DI,B,DEBUG)
global muzero

% load variables created in HPMsetup/nda
% DL = [Rfi g tsc l tarm lama]
Rfi=D(1);             % Super-c inner radius
g=D(2);               % air gap
tsc=D(3);             % field coil thickness => outer radius
lrot=D(4);            % active length
tarm=D(5);            % armature thickness =>outer radius


% DIN = [pmax ncmax qmax]
p=DI(1);              % number of poles
nc=DI(2);             % Turns per coil
q=DI(3);              % number of phases


%B=[rpm Preq Vll thwfe siga P0 F0 B0 epb epf rhos rhosc rhoc rhosc
Jalim Psc...
%     Pcu Pfe Bisat vtip etamin psi lamf lama Dmax Mmax DoverLmax rm lamc
lame Jsc];
rpm = B(1);           % Rotational speed
Preq = B(2);          % Required power
Vll = B(3);           % line-line voltage
thwfe = B(4);         % Sc feild coil Electrical Angle
siga = B(5);          % Stator Conductivity
P0=B(6);              % Iron Model: Base Dissipation
F0=B(7);              % Base Frequency
B0=B(8);              % Base Flux Density
epb=B(9);             % Flux Exponent
epf=B(10);            % Frequency Exponent
rhos=B(11);           % Steel Density
rhosc=B(12);          % SC Density
rhoc=B(13);           % Conductor Density
rhocs=B(14);          % composite density
Jalim = B(15);        % armature current density limit [A/m2]
Psc = B(16);          % Superconductor: $/kg
Pcu = B(17);          % copper price: $/kg
Pfe = B(18);          % iron price: $/kg
Bisat = B(19);        % maximum iron flux density
vtip = B(20);         % max tip speed m/s
etamin = B(21);       % min efficiency
psi = B(22);          % Required power factor angle
lamf=B(23);           % field packing factor
lama=B(24);           % armature packing factor
Dmax=B(25);           % maximum overall diameter allowed
Mmax=B(26);           % maximum overall mass allowed
DoverLmax=B(27);      % maximum aspect ratio allowed
rm=B(28);             % minumim bend radius for SC tape
lamc=B(29);           % straight section space factor
lame=B(30);           % end turn space packing factor
Jsc=B(31);            % SC current density [A/m^2]
```

146

```
rhoss=B(32);          % density secondary damper structure

% Here are a few constants
muzero=pi*4e-7;           % free-space permeability
cpair = 1005.7;           % mass heat capacity of air
rhoair = 1.21;            % density of air
nuair = 1.46e-5;          % kinematic viscosity of air
etf = .25;                % efficiency of fan
dtt = 50;                 % allowable temperature rise
taus=250e6;               % yield stess of steel
sf=1.5;                   % safety factor
Asc=8.2*10^-7;            % cross section area of typical SC tape
[0.2x4.1mm^2]


C=0;     % machine not viable yet
A=[1 0 0 0 0 0 0 0]; % attribut array, poor machine but not empty

% calculate geometry
tkp=.002;                 % primary damper thickness
ts=.11;                   % secondary damper support structure
tks=.006;                 % secondary damper thickness
Rfo=Rfi+tsc;              % outer radius of rotating rotor
Rkpi=Rfo;                 % inner radius of primary damper
Rkpo=Rkpi+tkp;            % outer radius of primary damper
Rsi=Rkpo;                 % inner radius of secondary support
Rso=Rsi+ts;               % outer radius of secondary support
Rksi=Rso;                 % inner radius of secondary damper
Rkso=Rksi+tks;            % outer radius of secondary damper
Rai=Rkso+g;               % inner radius of armature
Rao=Rai+tarm;             % outer radius of armature

thwa=pi/(p*q);            % armature pole physical angular extent (sec
10.5.0)
thwae=p*thwa;             % armature pole electrical extent
Aacoil=thwa/2*(Rao^2-Rai^2); % physical armature area per phase (sec
10.5.1)
Aac=Aacoil*lama/(2*nc); % Area of armature conductor per phase
Nat=2*p*nc;               % number of armature turns per phase

% end turn cone length
laz=.5*pi*Rai/p;          % 1/2 total end turn asmuthial traverse
thte=acos(lamc/lame);  % 90-end turn departure angle
le1=laz/tan(thte);;       % end length (axial)
le2=laz*laz/tan(thte);  % end length (half cone)

thwf=thwfe/p;             % super-c pole physical extent

% Electrical frequency
r=Rkso;                        % outer radius of rotating mass
f = p*rpm/60;
om = 2*pi*f;
stip = Rfo*om/p;.               % surface speed

% check surface speed
if stip > vtip,
   C = 0;
   if DEBUG==1, fprintf('stip= %g\n',stip); end
```

```
    return;
end;


Rs=Rao;       % flux shield inner radius
dl=Rai+Rao; % end turn length estimate
loa=lrot+2.6*dl;   % effective armature length, for self inductance
calcs
lab=lrot+1.2*dl;  % effective armature length, for mutual inductance
calcs
lm=lrot;      % effective armature length field-to-armature mutual
inductance
x=Rai/Rao;   % ratios used later
y=Rfi/Rfo;
w=Rao/Rs;
z=Rfo/Rs;


% n is summing variable only odd values used
n=1:2:17;
% n=1;
npp=n*p+2; npm=n*p-2; x2=(1-x^2); y2=(1-y^3); np=n*p;
fact=4/pi*muzero./np;


% winding factors
kwa=sin(n*thwae/2)./(n*thwae/2);
kwf=1;
%kwf=sin(n*thwfe/2)./(n*thwfe/2);


% geometric coeficient mutual inductance
Cm1b=1-x.^-npp+(npm./npp).*(1-x.^(npp)).^2.*(w).^(2*np);
Cm1a=(1-y.^npp).*(Rfo/Rao).^np;
Cm1=Cm1a.*Cm1b;
Cm2=4-np.^2;
if p == 2,
    Cm1(1)=-log(x)+x2/4*w^4;
    Cm2(1)=8;
end
Cm=Cm1./Cm2;
MavoNf=2*(fact./(x2.*y2))*lm*Nat.*kwa.*kwf.*Cm;
MaoNf=MavoNf(1);


% geometric coefficient self inductance of armature
Csa1=(npm)+4*x.^(npp)-(npp)*x^4+2*(npm./npp).*(1-
x.^(npp)).^2.*(w).^(2*np);
Csa2=np.^2-4;
if p == 2,
    Csa1(1)=(x^4*log(x)/2+(1-x^4)/8+(1-x^4)^2/16*w^4);
    Csa2(1)=1;
end
Csa=Csa1./Csa2;
% self inductance of armature phase-a
La=(fact./x2.^2)*loa*Nat^2.*Csa.*kwa.^2;
% Mutual inductance, phase-to-phase
Lab=(fact./x2.^2)*lab*Nat^2.*cos(2*n*pi/3).*Csa.*kwa.^2;
Xsv=om*(La-Lab);        % synchronous reactance
Xs=Xsv(1);
```

```
% Supply voltage is assumed as a rectified AC signal of RMS value Vll.
The entire
% rectified voltage, or portions there of could be applied to any given
phase if needed.
Va=Vll;

% Speed voltage (|Eaf|=w*Ma*If)
NftIf=.5*Jsc*thwfe*Rfo^2*(1-y^2);
Eafv=om*MaoNf*NftIf;
Eaf=Eafv(1)/sqrt(2);

if (Eaf > Va) | (Eaf < 0),
   C = 0;
   if DEBUG==1, fprintf('Eaf = %g, Va= %g\n',Eaf,Va); end
   return;
end


Rp=Rs;
t1=2*Jsc*Rp.*((Rfo/Rp).^npp).*(1-y.^npp).*(1+(Rp/Rs).^(2*np));
Hrfov=(t1.*kwf*thwfe.*n/2)./(n.*npp);
Brfo=muzero*Hrfov(1);            % radial flux at flux shield (egn pg 27)
dc=(Brfo/(sqrt(2)*Bisat))*r/p;% fs minimum thickness (RMS value of
Brfo)
fbi=dc*p/r;                      % fs thickness ratio (comparison term)
Bb = Brfo*r/(sqrt(2)*p*dc);   % fs flux density (RMS, should be Bisat)


% Misc. Lengths, Volumes and Weights
wcoil=2*Rfi*sin(.5*thwf);  % chord length of field winding pole
if wcoil>(2*(tsc+rm)),
    wsc=tsc;              % square coil windings with 2m seperation
    lsc=wcoil-2*tsc;  % field coil end turn connect length
else if wcoil>2*rm,
        wsc=(wcoil-2*rm)/2;  % rectangular coil winding with 2Rscmin
seperation
        lsc=0;
    else,
        C = 0;
        if DEBUG==1, fprintf('pole heads too narrow %g, \n',wcoil); end
        return;
    end
end


Afcoil=wsc*tsc;        % physical field area per phase per side
Acond=Afcoil*lamf;
Nft=Acond/Asc;         % Number of field coil turns per pole
If=Jsc/Asc;            % resulting SC current

Lac = 2*Nat*(lrot+2*le2);   % Armature Conductor Length;
Ra = Lac/(siga*Aac);        % stator resistance
Lover = lrot+2*le1;         % Overall machine length
rco = Rao+dc;               % Core Outside Radius
Dover = 2*rco;              % Overall Diameter
if Dover > Dmax,
   C = 0;
   if DEBUG==1, fprintf('Dover too big = %g, Dmax= %g\n',Dover,Dmax);
end
   return;
```

149

```
end

DoverL=Dover/Lover;
if DoverL > DoverLmax,
   C = 0;
   if DEBUG==1, fprintf('D/L too big = %g, D/Lmax=
%g\n',DoverL,DoverLmax); end
   return;
end

% Estimate of gap friction loss
omegam = om/p;                          % mechanical rotational speed
ren = omegam*r*g/nuair;                 % Reynold's Number in the gap
ff = .0076/ren^.25;                     % that gives a friction
factor
Pwind = 2*pi*r^4*omegam^3*lrot*rhoair*ff; % windage loss
Pereq=Preq+Pwind;

% thickness of torque tube
Torque = Pereq/omegam;      % required torque
Rbo=Rfi;
ttt=.01*Rbo;                % initial guess
notdone=1;
while notdone,
    if ttt>Rbo,      % not enough material to handle torque
        C = 0;
        if DEBUG==1, fprintf('tt too thick = %g\n',ttt); end
   return;
end
    tautt=2*Torque*Rbo/(pi*(Rbo^4-(Rbo-ttt)^4));
    if abs(sf*tautt-taus)>taus/100,
        ttt=ttt+ttt/2*sign(sf*tautt-taus);
    else
        notdone=0;
    end
end
Rbi=Rbo-ttt;

rci=Rao;
Mcbtube = rhos*lrot*pi*(rco^2-rci^2);      % Back Iron
Mcbend=rhos*pi*dc*(rci+dc)^2;              % end bells
Mcb=Mcbtube+2*Mcbend;
Ma = q*Lac*Aac*rhoc;                       % Mass of Armature Conductor:
Vsccoil=lrot*tsc*wsc;
Vcoil=2*pi*(Rfo^2-Rfi^2);                  % total volume in field section
Vscoil=Vcoil-(2*p*Vsccoil);                % volume of steel in field
sections
Vscend=tsc*(pi/2*((rm+wsc)^2-rm^2)+lsc*wsc);
Vsc=2*(Vsccoil+Vscend)*lamf;               % SC volume per pole
Msc = 2*p*rhosc*Vsc;                       % super-c field coil Mass
Mdampp=rhoc*lrot*pi*(Rkpo^2-Rkpi^2);       % primary damper mass
Mdamps=rhoc*lrot*pi*(Rkso^2-Rksi^2);       % secondary damper mass
Mdamp=Mdampp+Mdamps;
Mss=rhoss*lrot*pi*(Rso^2-Rsi^2);           % support structure mass
Mtt=rhos*lrot*pi*(Rbo^2-Rbi^2);            % torque tube mass
Ms = pi*Rfi^2*lrot*rhocs;                  % Shaft Mass (rhocs=fraction rhos)
Mscoil=Vscoil*rhos;
```

```
Mr=Msc+Ms+Mscoil+Mdamp+Mss+Mtt;        % rotating mass
Mass=Mr+Ma+Mcb;                        % total mass
if Mass/1000 > Mmax,
   C = 0;
   if DEBUG==1, fprintf('Mass too big = %g, Mmax= %g\n',Mass/1000,Mmax);
end
   return;
end

% Calculation of Losses
Pcb = Mcb*P0*abs(Bb/B0)^epb*abs(f/F0)^epf;   % Core Iron Loss
Pdamp=Mdamp*P0*abs(Bb/B0)^epb*abs(f/F0)^epf; % damper losses
Pd=Pcb+Pdamp;

Pereq = Preq+Pwind+Pd;                 % must be converted
Iq=2*Pereq/(q*p*Eaf);   % Required quadrature current for required
power

% For viability check assume Ia is inline with Eaf, (requiring a
lagging pf)
Iamax=sqrt(2)*Jalim*Aac;   % peak allowable armature current
if Iq > Iamax,
   C = 0;
   if DEBUG==1, fprintf('can not make min power, Iqmin = %g, Iamax=
%g\n',Iq,Iamax); end
   return;
end

% now assuming full line voltage applied at required pf (psi). The
required torque angle
% this will also define the operating current
num=Pereq*Xs;
denom=q*Va*Eaf;
if num > denom,
   C = 0;
   if DEBUG==1, fprintf('can not make power, negative torque angle\n');
end
   return;
end
delt=asin((Pereq*Xs)/(q*Va*Eaf));
thetapf=acos(psi)*sign(psi);
Ia=Iq/cos(delt-thetapf);
if Ia > Iamax,
   C = 0;
   if DEBUG==1, fprintf('Ia = %g, Iamax= %g\n',Iq,Iamax); end
   return;
end

% assuming a forced air fan, required pumping power is:
Pa=Ia^2*Ra;
Paq=q*Pa;
mdot=(Pd+Paq+Pwind)/(cpair*dtt); % mass flow based on temperature rise
Qdot=mdot/rhoair;               % volumetric flow rate
Agap=pi*(Rai^2-Rkso^2);         % air gap area
Vel=Qdot/Agap;                  % flow velocity
Dh=2*(Rai-Rkso);                % hydraulic diameter
Ren=rhoair*Dh*Vel/nuair;        % Reynolds number
```

151

```
deltap1=8/pi*nuair*lrot*Qdot;
deltap2=Rai^4-Rkso^4-(Rai^2-Rkso^2)^2/(log(Rai/Rkso));
deltap=deltap1/deltap2;        % pressure drop across rotor
Pfan=mdot*deltap/(rhoair*etf); % fan power is volume flow times
pressure drop

% Performance Characterization
Pwrcryo=(Pereq)*(0.3/100);     % estimate .3% machine rating for cryo
cooler
Ploss=Pwind+Pd+Pfan+Paq+Pwrcryo; % total losses
eff=Preq/(Preq+Ploss);             % efficiency

% Cost estimate
Costsc = Psc*Msc;
Costcu = Pcu*Ma;
Costfe = Pfe*Mcb;
Cost = Costsc + Costcu +Costfe;   % Materials Cost

% check efficiency addequate
if etamin > eff,
  C = 0;
  if DEBUG==1, fprintf('eff= %g\n',eff); end
  return;
end;

Ja=Ia/Aac;
Vt=Eaf*cos(delt)+Ia*Ra;

if Vt > Va,
  C = 0;
  if DEBUG==1, fprintf('Vt required= %g\n',Vt); end
  return;
end;

% check current density, Redundant check but oh, well
if Ja > Jalim,
  C = 0;
  if DEBUG==1, fprintf('Ja= %g\n',Ja); end
  return;
end;

% some quick checks...
Torque = Preq/omegam;                      % required torque
shear1 = Torque/(2*pi*r^2*lrot);           % required shear (stator
surf)
Ksubz = 1.5*Nat*sqrt(2)*2*Ia/(pi*r);         % PEAK surface current
density
shear2 = .5 * Ksubz * Brfo * cos(delt+psi); % another guess at shear
volts2 = 2*Nat*r*lrot*omegam*kwa(1)*Brfo/sqrt(2);     % RMS voltage by
blv...

% rotational inertia constant
Jr = .5*Ms*(Rbi)^2;              % rotor moment of inertia
Jsc = .5*Msc*(Rfo^2+Rfi^2);    % SC moment of inertia
Js = .5*Ms*(Rfo^2+Rfi^2);      % steel pole head moment of inertia
Jdampp=.5*Mdampp*(Rkpo^2+Rkpi^2); % primary damper moment of inertia
Jdamps=.5*Mdamps*(Rkso^2+Rksi^2); % secondary damper moment of inertia
```

```
Jss=.5*Mss*(Rso^2+Rsi^2);      % secondary support moment of inertia
Jtt=.5*Mtt*(Rbo^2+Rbi^2);      % torque tube moment of inertia
J=Jr+Jsc+Js+Jdampp+Jdamps+Jss+Jtt;   % total moment of inertia

C=1;
A = [Preq+Ploss 1/Cost 1/Mass 1/Dover 1/Lover eff 1/J 1/Ja ];
if DEBUG==3, fprintf('A= %6.4f %6.4f %6.4f %6.4f %6.4f %6.4f %6.4f
%6.4f \n',A(:));
    fprintf('A=[1/Pmax 1/Cost 1/Mass 1/Dover 1/Lover eff 1/J 1/Ja] \n');
    fprintf('inverse A= %6.4f %6.4f %6.4f %6.4f %6.4f %6.4f %6.4f %6.4f
\n',1./A(:));
end;
```

```
% OMOE calc data storage for sc% needs number of designs
% needs an array of attributes all increasing goodness
% MA=[Preq+Ploss 1/Cost 1/Mass 1/Dover 1/Lover eff 1/J 1/Ja ];
% need to initialize a weighting factor array should sum to zero

fp=fopen('scomoe.dat','w');   % create/write over file


% wf=[Pwr Cost Mass Dover Lover eff J Ja]
WF=[0 0 1 1 1 1 0 0];  WFV=1; % relative weighting factors
% WFV is the relative weighting factor for volume
V=pi/4*(1./MA(:,4)).^2.*(1./MA(:,5));
Vin=1/V;    % Volume with increasing value good
te=sum(WF')+WFV
wf=WF/te;
wfv=WFV/te;
MAmin=min(MA);
MAmax=max(MA);
Vmin=min(Vin);
Vmax=max(Vin);
range=MAmax-MAmin;
rangev=Vmax-Vmin;
for ii=1:NDE;
    dif(ii,:)=MA(ii,:)-MAmin;
    difv(ii)=Vin(ii)-Vmin;
    OMOEvol(ii)=difv(ii)/rangev*wfv;
    OMOEv(ii,:)=dif(ii,:)./range.*wf;
    OMOEt(ii)=sum(OMOEv(ii,:)')+OMOEvol(ii);;
end
OMOE=OMOEt';    % make column vector

for rr = 1:NDE,
    cost=10^-6/MA(rr,2);
    omoe=OMOE(rr);
    omoedat(rr,:)=[rr cost omoe];
    fprintf('%3d %7.5g %7.5g\n',rr,cost,omoe);
    fprintf(fp,'%3d %7.5g %7.5g\n',rr,cost,omoe);
end
err=fclose(fp);
[Y,I] = max(OMOE);
plot(omoedat(:,2),omoedat(:,3),'bo');
xlabel('cost');
ylabel('OMOE');
title('SC synch');
fprintf('highest OMOE is design # %2d, OMOE= %4g\n',I,Y);
fprintf('wf= %5.4f %5.4f %5.4f %5.4f %5.4f %5.4f %5.4f %5.4f\n',wf);
```

```
% This script displays motor details for scacsync
fp=fopen('sc.dat','w');  % create/write over file sc.dat
fprintf('Summary SC Motor Attribute  %s\n',date);
fprintf('Number of viable candidates optimized %7g\n',viable);
fprintf(' #  Pwr     Cost     Mass  Dia    Length   Gen     Inerti
Ja\n');
fprintf('    MW      M$       tonne  m      m        Eff     Mg/m^2
A/cm^2\n');
fprintf(fp,'Summary SC Motor Attribute  %s\n',date);
fprintf(fp,'Number of viable candidates optimized %7g\n',viable);
fprintf(fp,' #  Pwr     Cost     Mass  Dia    Length   Gen     Inerti
JA\n');
fprintf(fp,'    MW      M$       tonne  m      m        Eff     Mg/m^2
A/cm^2\n');


for r = 1:NDE,
    if MD(r,1)==0  % Avoid division by 0
        MA(r,:)=1e-7;
        MDI(r,1)=1;
    end
  Pwr = 10^-6*MA(r,1);
  Cost = 10^-6/MA(r,2);
  Mass = 10^-3/MA(r,3);
  Dia = 1/MA(r,4);
  Len = 1/MA(r,5);
  Eff = MA(r,6);
  J = 10^-3/MA(r,7);
  Ja = 10^(-4)/MA(r,8);

  fprintf('%2g  %4.2f %7.2f %7.1f %7.3f %7.3f %7.3f %6.1f
%7.2f\n',...
            r,Pwr,Cost,Mass,Dia,Len,Eff,J,Ja);
  fprintf(fp,'%2g  %4.2f %7.2f %7.1f %7.3f %7.3f %7.3f %6.1f
%7.2f\n',...
            r,Pwr,Cost,Mass,Dia,Len,Eff,J,Ja);

end


% This script displays motor geometry for SC.m
fprintf('\nSummary SC synch geometry\n');
fprintf(' #  Rfi  air-gap   tsc   lrot    tarm   p  nc  q\n');
fprintf('    m    mm        mm    m       mm\n');
fprintf(fp,'\nSummary SC synch geometry\n');
fprintf(fp,' #  Rfi  air-gap   tsc   lrot    tarm   p  nc  q\n');
fprintf(fp,'    m    mm        mm    m       mm\n');

for r = 1:NDE,
  % MD = [Rfi g tsc lrot tarm];
  % MDI = [pmax ncmax qmax];
  p =MDI(r,1);
  nc = MDI(r,2);
  q = MDI(r,3);
  Rfi = MD(r,1);
  g = 1000*MD(r,2);
  tsc = 1000*MD(r,3);
  lrot = MD(r,4);
  tarm = 1000*MD(r,5);
```

```
    fprintf('%2g  %3.2f  %6.2f   %6.2f %5.2f  %3.2f  %2d %2d %2d\n',...
          r,Rfi,g,tsc,lrot,tarm,p,nc,q);
    fprintf(fp,'%2g  %3.2f  %6.2f   %6.2f %5.2f  %3.2f  %2d %2d
%2d\n',...
          r,Rfi,g,tsc,lrot,tarm,p,nc,q);

   end
   fprintf(fp,'\nDM =     Rfi      g       tsc      lrot    tarm\n');
   fprintf(fp,'DU = %6.4f  %6.4f  %6.4f   %6.4f  %6.4f\n',DU);
   fprintf(fp,'DM = %6.4f  %6.4f  %6.4f   %6.4f  %6.4f\n',DM);
   fprintf(fp,'DL = %6.4f  %6.4f  %6.4f   %6.4f  %6.4f\n',DL);
   fprintf(fp,'DS = %6.4f  %6.4f  %6.4f   %6.4f  %6.4f\n',DS);
   fprintf(fp,'DIN =  pmax  ncmax qmax\n');
   fprintf(fp,'DIN = %4d  %4d  %4d\n',DIN);

   fprintf('\nDM =     Rfi      g       tsc      lrot    tarm\n');
   fprintf('DU = %6.4f  %6.4f  %6.4f   %6.4f  %6.4f\n',DU);
   fprintf('DM = %6.4f  %6.4f  %6.4f   %6.4f  %6.4f\n',DM);
   fprintf('DL = %6.4f  %6.4f  %6.4f   %6.4f  %6.4f\n',DL);
   fprintf('DS = %6.4f  %6.4f  %6.4f   %6.4f  %6.4f\n',DS);
   fprintf('DIN =  pmax  ncmax  qmax\n');
   fprintf('DIN = %4d  %4d   %4d\n',DIN);

err=fclose(fp);
```

```
% scdata
% saves design parameters to be read in manually for further analysis

fp=fopen('scdata.dat','w');   % create/write over file

fprintf(fp,'%7d  %7d\n',NDE,viable);
for rr = 1:NDE,
    % MD = [Rfi g tsc lrot tarm Jsc];
    % MDI = [pmax ncmax qmax];
  Rfi = MD(rr,1);
  g = MD(rr,2);
  tsc = MD(rr,3);
  lrot = MD(rr,4);
  tarm = MD(rr,5);
  p = MDI(rr,1);
  nc = MDI(rr,2);
  q = MDI(rr,3);
  fprintf(fp,'%7.5f %7.5f %7.5f %7.5f %7.5f ',...
      Rfi,g,tsc,lrot,tarm);
  fprintf(fp,'%7d %7d %7d\n',p,nc,q);
end

err=fclose(fp);
```

```
% reads in data (should be dominate) and runs attribute for designs
% run SC setup first to initialize B and NA
scsetup;
DEBUG=4

fp=fopen('scdata.dat','r');  % open file to read

NDEt=fscanf(fp,'%7d',1);
viable=fscanf(fp,'%7d',1);
for rr = 1:NDEt,
    % Dt = [Rfi g tsc lrot tarm Jsc];
    % DIt = [pmax ncmax qmax]
  Rfi = fscanf(fp,'%7g',1); Dt(rr,1) = Rfi;
  g = fscanf(fp,'%7g',1); Dt(rr,2) = g;
  tsc = fscanf(fp,'%7g',1);  Dt(rr,3) = tsc;
  lrot = fscanf(fp,'%7g',1); Dt(rr,4) = lrot;
  tarm = fscanf(fp,'%7g',1); Dt(rr,5) = tarm;
  p = fscanf(fp,'%7g',1); DIt(rr,1) = p;
  nc = fscanf(fp,'%7g',1); DIt(rr,2) = nc;
  q = fscanf(fp,'%7g',1); DIt(rr,3) = q;
  if Rfi == 0,
      return
  end

  [A, gg] = attributsc(Dt(rr,:), DIt(rr,:), B, DEBUG);
  if gg ~= 0,
      fprintf(' motor %2d viable\n',rr);
      MA(rr, :) = A;       % if still viable it goes here
      MD(rr, :) = Dt(rr,:);    % save design too!
      MDI(rr, :) = DIt(rr,:);
  end % if

  DM=Dt(1,:);          % initialize mean variable vector to first
optimized design

end
err=fclose(fp);
```

Appendix I

HPM MATLAB™ Code

```
% HPMsetup.m
% Rotor parameters
clear
NA = 8;              % attributes
NDE = 30;            % designs to keep
NITER = 1000;        % shots to try
DEBUG=1;             % 1=debug output, 2=screen output
                     % 3=attribute output, 4=std reduction optimization
DF=.999;             % Standard deviation reduction factor
viable=0;            % index of viable designs

% Lower limit
Lrot=.5;             % active rotor length (inside field coils)
Rri=.25;             % rotor inner radius
trot=.001;           % rotor can thickness
tins=.001;           % rotor insulation/cooling thickness
Rc=.25;              % field coil radius
tc=.02;              % field coil thickness
wc=.05;              % field coil width
DL=[Lrot Rri trot tins Rc tc wc];

% Upper limit
Lrot=4;              % active rotor length (inside field coils)
Rri=4;               % rotor inner radius
trot=.1;             % rotor can thickness
tins=.01;            % rotor insulation/cooling thickness
Rc=5;                % field coil radius
tc=1;                % field coil thickness
wc=1;                % field coil width
DU=[Lrot Rri trot tins Rc tc wc];

ND = size(DL,2);        % continuous design space
DM=(DL+DU)/2;           % Mean value array
DS=(DU-DL)/2;           % initial standard normal multplier vector

% Limits of integer variables
Nturnsmax=30;           % number of series connected rotors
% Integer upper limit vector
DIN = [Nturnsmax];

% fixed inputs
Jc=2*10^8;       % (A/m^2) field coil current density
                 % HTS BSCCO 20,000A/cm^2, LTS Nb-Ti 200,000A/cm^2
divcz=1;         % segmentation of coil axially
divcr=1;         % segmentation of coil radially
tpu=.05;         % rotor to brush minimum pickup length
tcr=.01;         % rotor to coil clearance
rpm = 100;       % Rotational speed
Preq = 21*10^6;% Required power
Vll = 1100;      % line-line voltage
siga = 5.917e5;% Stator Conductivity [1/(ohm*m)]
rhos=7800;       % Steel Density
rhosc=10510;     % Superconductor Conductor (silver) Density
rhoco=.2*rhos; % Composite Density
rhoins=500;      % Insulation density
kins=0;          % insulation thermal conductivity
rhoc=8960;       % Conductor (copper) Density
```

```
krot=0;          % conductor thermal conductivity
Jalim = 4e6;     % armature current density limit [A/m^2]
Psc = 100;       % Superconductor price: $/kg
Pcu = 5;         % copper price: $/kg
Pfe = 2;         % iron price: $/kg
Pins = 5;        % insulation price: $/kg
Pcryo = .0001;   % cryo system price: $/J
Bisat = 2;       % maximum iron flux density
vtip = 140;      % max tip speed m/s
tbrush=.01;      % brush length
Jmax=1.5e6;      % max current density in copper brushes [A/m^2]
effmin=.8;       % minimum efficiency
Mmax=100;        % maximum weight
dT=10;           % temperature rise along rotor

B = [Jc divcz divcr tpu tcr rpm Preq Vll siga rhos rhosc rhoco rhoins
rhoc...
    Jalim Psc Pcu Pfe Pins Pcryo Bisat vtip tbrush Jmax effmin Mmax
dT];

% Here are the matrices that NDA will fill out

MA = zeros(NDE, NA);    % design attributes across rows
MD = zeros(NDE, ND);    % design variables (continuous)
NI = length(DIN);       % number of integer variables
MDI = zeros(NDE, NI);   % design variables (integers)
DI = zeros(size(DIN));  % space for integer variables

% Run NdaHPM
```

```
% HPMattribut.    Joe Harbour 01/04/01
% used in conjunction with HPMsetup to find
% solution to drum type HMP motor with multiple
% rotor turns and opposing superconducting coils.
%
% uses following variables previously initialized
% Lrot active rotor length (inside field coils)
% Rri rotor inner radius
% Nturns number of series connected rotors
% trot rotor can thickness
% tins rotor insulation/cooling thickness
% tpu rotor to brush minimum pickup length
% Rro rotor outer radius
% divr, divz radial/axial segments of rotor field array
%
% brush parameters
% tbrush collector brush radial thickness
% Ia armature current full load
%
% Flux shield parameters
% tfs flux shield thickness
% Rfs flux shield radius
%
% field coil parameters
% Rc field coil radius
% Jc field coil current density
% wc field coil width
% tc field coil thickness
% divcw segmentation of coil axially
% divct segmentation of coil radially
% dlfs length of fs segment
% dlcw length of coil width segment
% dlct length of coil thickness segment
% dlJc elemental field current density
% Jfs flux shield surface current storage array

function[A,C] = attributHPM(D,DI,B,DEBUG)
global mew0

% load variables created in HPMsetup/nda
Lrot=D(1);          % active rotor length (inside field coils)
Rri=D(2);           % rotor inner radius
trot=D(3);          % rotor can thickness
tins=D(4);          % rotor insulation/cooling thickness
Rc=D(5);            % mean coil radius
tc=D(6);            % coil axial thickness
wc=D(7);            % coil radial thickness

Nturns=DI(1);       % number of series connected rotors

Jc=B(1);            % (A/cm^2) field coil current density
divcz=B(2);         % segmentation of coil axially
divcr=B(3);         % segmentation of coil radially
tpu=B(4);           % rotor to brush minimum pickup length
tcr=B(5);           % rotor to coil clearance
```

```
% B = [Jc divcz divcr tpu tcr rpm Preq Vll siga rhos rhosc rhoco rhoins
rhoc...
%   Jalim Psc Pcu Pfe Pins Pcryo Bisat vtip tbrush Jmax effmin Mmax dT];

% Material parameters
rpm = B(6);
Preq = B(7);
Vll = B(8);
siga = B(9);
rhos=B(10);
rhosc=B(11);
rhoco=B(12);
rhoins=B(13);
rhoc=B(14);
Jalim = B(15);
Psc = B(16);
Pcu = B(17);
Pfe = B(18);
Pins= B(19);
Pcryo= B(20);
Bisat = B(21);
vtip = B(22);
tbrush=B(23);                 % collector brush radial thickness
Jmax=B(24);
effmin=B(25);
Mmax=B(26);
dT=B(27);


% Here are a few constants
mew0=pi*4e-7;            % free-space permeability
cpco2 = 844;            % mass heat capacity of wetted CO2 [J/(kg*K)]
rhoco2 = 1.83;          % density of wetted CO2 [kg/m^3]
cph2o = 4190;           % mass heat capacity of H2O [J/(kg*K)]
rhoh2o = 1000;          % density of H2O [kg/m^3]
nuair = 1.79e-5;        % kinematic viscosity of air [N*s/m^2]
nuh2o = 1.12e-3;        % kinematic viscosity of H2O [N*s/m^2]
tol=.0001;              % iterative loop tolerance
kins=0;                 % insulation thermal conductivity [W/m*K]
krot=400;               % conductor thermal conductivity [W/m*K]
elpc=.004*(.5^.333)*11^10; % average contact pressure of brush (eq
20.11 Slade)
PB=5;                   % applied pressure on brush [N]
sigaF=1*10^-12;         % film resistivity of metal brushes [ohm*m^2]
epsilon=.0015;          % equivalent roughness of drawn tubing

C=0;                    % machine not viable yet
A=[1 0 0 0 0 0 0 0];    % attribut array, poor machine but not empty

% Calculate dependant geometry
Ttrot=Nturns*(tins+trot)-tins;
divr=10;                % radial/axial segments of rotor field array
divz=divr;
Icoil=Jc*(tc*wc);

om=rpm*(2*pi)/60;
stip=(Rri+Ttrot)*om;
```

```matlab
% check surface speed (brush wear rates proven for <20m/s)
if stip > vtip,
   C = 0;
   if DEBUG==1, fprintf('stip= %g\n',stip); end
   return;
end;

% check that rotor radial turns fit into total rotor length
if 2*Ttrot>Lrot,              %too many turns to fit in rotor length
    if DEBUG==1,
        fprintf('Too many turns. 2*Ttrot = %g Lrot = %g\n',2*Ttrot,Lrot);
    end
    return
end

% check that coil fits in machine
if tc/2>Rc,                  %coil too thick
    if DEBUG==1,
        fprintf('coil too thick. tc/2 = %g Rc = %g\n',tc/2,Rc);
    end
    return
end

Rro=Rri+Ttrot;               % rotor outer radius
Rfs=Rro+tpu+tbrush;          % flux shield inner radius
if (Rc+.5*tc>Rfs),           % field coil too big for flux shield
    if DEBUG==1,
       fprintf('Rc outer radius= %5.1f m  Rfs inner radius= %1.1f
m\n',...
         Rc+.5*tc, Rfs);
    end
    return
end

dlz=Lrot/(2*divz);           % radial & axial differential element length
dlr=Ttrot/divr;

% calculate position array in rotor turn area (two vectors)
posr=zeros(1,divz);          % radial position vector (outer to inner)
posz=zeros(divr,1);          % axial position vector (left to right)
I=1:divr; J=1:divz;
posr=Rro-dlr*(I-.5);
posz=wc/2+tcr+dlz.*(J-.5);

% Calculate magnetic flux at each position due to coil
Brotr=zeros(divr,divz);
Brotz=zeros(divr,divz);
Bfsr=zeros(1,divz);          % radial flux at fs; used for fs thickness calc.
Bfsz=zeros(1,divz);          % axial flux at fs; Boundary condition must be
zero
dlcr=tc/divcr; dlcz=wc/divcz;    % coil elements
dlJc=Jc*dlcr*dlcz;               % elemental field current density
zc=zeros(1,divcz);               % vectors for coil position array
rc=zeros(divcr,1);
for II=1:divcz;  % coil axial loop
    zc(II)=-wc/2+dlcz*(II-.5);
    for JJ=1:divcr; % coil radial loop
```

164

```
            rc(JJ)=Rc-tc/2+dlcr*(JJ-.5);
        for K=1:divz; % axial position loop
            Bfsr(K)=Bfsr(K)+Brcoil(dlJc,rc(JJ),Rfs,(posz(K)-zc(II)));
            Bfsz(K)=Bfsz(K)+Bzcoil(dlJc,rc(JJ),Rfs,(posz(K)-zc(II)));
            for I=1:divr;    % radial position loop
                Brotr(I,K)=Brotr(I,K)+Brcoil(dlJc,rc(JJ),posr(I),(posz(K)-
zc(II)));
                Brotz(I,K)=Brotz(I,K)+Bzcoil(dlJc,rc(JJ),posr(I),(posz(K)-
zc(II)));
            end %radial position loop
        end %axial position loop
    end %coil radial loop
end % coil axial loop

% calculate amperian current in fs segment (I) to cancel axial flux of
coil at
% inner surface of fs; Boundary Condition for ferrous flux shield.
Jfs=zeros(1,divz);
Kfs=zeros(1,divz);
Kfs=2*(Bfsz/mew0);       %K=2*H, H=B/mew0
Jfs=Kfs*dlz;             %J=k*dlz

%  Add in contribution due to flux shield current
for I=1:1:divz;          % Jfs current in question
    for J=1:divz;        % axial position for analysis
        % distance from fs(I) to fs(J) element
        rfs=posz(J)-posz(I);
        if rfs==0;
            Bfsr(J)=Bfsr(J);
            Bfsz(J)=Bfsz(J)-.5*Kfs(J)*mew0;     % should be zero
        else
            Bfsr(J)=Bfsr(J)+Bwire(Jfs(I),abs(rfs))*sign(rfs);
        end %if
        for K=1:divr    % radial position for analysis
            % distance from fs point to rotor element, pythagorean formula
            rtemp=sqrt((posz(J)-posz(I))^2+(posr(K)-Rfs)^2);
            if (posz(J)-posz(I))==0;
                theta=-pi/2;
            else
                theta=atan((posr(K)-Rfs)/(posz(J)-posz(I)));
            end %if
            Brotr(K,J)=Brotr(K,J)-Bwire(Jfs(I),rtemp)*cos(theta);
            Brotz(K,J)=Brotz(K,J)-Bwire(Jfs(I),rtemp)*sin(theta);
        end % rotor radial loop
    end % rotor axial loop
end % fs current loop

% check flux shield thickness. Total flux integrated over all divz's
flux=0;
flux=sum(Bfsr*dlz);
%B=flux/area=flux/2*pi*Rfs*tfs
tfs=flux/(Bisat*2*pi*Rfs);    % set tfs to smallest allowed.

% now calculate torque production and back emf
% create arrays with 1's if rotor is perpendicular to magnetic flux's
Brotr
% and Brotz, else 0's
```

165

```
ptr=zeros(divr,divz);    % radially laying rotor turns
ptz=zeros(divr,divz);    % axially laying rotor turns
dtr=dlr/(trot+tins);     % maximum number of rotor turns per radial
element
dtz=dlz/(trot+tins);     % maximum number of rotor turns per axial
element
Mr=zeros(divr,divz);     % radial position matrix
for J=1:divz
    Mr(J,:)=posr;
    for I=1:divr
        zprime=posz(J)-(wc/2+tcr);
        rprime=posr(I)-Rri;
        if zprime>rprime,
            ptz(I,J)=1;
        else
            ptr(I,J)=1;
        end
    end
end
Mr=Mr';


% Heres the torque and power per unit amp through the armature
% F=(i*l) X B, T=(F)*moment arm
Fz=Brotr.*(ptz*dtz)*dlz;          % force per amp  due to radial
flux/axial turns
Tze=Fz.*Mr;                       % elemental torques
Tz=sum(Tze);                      % column sums
Fr=Brotz.*(ptr*dtr)*dlr;          % force due to axial flux/radial turns
Tre=Fr.*Mr;
Tr=sum(Tre);
Torquem=2*(sum(Tz')+sum(Tr'));    % total torque [N*m/A] (sum of
transpose)
% Pwr=RPM*Torquem;
om=rpm*(2*pi)/60;
Pmaxa=om*Torquem; % [W/A]


% Here is the back emf calc.  Only the axial turns will generate a
voltage at the brushes
% The voltage generated by the radial turns at opposite ends will
cancel each other.
% Faraday (constant field); dv=integral (v X B)dl.  Only half of rotor
solved for.
Eturn=((om*Mr).*Brotr.*ptz*dlz)*dtr;
Eaf=2*sum(sum(Eturn)');


% Now determine operating current (P=IV) and maximum current
% Imax=(Vt-Eaf)/Ra.  Determine maximum armature current
Aturns=pi*(Rro^2-Rri^2)*(trot/(trot+tins));  %x-section area of copper
Rturns=Lrot/(siga*Aturns);      % total resistance of armature turns
Abrush=.6*(2*pi*(Rro+tpu)*trot);
% Rbrush=.000001;
Rbrush=sigaF*(elpc/PB);           % resistance per end, per turn, due to
brushes
Ra=Rturns+2*(Rbrush*Nturns);
Iamax=(Vll-Eaf)/Ra;               % max armature current

Pmax=Pmaxa*Iamax;                 % ignores losses
```

166

```matlab
% Determine operating current
% First determine non-dependate losses
% Estimate of gap friction loss
gap=Rfs-Rro;
l=Lrot-2*Ttrot;
ren = om*Rro*gap/nuair;              % Reynold's Number in the gap
ff = .0076/ren^.25;                  % that gives a friction factor
Pwind = 2*pi*Rro^4*om^3*l*rhoco2*ff; % windage loss
Pereq=Preq+Pwind+Iamax^2*Ra;

% Check sufficient power capacity
if Pmax<Pereq                    % the thing won't do what is required
    if DEBUG==1,
        fprintf('Max converted P = %10.1f MW. Required = %10.1f MW\n',...
            Pmax/1000000, Pereq/1000000);
    end
    return
end

% Operating current requires an iterative loop.
Ierror=tol*100.1;
Ia=Preq/Eaf;
while abs(Ierror)>(tol*100)
    Itemp=(Preq+Ia^2*Ra)/Eaf;
    Ierror=Ia-Itemp;
    Ia=Ia-Ierror/2;
end

% Dependant losses
Pturns=Ia^2*Rturns;              % drum losses
Pbrush=Ia^2*Rbrush*2;            % brush losses
Pa=Pturns+Pbrush;                % armature loss
Ploss=Pwind+Pa;
Pereq=Preq+Ploss;

% Check maximum current density
% Determine required cooling
Ainturn=pi*((Rri+tins+trot)^2-(Rri+tins)^2);
Imax=Jalim*Ainturn;
if Ia>Imax                % rotor too thin for required current
    if DEBUG==1,
        fprintf('Current density in rotor too high    = %10.1f A/cm^2
limit= %10.1f A/cm^2\n',...
            Ia/(Ainturn*10^4), Jalim/10^4);
    end
    return
end

Ibmax=Jmax*Abrush;
if Ia>Ibmax              % Brush current density too high
    if DEBUG==1,
        fprintf('Brush current density too high = %10.1f A/cm^2   limit=
%10.1f A/cm^2\n',...
            Ia/(Abrush*10^4), Jmax/10^4);
    end
    return
```

167

```
end

Vol=(Pturns+Pwind)/(rhoh2o*cph2o*dT);   % total volumetric flow rate of
water required
% in composite rotor [m^3/sec] (assumes brushes cooled by wetted CO2.
% Determine required dp and pump loss across rotor. first find minimum
xsection
% to maintain flow velocity less than 10m/s; limits flow noise in
motor.
% Assume 60% of Rri surface can be used for heat transfer (Wcool).
Coolant channel is
% rectangular with height = .5*width.
Nchan=50;
arc=.6*2*pi/10;    % azmuthal extent of each channel
wchan=2*Rri*sin(arc/2); % chord length of channel
hchan=.5*wchan;
Achan=Nchan*(wchan*wchan);
Vel=Vol/Achan;
if Vel>10              % Too much flow noise
    if DEBUG==1,
        fprintf('Vel = %5gm/s, max allowed is 10m/s\n',Vel);
    end
    return
end
Xcool=Vol/Vel;
Dpipei=sqrt(4*Xcool/pi);       % radius of coolant return pipe.
Dh=((2*hchan*wchan)/(hchan+wchan));   % hydraulic diameter for square
pipe.

Rens=(rhoh2o*Dh*Vel)/nuh2o;              % reynolds number
% check if laminar or turbulent flow
if (Rens>2100),    % Turbulent coolant flow
  if DEBUG==1,
      fprintf('Turbulent coolant flow in channel Re= %5.1f Recrit=2100
\n',...
          Rens);
  end
  fs=.001;      % initial guess at friction factors
  ferrors=tol*10;
    while ferrors>tol
    fact=-2*log10(epsilon/Dh/3.7+2.51/(Rens*sqrt(fs))); % eqn 8.35
"Fund Fluid Mech"
                        % the "Colebrook formula" applied to square
tube (see pg 519)
    fit=1/fact^2;
    ferrors=abs(fit-fs);
    fs=fit;
  end
else  % Laminar flow
  if DEBUG==1,
      fprintf('Laminar coolant flow in channels Re= %5.1f Recrit=2100
\n',...
          Rens);
  end
  fs=62.2/Rens;              % square tube a/b=.5 C=62.2 Table 8.4
end
```

```
Reni=(rhoh2o*Dpipei*Vel)/nuh2o;              % reynolds number
% check if laminar or turbulent flow
if (Reni>2100),     % Turbulent coolant flow
   if DEBUG==1,
      fprintf('Turbulent coolant flow in return Re= %5.1f Recrit=2100
\n',...
         Reni);
   end
   fi=.001;       % initial guess at friction factors
   ferrori=tol*10;
     while ferrori>tol
      fact=-2*log10(epsilon/Dpipei/3.7+2.51/(Reni*sqrt(fi))); % eqn 8.35
"Fund. Fluid Mech"
                                                    % the
"Colebrook formula"
      fit=1/fact^2;
      ferrori=abs(fit-fi);
      fi=fit;
   end
else  % Laminar flow
   if DEBUG==1,
      fprintf('Laminar coolant flow in return Re= %5.1f Recrit=2100
\n',...
         Reni);
   end
   fi=64/Reni;
end

% Determine required differential pressure for coolant and pump HP.
dp=(Lrot*.5*rhoh2o*Vel^2)*(fs/Dh+fi/Dpipei);     % eqn 8.33
Ppump=dp*Vol;

% calculate physical parameters
Rpu=Rro+tpu;
Ma=rhoc*Aturns*Lrot;
Ains=pi*(Rro^2-Rri^2)*(tins/(trot+tins)); %x-section area of ins
Mins=rhoins*(Ains*Lrot+(tpu*Nturns*tins*2*pi*Rro));
Mturns=Ma+Mins;
Jturns=.5*Mturns*(Rro^2-Rri^2);
Mrotor=Lrot*pi*(rhoco*Rri^2);
Jrot=.5*Mrotor*Rri^2;
Mpuc=rhoc*pi*((Rro+tpu)^2-(Rro)^2)*Nturns*trot;
Mpuins=rhoins*pi*((Rro+tpu)^2-(Rro)^2)*Nturns*tins;
Mpu=Mpuc+Mpuins;
Jpu=5*Mpu*(Rpu^2-Rro^2);
J=Jrot+Jturns+Jpu;

Dover=2*Rfs;                              % overall diameter
Lover=Lrot+(2*tcr)+(2*wc)+(2*tfs);        % overall length

% cylinder plus two end caps
Mfsdrum=rhos*pi*Lover*((Rfs+tfs)^2-Rfs^2);
Mfsend=rhos*pi*tfs*(Rfs+tfs)^2;
Mfs=2*Mfsend+Mfsdrum;
Areasc=2*(wc*pi*Rc*tc);
lamasc=.85;
Mcoils=rhosc*lamasc*Areasc;
```

169

```
Mcryo=500;           % estimated weight for two mechanical conduction
cryo coolers
Mass=Mturns+Mrotor+Mpu+Mfs+Mcoils+Mcryo;

if Mass/1000>Mmax          % Too heavy
    if DEBUG==1,
        fprintf('Weight= %4.1\n',Mass);
    end
    return
end

% Cost estimate
Costfs = Pfe*Mfs;
Costc = Pcu*(Ma+Mpuc);
Costins=Pins*(Mins+Mpuins);
Costcryo=Pcryo*Jc;
Cost = Costfs+Costc+Costins+Costcryo;      % Materials Cost

Ja=Ia/Abrush;

Pwrcryo=(Pereq)*(0.3/100);     % estimate .3% machine rating for cryo
cooler (AMSC data)
Pereq=Pereq+Pwrcryo+Ppump;
eff=Preq/Pereq;
% check eff
if eff < effmin                % efficiency too low
    if DEBUG==1,
        fprintf('low efficiency =  %4.3fn\n',eff);
    end
    return
end

C=1;       % Machine viable
A = [Pereq 1/Cost 1/Mass 1/Dover 1/Lover eff 1/J 1/Ja ];
if DEBUG==1,
    geo=[Ttrot Rro Rfs];
    Pwr=[Pturns Pbrush Pwind Pa Pwrcryo Ppump Pereq];
    Masss=[Mturns Mrotor Mpu Mfs Mcoils Mcryo];
    Costs=[Costfs Costc Costins Costcryo];
    temp=[divr,divz,Ia,Eaf];

HPMout(A,D,DI,Brotr,Brotz,posr,posz,Bfsr,Bfsz,temp,geo,Tre,Tze,Pwr,Mass
s,Costs);
    fprintf('Load "hpmout.dat" in Debugger menu to print out results. It
any key to continue.\n');
    pause;
end

if DEBUG==3, fprintf('A= %6.4f %6.4f %6.4f %6.4f %6.4f %6.4f %6.4f
%6.4f \n',A(:));
    fprintf('A=[Pmax 1/Cost 1/Mass 1/Dover 1/Lover eff 1/J 1/Ja ] \n');
    fprintf('inverse A= %6.4f %6.4f %6.4f %6.4f %6.4f %6.4f %6.4f %6.4f
\n',1./A(:));
end;
```

```
% radial magnetic field due to coil radius a, current J, at r,z
function B=Brcoil(J,a,r,z)
global mew0

k=modulus(a,r,z);
[K,E]=ellipke(k^2);
amp1=(mew0*J)/(2*pi)*(z/r)/sqrt((a+r)^2+z^2);
amp2=-K+(a^2+r^2+z^2)/((a-r)^2+z^2)*E;
B=amp1*amp2;




% axial magnetic field due to coil radius a, current J, at r,z
function B=Bzcoil(J,a,r,z)
global mew0

k=modulus(a,r,z);
[K,E]=ellipke(k^2);
amp1=(mew0*J)/(2*pi)*1/sqrt((a+r)^2+z^2);
amp2=K+(a^2-r^2-z^2)/((a-r)^2+z^2)*E;
B=amp1*amp2;




% Calculates phi directed field at radius r due to wire with current I
% assumes Length of wire much greater than radius r
function Bphi=Bwire(Iw,rf)
global mew0
Bphi=(mew0*Iw)/(2*pi*rf);
```

```
% This script displays motor details for HPM
fp=fopen('hpm.dat','w');  % create/write over file hpm.dat
fprintf('Summary HPM Motor Attributes  %s\n',date);
fprintf('Number of viable candidates optimized %7g\n',viable);
fprintf(' #  Pwr      Cost    Mass    Dia    Length  Gen    Inerti   Ja
\n');
fprintf('    MW       M$      tonne   m      m       Eff    Mg/m^2
A/cm^2     \n');
fprintf(fp,'Summary HPM Motor Attribute  %s\n',date);
fprintf(fp,'Number of viable candidates optimized %7g\n',viable);
fprintf(fp,' #  Pwr      Cost    Mass    Dia    Length  Gen    Inerti
Ja       \n');
fprintf(fp,'    MW       M$      tonne   m      m       Eff    Mg/m^2
A/cm^2     \n');

for r = 1:NDE,
  Pwr = 10^-6*MA(r,1);
  Cost = 10^-6/MA(r,2);
  Mass = 10^-3/MA(r,3);
  Dia = 1/MA(r,4);
  Len = 1/MA(r,5);
  Eff = MA(r,6);
  J = 10^-3/MA(r,7);
  Ja = 10^(-4)/MA(r,8);

  fprintf('%2g  %4.2f %7.2f %7.1f %7.3f %7.3f %7.3f  %6.1f   %7.5f
\n',...
          r,Pwr,Cost,Mass,Dia,Len,Eff,J,Ja);
  fprintf(fp,'%2g  %4.2f %7.2f %7.1f %7.3f %7.3f %7.3f  %6.1f   %7.5f
\n',...
          r,Pwr,Cost,Mass,Dia,Len,Eff,J,Ja);

end

% This script displays motor geometry for hpm
fprintf('\nSummary HPM Motor geometry\n');
fprintf(' #  Lrot  Rri    trot  tins  Rc   tc    wc   Nturns\n');
fprintf('    m     m      m     m     m    m     m    \n');
fprintf(fp,'\nSummary HPM Motor geometry\n');
fprintf(fp,' #  Lrot  Rri    trot  tins  Rc   tc    wc   Nturns\n');
fprintf(fp,'    m     m      m     m     m    m     m    \n');

for r = 1:NDE,

  % MD= [Lrot Rri trot tins Rc tc wc]
  % MDI = [Nturns];
  Nturns =MDI(r,1);
  Lrot = MD(r,1);
  Rri = MD(r,2);
  trot = MD(r,3);
  tins = MD(r,4);
  Rc = MD(r,5);
  tc = MD(r,6);
  wc = MD(r,7);

  fprintf('%2g %3.2f   %3.2f    %4.3f %4.3f  %3.2f   %4.3f   %4.3f
%2d\n',...
```

172

```
            r,Lrot,Rri,trot,tins,Rc,tc,wc,Nturns);
    fprintf(fp,'%2g  %3.2f %3.2f   %4.3f %4.3f  %3.2f  %4.3f  %4.3f
%2d\n',...
            r,Lrot,Rri,trot,tins,Rc,tc,wc,Nturns);


    end
    fprintf(fp,'\nDM =  Lrot      Rri      trot     tins      Rc         tc
wc\n');
    fprintf(fp,'DU = %6.4f   %6.4f   %6.4f   %6.4f   %6.4f   %6.4f
%6.4f\n',DU);
    fprintf(fp,'DM = %6.4f   %6.4f   %6.4f   %6.4f   %6.4f   %6.4f
%6.4f\n',DM);
    fprintf(fp,'DL = %6.4f   %6.4f   %6.4f   %6.4f   %6.4f   %6.4f
%6.4f\n',DL);
    fprintf(fp,'DS = %6.4f   %6.4f   %6.4f   %6.4f   %6.4f   %6.4f
%6.4f\n',DS);
    fprintf(fp,'DIN =  Nturns\n');
    fprintf(fp,'DIN = %4d\n',DIN);


    fprintf('\nDM =  Lrot      Rri      trot     tins      Rc         tc
wc\n');
    fprintf('DU = %6.4f   %6.4f   %6.4f   %6.4f   %6.4f   %6.4f
%6.4f\n',DU);
    fprintf('DM = %6.4f   %6.4f   %6.4f   %6.4f   %6.4f   %6.4f
%6.4f\n',DM);
    fprintf('DL = %6.4f   %6.4f   %6.4f   %6.4f   %6.4f   %6.4f
%6.4f\n',DL);
    fprintf('DS = %6.4f   %6.4f   %6.4f   %6.4f   %6.4f   %6.4f
%6.4f\n',DS);
    fprintf('DIN =  Nturns\n');
    fprintf('DIN = %4d\n',DIN);

err=fclose(fp);
```

```
% OMOE calc data storage for hpm% needs number of designs
% needs an array of attributes all increasing goodness
% MA=[Preq+Ploss 1/Cost 1/Mass 1/Dover 1/Lover eff 1/J 1/Ja ];
% need to initialize a weighting factor array should sum to zero

fp=fopen('hpmomoe.dat','w');  % create/write over file

% wf=[Pwr Cost Mass Dover Lover eff J Ja]
WF=[0 0 1 1 1 1 0 0];  WFV=1; % relative weighting factors
% WFV is the relative weighting factor for volume
V=pi/4*(1./MA(:,4)).^2.*(1./MA(:,5));
Vin=1/V;    % Volume with increasing value good
te=sum(WF')+WFV;
wf=WF/te;
wfv=WFV/te;
MAmin=min(MA);
MAmax=max(MA);
Vmin=min(Vin);
Vmax=max(Vin);
range=MAmax-MAmin;
rangev=Vmax-Vmin;
for ii=1:NDE;
    dif(ii,:)=MA(ii,:)-MAmin;
    difv(ii)=Vin(ii)-Vmin;
    OMOEvol(ii)=difv(ii)/rangev*wfv;
    OMOEv(ii,:)=dif(ii,:)./range.*wf;
    OMOEt(ii)=sum(OMOEv(ii,:)')+OMOEvol(ii);;
end
OMOE=OMOEt';    % make column vector

for rr = 1:NDE,
    cost=10^-6/MA(rr,2);
    omoe=OMOE(rr);
    omoedat(rr,:)=[rr cost omoe];
    fprintf('%3d %7.5g %7.5g\n',rr,cost,omoe);
    fprintf(fp,'%3d %7.5g %7.5g\n',rr,cost,omoe);
end
err=fclose(fp);
plot(omoedat(:,2),omoedat(:,3),'bo');
xlabel('cost');
ylabel('OMOE');
title('HPM');
[OMOEmax,OMOEd] = max(OMOE);
fprintf('highest OMOE is design # %2d, OMOE= %4g\n',OMOEd,OMOEmax);
fprintf('wf= %5.4f %5.4f %5.4f %5.4f %5.4f %5.4f %5.4f %5.4f\n',wf);
```

```
% hpmdata
% saves design parameters to be read in manually for further analysis

fp=fopen('hpmdata.dat','w');   % create/write over file

fprintf(fp,'%7d  %7d\n',NDE,viable);
for r = 1:NDE,
  % MD= [Lrot Rri trot tins Rc tc wc]
  % MDI = [Nturns];
  Nturns =MDI(r,1);
  Lrot = MD(r,1);
  Rri = MD(r,2);
  trot = MD(r,3);
  tins = MD(r,4);
  Rc = MD(r,5);
  tc = MD(r,6);
  wc = MD(r,7);
  fprintf(fp,'%7.5f %7.5f %7.5f %7.5f %7.5f %7.5f %7.5f %7d\n',...
          Lrot,Rri,trot,tins,Rc,tc,wc,Nturns);
end

err=fclose(fp);
```

```
% reads in data (should be dominate) and runs attribute for designs
% run HPM setup first to initialize B and NA
hpmsetup;
DEBUG=4;

fp=fopen('hpmdata.dat','r');   % open file to read

NDEt=fscanf(fp,'%7d',1);
viable=fscanf(fp,'%7d',1);
for r = 1:NDEt,
   % Dt= [Lrot Rri trot tins Rc tc wc]
   % DIt = [Nturns];
   Lrot = fscanf(fp,'%7g',1);
   Dt(r,1) = Lrot;
   Rri = fscanf(fp,'%7g',1);
   Dt(r,2) = Rri;
   trot = fscanf(fp,'%7g',1);
   Dt(r,3) = trot;
   tins = fscanf(fp,'%7g',1);
   Dt(r,4) = tins;
   Rc = fscanf(fp,'%7g',1);
   Dt(r,5) = Rc;
   tc = fscanf(fp,'%7g',1);
   Dt(r,6) = tc;
   wc = fscanf(fp,'%7g',1);
   Dt(r,7) = wc;
   Nturns = fscanf(fp,'%7g',1);
   DIt(r,1) = Nturns;

   [A, g] = attributHPM(Dt(r,:), DIt(r,:), B, DEBUG);
   if g ~= 0,
      fprintf(' motor %2d viable\n',r);
      MA(r, :) = A;        % if still viable it goes here
      MD(r, :) = Dt(r,:);        % save design too!
      MDI(r, :) = DIt(r,:);
   end % if

   DM=Dt(1,:);         % initialize mean variable vector to first
optimized design

end
err=fclose(fp);
```

176

AD NUMBER

DATE 13 AUG 01	DTIC ACCESSION

20010816 041

1. REPORT IDENTIFYING INFORMATION

   A. ORIGINATING AGENCY

   NAVAL POSTGRADUATE SCHOOL, MONTEREY, CA 93943

   B. REPORT TITLE AND/OR NUMBER
   EVALUATION AND COMPARISON OF ELECTRIC PROPULSION
   MOTORS FOR SUBMARINES

   C. MONITOR REPORT NUMBER

   BY JOEL P. HARBOUR, MIT

   D. PREPARED UNDER CONTRACT NUMBER

   N62271-97-G-0026

2. DISTRIBUTION STATEMENT

   **APPROVED FOR PUBLIC RELEASE:
   UNLIMITED DISTRIBUTION**

REQUE

1. Put you
   on reve

3 Comple

ION h i
   mailed

4. Use un
   inform

5. Do not (
   for 6 tc

DTIC:

1. Assign

2. Return

DTIC F
JUL 96